THE UNIVERSITY *of* EDINBURGH

This thesis has been submitted in fulfilment of the requirements for a postgraduate degree (e.g. PhD, MPhil, DClinPsychol) at the University of Edinburgh. Please note the following terms and conditions of use:

This work is protected by copyright and other intellectual property rights, which are retained by the thesis author, unless otherwise stated.
A copy can be downloaded for personal non-commercial research or study, without prior permission or charge.
This thesis cannot be reproduced or quoted extensively from without first obtaining permission in writing from the author.
The content must not be changed in any way or sold commercially in any format or medium without the formal permission of the author.
When referring to this work, full bibliographic details including the author, title, awarding institution and date of the thesis must be given.

Predictive modelling and uncertainty quantification of UK forest growth

Jack Lonsdale

THE UNIVERSITY
of EDINBURGH

Thesis submitted in fulfilment of
the requirements for the degree of
Doctor of Philosophy
to the
University of Edinburgh — 2014

Declaration

I declare that this thesis has been composed solely by myself and that it has not been submitted, either in whole or in part, in any previous application for a degree. Except where otherwise acknowledged, the work presented is entirely my own.

Jack Lonsdale

October 2014

Abstract

Forestry in the UK is dominated by coniferous plantations. Sitka spruce (*Picea sitchensis*) and Scots pine (*Pinus sylvestris*) are the most prevalent species and are mostly grown in single age mono-culture stands. Forest strategy for Scotland, England, and Wales all include efforts to achieve further afforestation. The aim of this afforestation is to provide a multi-functional forest with a broad range of benefits. Due to the time scale involved in forestry, accurate forecasts of stand productivity (along with clearly defined uncertainties) are essential to forest managers. These can be provided by a range of approaches to modelling forest growth. In this project model comparison, Bayesian calibration, and data assimilation methods were all used to attempt to improve forecasts and understanding of uncertainty therein of the two most important conifers in UK forestry.

Three different forest growth models were compared in simulating growth of Scots pine. A yield table approach, the process-based 3PGN model, and a Stand Level Dynamic Growth (SLeDG) model were used. Predictions were compared graphically over the typical productivity range for Scots pine in the UK. Strengths and weaknesses of each model were considered. All three produced similar growth trajectories. The greatest difference between models was in volume and biomass in unthinned stands where the yield table predicted a much larger range compared to the other two models. Future advances in data availability and computing

power should allow for greater use of process-based models, but in the interim more flexible dynamic growth models may be more useful than static yield tables for providing predictions which extend to non-standard management prescriptions and estimates of early growth and yield.

A Bayesian calibration of the SLeDG model was carried out for both Sitka spruce and Scots pine in the UK for the first time. Bayesian calibrations allow both model structure and parameters to be assessed simultaneously in a probabilistic framework, providing a model with which forecasts and their uncertainty can be better understood and quantified using posterior probability distributions. Two different structures for including local productivity in the model were compared with a Bayesian model comparison. A complete calibration of the more probable model structure was then completed. Example forecasts from the calibration were compatible with existing yield tables for both species. This method could be applied to other species or other model structures in the future.

Finally, data assimilation was investigated as a way of reducing forecast uncertainty. Data assimilation assumes that neither observations nor models provide a perfect description of a system, but combining them may provide the best estimate. SLeDG model predictions and LiDAR measurements for sub-compartments within Queen Elizabeth Forest Park were combined with an Ensemble Kalman Filter. Uncertainty was reduced following the second data assimilation in all of the state variables. However, errors in stand delineation and estimated stand yield class may have caused observational uncertainty to be greater thus reducing the efficacy of the method for reducing overall uncertainty.

Acknowledgements

First and foremost I would like to thank my supervisors: Maurizio Mencuccini, Mike Perks, and Mat Williams. They have provided me with some amazing guidance, support and lively debate throughout the trials and tribulations of my PhD.

I would also like to thank my co-authors and the many people at Forest Research, Edinburgh University and Center for Ecology and Hydrology who have helped in providing information, support and data essential to this work. Special mentions should go to Francesco Minunno, Georgios Xenakis, Juan Suarez, Richard Nair, and Iain McNicol, who have gone out of their way to talk to me and help me with my thesis.

Additionally, I would like to thank my examiners Maarten Nieuwenhuis and Marcel Van Oijen for their constructive input and challenging examination.

The Hyperspectral and LiDAR research group were more than wonderful as hosts to me while I spent a year in Victoria, BC. I would like to thank Olaf Niemann, Roger Stephen, Geoff Quinn, Fabio Visintini, and Diana Parton having me in the lab and giving me insight and information on using LiDAR for forest inventory.

Special thanks go to Oscar Garcia for introducing me to the stand level dynamic growth models more than 6 years ago. I have found him to be an inspiring forest

modeller, who has always had time to read over what I have been working on, and that has been greatly appreciated.

I must also thank all the medical professionals who helped put me back together following a road accident in the first year of my PhD. Without them I would not have been able to get back to work so quickly.

Finally comes the very important group of friends and family. I would like to thank all of my parents, brothers, sisters, grandparents and other wider family for always being there for me. I would like to give special mention to my uncle John, and Mike and Cathy for supporting me at certain difficult times. All of my friends have been amazing throughout. So thank you Edinburgh and Glasgow friends, C.O.L. friends, Victoria friends, and all the other PhD students in the Attic. Lastly, I would like to thank my girlfriend Hayley for all her support in getting to the finish line.

Contributions to Chapters

- Chapters 1 and 5 were the work of Jack Lonsdale
- Chapter 2 & Appendix A: Jack Lonsdale performed the model calibration of the SLeDG model for Scots pine, performed all analyses, produced all figures and tables, and wrote the text. Georgios Xenakis ran the 3PGN model for the model comparison. Maurizio Mencuccini and Mike Perks gave feedback and comments on drafts of the chapter.
- Chapter 3: Jack Lonsdale performed all Bayesian Calibrations and analysis of the SLeDG model included in the chapter, produced all figures and tables, and wrote the text. Francesco Minunno provided the code for the DE-MC method and provided initial advice as to how to implement models in the code, feedback on drafts of the paper was also provided. Maurizio Mencuccini and Mike Perks provided feedback on drafts of the chapter.
- Chapter 4: Jack Lonsdale adapted the EnKF to work at the stand level, performed all runs of the EnKF and associated analyses, produced all tables and figures, and wrote the text. Maurizio Mencuccini and Mike Perks provided feedback on drafts of the chapter.

Contents

List of Tables

List of Figures

List of Acronyms

3PG Physiological Principles Predicting Growth

AIC Akaike Information Criterion

BEF Biomass Expansion Factors

BMC Bayesian Model Comparison

CAI Current Annual Increment

CCF Continuous Cover Forestry

dbh Diameter At Breast-height

DE-MC Differential Evolution Markov Chain

EnKF Ensemble Kalman Filter

FR Fertility Rating

GPP Gross Primary Production

LAI Leaf Area Index

LiDAR Light Detection And Ranging

LULUCF Land Use, Land Use Change And Forestry

MAI Mean Annual Increment

MCMC Markov Chain Monte Carlo

NPP Net Primary Production

PAR Photosynthetically Active Radiation

PDF Probability Density Function

PSP Permanent Sample Plot

QE Quantum Efficiency

RMSE Root Mean Standard Error

SCDB Sub-compartment Database

SI Site Index

SLeDG Stand Level Dynamic Growth

VPD Vapour Pressure Deficit

YC Yield Class

Chapter 1

Introduction

1.1 Background

1.1.1 UK forestry

Forestry in the UK is dominated by coniferous plantations. Foresters have planted Sitka spruce (*Picea sitchensis* (Bong.) Carr.) in the UK since the beginning of the Twentieth century (McIntosh, 1995), and Sitka spruce makes up almost half of the area of coniferous forests in the UK (Forestry Commission, 2011). Seeds were acquired from various locations in the Pacific North-West of North America and imported to the UK for planting (Aldhous, 1961). Its productivity over a range of sites, including poor quality upland areas has led to extensive planting across the UK (Low, 1987; McIntosh, 1995). Until recently, Sitka spruce has been managed as single species, even-aged stands, which are ideally clear-felled at the point of maximum mean annual increment (MAI) (Hibberd, 1991; Hamilton and Christie, 1971). More recently, there has been a shift in silvicultural methods with more emphasis on the use of native species (Scottish Executive, 2006; Forestry Commission, 1998; Welsh Assembly Government, 2009). This has resulted in an increased role of Scots pine (*Pinus sylvestris* L.), which is the most abundant of the three conifers native to the UK (Forestry Commission, 2011). Additionally, mixed species stands (Kerr, 1999), the use of natural regeneration and more varied spatial vertical structure associated with continuous cover forestry (CCF) (Pommerening and Murphy, 2004), and thinning/pruning regimes are becoming more prevalent (Kerr, 1999).

In addition to increased structural variety in UK forests, there is also a drive to increase the forest land cover. The forest strategy for Scotland (Scottish Executive, 2006), England (Defra, 2007), and Wales (Welsh Assembly Government, 2009) all mention efforts for further afforestation of between 5% and 8% of land area by 2050 (Scottish Executive, 2006; Forestry Commission, 1998). Accordingly,

between 2012 and 2013 twenty-four thousand hectares of forests were planted in the UK, of which eleven thousand hectares were new forest areas (Forestry Commission, 2013).

The aim of this afforestation is to provide a multi-functional forest with a broad range of social, environmental, and financial benefits (Scottish Executive, 2006). Additionally, afforestation may be considered in land use, land use change and forestry (LULUCF) reports to offset national carbon emissions (Dyson *et al.*, 2009) as part of the commitment to the Kyoto protocol (UNFCCC, 1997). Due to the time scale involved in forestry, accurate forecasts of stand productivity are essential for effective management to provide these benefits (Vanclay, 1994).

1.1.2 Growth and yield models

Yield tables to forecast growth have been employed since the late 1700s, and have been continually refined and improved since then (Assmann, 1970). Historically, only forest yield (merchantable timber volume) was given in a table based on a measure of site productivity and the stand age using graphical techniques (Vuokila, 1965). However, as analytical methods and computing power have increased the complexity of yield tables has also increased (Vanclay, 1994). Modern forest growth models can broadly be split into three main approaches: empirical, process based, and hybrid (Weiskittel *et al.*, 2009). There are also a variety of scales which growth models may operate at. The ranges of approach and scale in forest growth modelling are shown in Figure 1.1.

Empirical models provide forecasts of stand growth based on statistical relationships between state variables describing a forest stand such as top height, basal area, and spacing (or stems per hectare) (Monserud, 2003). Ideally empirical models should provide a logical relationship between growth and yield in that the

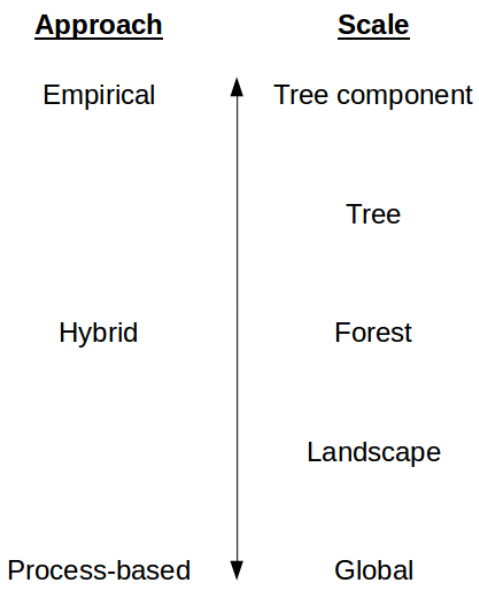

Figure 1.1: Forest growth model ranges in approach and scale

function for yield should equal the integral of a growth function (as per Clutter (1963)). Empirical models aim for parsimony, with relatively simple equations describing stand development through time (Vanclay, 1994).

Process based models attempt to represent the underlying physical and mechanistic processes of growth in forest stands (van Oijen *et al.*, 2005). Process based models have shown a recent increase in favour, as they have the potential to allow forecasting of forest stands under changes in climatic conditions (Coops and Waring, 2011). Process models usually represent a system at one level of hierarchy, which is important as a process considered mechanistically in a model at one level of hierarchy may be considered empirical at a higher level model (Mäkelä *et al.*, 2000). A consequence of trying to represent underlying processes mechanistically is an increase in model complexity and the number of parameters (Weiskittel *et al.*, 2009; Mason *et al.*, 2011). Such parameters may not be easily defined, introducing large uncertainty (Mäkelä *et al.*, 2000), thus limiting the utility of process based models to 'models for understanding' (Vanclay, 1994).

Hybrid models represent a combination of empirical and process based models. Hybrid models include both processes and empirical relationships, which may give the advantages of each modelling approach whilst minimising the disadvantages (Mäkelä *et al.*, 2000). For example, the Bridging model of Valentine and Mäkelä (2005) used a simple carbon balance growth model and fitted it empirically using commonly measured forest inventory variables. There are also examples such as Pérez-Cruzado and Muñoz Sáez (2011), where empirical models were used for parameterising process based models. Thus, process models which may not provide estimates of tree height, or basal area may be hybridised with empirical models to provide these values (Landsberg, 2003). It has been shown that this approach often increases the accuracy of model predictions over empirical growth models, whilst reducing the number of parameters required to be estimated (Woollons *et al.*, 1997; Pinjuv *et al.*, 2006; Weiskittel *et al.*, 2009).

A number of reviews exist of these different approaches to forest modelling. Most convey the idea that process models are underused in forest management (Mäkelä *et al.*, 2000; Landsberg, 2003), perhaps unsurprising given the authors backgrounds in process based modelling. However, this may be in response to the opinion that process models are unsuitable for management, a concept that is prevalent in earlier comparisons of empirical and process models (Sharpe and Rykiel, 1991; Mohren *et al.*, 1994). Korzukhin *et al.* (1996) provide a thorough review of a number of comparisons between empirical and process models, arguing that process based models are specifically advantageous in ecosystem management of forests, where management is aiming to maximise ecosystem services rather than timber production. Ideally, models should provide data to allow effective stand management in terms of both timber and ecosystem services. Hybrid models are cited to have the ability of providing these data (Weiskittel *et al.*, 2009), and appear to be the approach taken in a number of forest growth models over the last two decades (Mason *et al.*, 2011; Weiskittel *et al.*, 2009; Waterworth *et al.*, 2007;

Valentine and Mäkelä, 2005; Woollons *et al.*, 1997; Landsberg and Waring, 1997). Indeed, numerical comparisons of the three approaches have shown superior performance of hybrid models compared to both process and empirical models. All things considered, it is perhaps best to infer that all models sit somewhere in the spectrum between pure process and empirical models (Korzukhin *et al.*, 1996).

In addition to the approach taken to model a forest, the scale at which a model operates is also important (Vanclay, 1994). Forests may be modelled from the global scale down to the scale of roots, branches, and foliage. As with the issue of the choice of the modelling approach, each scale is appropriate for different uses. The smaller scale (tree component) models, are useful in providing estimates of wood properties. This can be observed in the timber quality models of Leban (2003) for Sitka spruce, or the stem form model of Valentine and Green (2012). Individual tree models such as TASS (Mitchell, 1975) and Prognosis (Stage, 1973), are well suited to modelling complex stands with mixtures of species and ages. Stand level predictions are usually applied to situations of even-aged monocultures: such is the case with Physiological Principles Predicting Growth (3PG) (Landsberg and Waring, 1997), and a number of dynamic stand level models (García, 2013; García *et al.*, 2011; García, 2010; Broad and Lynch, 2006; García and Ruiz, 2003). Larger scale models running at regional, national, or global scale tend to concentrate on the prediction of biomass development in forests (Vanclay, 1994) (for example the national carbon inventory model for the UK - CFLOW (Cannell and Dewar, 1995)), or are used in policy making (Wernsdörfer *et al.*, 2012).

It is also common to utilise smaller scale models within larger scale models to provide inputs: CFLOW utilises the yield tables of Edwards and Christie (1981) to provide stand estimates to the national scale; Houllier *et al.* (1995) uses a stand level growth model coupled with a timber quality model related to Leban (2003)

to provide stand level timber quality estimates; and SYLVER (Mitchell, 1988) uses a combination of smaller scale models (including TASS (Mitchell, 1975)) to predict stand level wood properties and timber quality in addition to standing yield.

Most production forest stands in the UK are even aged monocultures (Forestry Commission, 2003), therefore a stand level model is often most appropriate. When forests are measured in the UK it is most often at stand level and the additional variables that would need to either be measured (resulting in increased cost), or estimated (resulting in increased model uncertainty) limit the usefulness of a model at a smaller spatial scale such as at individual tree level. Forest managers are also used to the utilisation of stand level models, through the extensive use of yield tables (Edwards and Christie, 1981).

1.1.3 UK growth models

The UK (perhaps more specificially the Forestry Commission) mainly utilises the M1 growth model for predicting forest growth. Over recent years there has been greater interest in using more process based models such as 3PG (Xenakis *et al.*, 2008; Minunno *et al.*, 2010), as well as the MOSES (MOdelling Stand rESponse) model (Hasenauer, 1994) for predicting mixed-species and continuous cover forests. Nonetheless, it is the M1 which dominates forest forecasting.

The M1 yield model has its origin in the graphically derived, imperial unit yield tables of Hummel and Christie (1953). These were converted to metric units (Hamilton and Christie, 1971), before Edwards and Christie (1981) fitted polynomial equations to the yield curves to provide a numerically derived set of density-dependent yield tables. More recent development of the M1 model further updated the yield tables of Edwards and Christie (1981) to provide interpolated

values for any stands which are not given in the tables (Davies and Kerr, 2011), increasing the number of thinnings and initial planting densities over the original. It is available through the software package ForestYield (Forest Research, 2001). However, the M1 model is limited to certain initial planting densities and thinning regimes which limits the management scenarios that can be forecast. Additionally, there is no measure of uncertainty provided by the model. As the M1 model's workings are not published (and there is no plan to do so (Jenkins, 2009)) there is no way to investigate the uncertainty in the model further.

Despite the limited documentation and flexibility of the M1 model, it still provides the forest growth basis of a number of other models used by forest managers. For example, it is used with taper equations for timber assortment predictions (Fonweban *et al.*, 2011), to provide growth predictions in ForestGALES for wind risk prediction (Gardiner and Quine, 2000), and in land-use change carbon reporting (Morison *et al.*, 2011).

1.1.4 Uncertainty

As models are abstractions of reality, they cannot be considered to give exact answers and so a measure of uncertainty should be included in all model predictions. Effective forest management relies on knowledge of accuracy and precision of growth models (Kangas, 1999). Thus, in most cases uncertainty is taken to be a numerical estimate of the performance of a model. However, both qualitative and quantitative assessment is possible (Soares *et al.*, 1995; Vanclay and Skovsgaard, 1997). Indeed, Clutter (1963) states that models may be improved without data, "Through a detailed consideration of the biological implications that are inherent in the current system", while Rykiel (1996) suggests that complex models may not require comparison with measured data and may be simply put forward based on theory alone without experimentation.

Uncertainty may lie in the inputs to the model in the form of measurement error, within models in parameter covariance, or the structure of the model itself may be uncertain (McRoberts and Lessard, 2000). Assessment of model structure may be as, or even more important than the fit of an individual model (van Oijen *et al.*, 2013). Prisley and Mortimer (2004) identify that there is no single model evaluation that can be used in all cases. A clear definition of what is meant by uncertainty is important, and model-specific definitions are suggested to be of greatest use (Smith and Heath, 2001).

Uncertainty may be quantified in a number of ways. This is best achieved with data that is separate from the data used for model parameterisation (Vanclay, 1994), although resampling methods such as bootstrapping and cross-validation can be used in cases where it is not possible to save data (Vanclay and Skovsgaard, 1997). Linear regression of observations against model predictions (Mayer and Butler, 1993) may provide an initial insight into model fit, with R^2 indicating precision, and the regressions slope and intercept indicating accuracy. Modelling efficiency as defined by Soares *et al.* (1995) may provide a simple index of model fit based on the difference between observations and model predictions. Other approaches include modelling previously observed errors to estimate future error observations and producing a simplified (elementary) model that has a variance representative of the original model (e.g. Kangas (1999)). Another common approach to assessing uncertainty in growth models is to use Monte Carlo methods (e.g Fortin and DeBlois (2010); Kangas (1997)). In these methods, a given model is run repeatedly with random perturbations (scaled by parameter or other uncertainties) to produce a range of outputs representative of the uncertainty in the model. Monte Carlo methods may also be used to consider uncertainty throughout the parameterisation of a model.

1.1.5 Bayesian methods

Bayesian calibration makes use of Monte Carlo methods to focus on quantifying uncertainty in model parameterisation. In a Bayesian calibration, uncertainties are represented by probability density function (PDF)s (van Oijen *et al.*, 2005). Bayesian calibration may provide a number of advantages when used to assess model uncertainty. These are outlined by Patenaude *et al.* (2008):

- It allows for the use of observation data with varying uncertainties, such as remote sensing and ground based data
- It enables quantification of uncertainty for parameters and outputs
- It allows for improvement of PDFs when further information is obtained

Bayesian calibrations seem to have been predominantly deployed in the calibration of process based models, and have been used in a large number of forest models (Xenakis *et al.*, 2008; Patenaude *et al.*, 2008; van Oijen *et al.*, 2005; Radtke *et al.*, 2002; Green *et al.*, 2000). However, their use in empirical models is less prevalent: Li *et al.* (2011) used a Bayesian method to calibrate a site-index model, Radtke and Robinson (2006) used Bayesian melding: where PDF outputs of an empirical growth model are used to calculate likelihoods used in the estimation of uncertainty in a process model, Green *et al.* (1992) used Bayesian statistics to predict site specific values of yield models for Honduran Pine, and likewise Gertner (1984) used a sequential Bayesian procedure to reduce uncertainty in predicting local values for diameter increment models for Douglas fir. To date it appears that Bayesian methods have not been used to parameterise empirical stand growth models, and certainly not at the national scale for multiple species. While in the past Bayesian methods have been restricted by computational costs (both financial and temporal), this is now much less of an issue with reductions in

the cost of computing and more advanced Markov Chain Monte Carlo (MCMC) algorithms (van Oijen *et al.*, 2005). Examples of how Bayesian methods can be applied to parameterise forest growth models may encourage wider scale adoption.

The natural progression from a simple Bayesian calibration is to calibrate iteratively, as is the case in data assimilation. Again, such methods are more prevalent in process based modelling, for example studies looking at forest carbon dynamics (Gao *et al.*, 2011; Quaife *et al.*, 2008; Williams *et al.*, 2005). Data assimilation works on the premise that both models and observations contain uncertainties and analysis of both will provide reduced uncertainty compared to using observations or model predictions alone. State variables, parameters or both may be updated by assimilating observations using methods such as the Kalman filter (Chen *et al.*, 2008). More complex problems with large numbers of parameters can also be considered by using Markov Chain methods such as the Ensemble Kalman Filter (EnKF) (Evensen, 2003). Data assimilation has been used with some success in crop yield models, especially those utilising remote sensing data (De Wit and van Diepen, 2007; Guerif and Duke, 2000), however its use outside of process-based models seems to be limited again to improving localised predictions of yield models (Walters *et al.*, 1991). Despite the fact that both Bayesian calibration and EnKF use Markov Chain methods, there are no examples of using a Bayesian Calibration of a forest growth model to provide the parameter PDFs used in data assimilation with EnKF.

1.1.6 Inventory and remote sensing

In order to use statistical methods such as data assimilation, regular surveys such as forest inventories are necessary. For example in the USA, annual surveys measure up to a fifth of the national forest, resulting in national reports every 5 years (Schreuder *et al.*, 2004). The UK does not have such a strict regime for

the national forest inventory, with the last report in 2003 (Forestry Commission, 2003), and the next report expected in 2014. Unfortunately, the UK National Inventory appears to concentrate on forest area cover and species composition rather than changes in forest variables such as top height and basal area, which are important in predicting forest growth (Vanclay, 1994). While certain forest districts may have regular surveys of forest growth variables, no central database of inventories has been available for this study.

In the stead of regular (ground-based) surveys, remote sensing technology can be used to provide measurements of forest growth. In particular light detection and ranging (LiDAR) has been identified as having great potential in forest inventory (Evans *et al.*, 2006). Large areas of forest may be surveyed rapidly, with attributes such as top height, stem number, and canopy dimensions as products (Suarez *et al.*, 2005).

Aerial LiDAR data has provided accurate estimates of top height, with errors less than 2 meters (Balzter *et al.*, 2007). Basal area is not directly measurable with non-terrestrial remote sensing technology. It has been estimated using linear equations that link crown diameter and height as estimated from LiDAR data with reasonable accuracy and precision ($R^2 = 0.87$) (Popescu, 2007; Popescu *et al.*, 2004). The only remote sensing technology for measuring basal area is terrestrial LiDAR. Although accuracy has in the past been comparable to allometry based estimates ($R^2 = 0.85$ compared to ground measures (Hopkinson and Chasmer, 2004)), more recent studies have reduced error to an average of 1.8 cm in individual tree diameter at breast-height (dbh) measures (Maas *et al.*, 2008). However, terrestrial LiDAR data is more time intensive to collect than aerial LiDAR data and is not so readily available. Number of stems may be derived from aerial LiDAR data by identifying local high points, which are assumed the tops of trees. The local area may either be defined using variable 'window' sizes and shapes (Popescu *et al.*, 2004), determined by a-priori knowledge of height-crown

diameter relationships, or by fitting wavelet functions with similar shape to tree crowns to the shape of the LiDAR surface models (Falkowski *et al.*, 2006).

Given the current innovation in LiDAR forest survey techniques, one might expect LiDAR data to have been used in data assimilation applications. Instead, it seems that the only forest growth model driven by LiDAR inputs to date is that of Härkönen *et al.* (2013), where LiDAR was used in the stead of ground based measurements in the parameterisation of a process-based model.

1.2 Objectives and overview

The broad aim of this work is to investigate methods for estimating forest growth in the UK and reduce the uncertainty in forest growth predictions. Reducing uncertainty in forest growth predictions not only provides better information for forest managers to decide on management and harvesting routines, but also allows for the reduction of uncertainty in the estimation of forest carbon stocks, wind risk, and timber quality.

First, in Chapter 2 two exisiting models for UK forest growth (The existing yield tables of Edwards and Christie (1981), and the 3PGN model of Xenakis *et al.* (2008)) are compared with a Stand Level Dynamic Growth (SLeDG) model (based on the work of García *et al.* (2011)) that has not been applied before in the UK. Scots pine is modelled over the hypothetical productivity ranges in the UK by all three models. All three models are demonstrated to be capable of producing similar forecasts. However, the strengths and weaknesses of the models are also considered to provide insight for future applications.

Then in Chapter 3 I present a Bayesian calibration of the SLeDG style model for both Sitka spruce and Scots pine across the UK. It is the first Bayesian calibration

of a stand level dynamic forest growth model. An innovative Markov Chain method called the Differential Evolution Markov Chain with snooker updater is used to reduce the computational expense of the calibration. Methods of including local productivity estimates are compared using Bayesian model comparison. The result is a set of parameter probability distributions for both species, as well as a framework for the parameterisation of other species in the future.

Chapter 4 then takes the probability distributions provided in Chapter 3 and uses them in concert with a time series of LiDAR remote sensing observations to perform data assimilation. This is achieved with an implementation of the Ensemble Kalman Filter (Evensen, 2003) and attempts to reduce uncertainty in the SLeDG model predictions further by incorporating regular observational data.

Finally, Chapter 5 brings together the findings from previous chapters and discusses areas for further investigation. The wider implications of this research are also addressed.

Chapter 2

A comparison of models for quantifying growth and standing carbon in UK Scots pine forests

J. Lonsdale[1,*], G. Xenakis[2], M. Mencuccini[1,3], M. Perks[2]

[1]School of Geosciences, University of Edinburgh, Edinburgh, EH9 3JN, UK

[2]Forest Research, NRS, Roslin, Midlothian, EH25 9SY, UK

[3]ICREA at CREAF, Cerdanyola del Valles, Barcelona, Spain

(Submitted to *iForest*)

Abstract

Scots pine is the most abundant native conifer in the UK. A stand level dynamic growth (SLeDG) model is parameterised for British Scots pine stands for the first time. This model predicts stand dynamics annually based on their current state, and allows for changes in forest management. Stand growth and carbon storage predictions using this model were compared with those of the yield look-up package ForestYield, and a process-based model (3PGN). Predictions were compared graphically over an 100 year rotation and strengths and weaknesses of each were considered. The SLeDG parameterisation provided forecasts of Scots pine growth with percentage mean absolute difference between model and observations $< 12\%$ for all state variables. The model comparison showed that similar outputs were predicted by all three models, with the greatest difference between models occuring in the predictions of volume and biomass in unthinned stands. Future advances in data availability and computing power should allow for greater use of process-based models, but in the interim more flexible dynamic based growth models may be more useful than static yield tables for providing predictions which extend to non-standard management prescriptions and estimates of early growth and yield.

2.1 Introduction

The combination of both spatial scale and rotation length of forest stands means that models of forest growth are essential for sustainable management (Blanco *et al.*, 2008). Historically, this has been achieved using yield models which use empirical relations between state variables such as top height, basal area, and number of stems to forecast stand development and timber volume production (Vanclay, 1994). For example, in the UK there is widespread use of the yield tables of Edwards and Christie (1981) provided through a lookup package ForestYield. Increased emphasis on providing a multi-function forest resource (Nijnik *et al.*, 2007) has meant that such models have had to be applied to activities such as carbon storage reporting (Dyson *et al.*, 2009). However, forest managers focusing on multi-function management are in turn more likely to deviate from management regimes aimed only at maximising timber production. Another shortcoming of such yield tables is that they fail to be linked causally to the drivers of productivity such as climate and nutrient availability, and are unable to account for changes in these drivers as might be expected in a changing climate (Monserud, 2003). A shift to more flexible forest models is appropriate to accommodate changes in environment or management objectives.

Hybrid models combine both empirical and process based modelling approaches: using simple mathematical relationships between stand variables, and representations of the underlying ecophysiological processes in stand development respectively. Through the combination, shortcomings of the empirical and process-based approaches may be ameliorated (Landsberg, 2003; Monserud, 2003), providing both traditional outputs for forest managers as well as estimates of carbon sequestration, whilst reducing the uncertainty in model outputs that occurs in complex process modelling (Valentine and Mäkelä, 2005). Additionally, prediction precision may be improved (Pinjuv *et al.*, 2006).

A number of hybrid models have been applied for varied species and locations globally (e.g. Mason *et al.* (2011); Weiskittel *et al.* (2007); Valentine and Mäkelä (2005)). Perhaps the most widely applied hybrid model is Physiological Principles Predicting Growth (3PG) developed by Landsberg and Waring (1997). It uses physiological principles to predict forest growth, combined with empirical relationships to output stand variables such as height and basal area. Thus model outputs can be used by forest managers to estimate timber production as well as estimates of carbon fixation. The model works in three stages: derivation of primary production, partitioning the production to above and below ground portions, and derivation of output variables (Landsberg *et al.*, 2003). It has been parameterised successfully for a number of species including: eucalyptus (*Eucalyptus* spp.) in Australia (Sands and Landsberg, 2001), Brazil (Almeida *et al.*, 2010), Spain (Pérez-Cruzado and Muñoz Sáez, 2011) and Portugal (Minunno *et al.*, 2012); ponderosa pine (*Pinus ponderosa* Douglas ex C.Lawson) and Douglas fir (*Pseudotsuga menziesii* (Mirb.) Franco) in the Pacific Northwest (Swenson *et al.*, 2005), and in the UK for Scots pine (*Pinus sylvestris* L.)(Xenakis, 2007) and Sitka spruce (*Picea sitchensis* (Bong.) Carr.) (Minunno *et al.*, 2010). However, while 3PG has the potential to be used over large areas where it has not been calibrated (Almeida *et al.*, 2010), it still requires a large number of parameters to be measured or estimated (both climatic and in the stand). This may increase both model uncertainty, especially in cases with limited data availability, and the cost of parameterisation.

Another class of models which can have elements of flexibility in the sense described above are dynamic yield models. Dynamic yield models allow forecasting of a stand based on its current state, as measured by a number of state variables (such as top height, basal area, and number of stems per hectare). Changes in a state variable are a function of only the current state of the stand. Thus variation in forest management strategies can easily be modelled by adjusting state

variables accordingly. For example, a thinning may be modelled by reducing the number of stems and the basal area in the state vector, creating an adjusted state vector. The trajectory of this adjusted state vector is then forecast. This would not be possible with a static yield model, where only predetermined points for thinnings can be simulated.

A number of Stand Level Dynamic Growth (SLeDG) models have been developed for a variety of species based on the initial work of García (1979). It should be noted that while other models may be dynamic and predict forest stands, here we specifically refer to SLeDG models as those based on García (1979). Previous example include models for eucalypts (*Eucalyptus globulus* Labill.) in Spain (García and Ruiz, 2003), Sitka spruce in Ireland (Broad and Lynch, 2006), interior spruce (a mix of white spruce (*Picea glauca* [Moench] Voss), Engelmann spruce (*Picea engelmannii* Parry) and their hybrids) in British Columbia (García, 2010), loblolly pine (*Pinus taeda* L.) in the Piedmont region of the USA (García *et al.*, 2011), and trembling aspen (*Populus tremuloides* Michx.) in Western Canada (García, 2013). This approach has an advantage in that SLeDG models may be parameterised providing acceptable extrapolations with relatively small permanent sample plot (PSP) datasets (García, 2010). This is especially useful as the UK has a robust but not particularly extensive network of PSPs (Scots pine $n = 51$ in Scotland). Changes in stand-level variables are predicted with biologically consistent differential equations. Recent versions of the model have moved towards more of a hybrid style, including variables which account for reduction of productivity following thinning or topping, in turn reducing the stand's photosynthetic (and nutrient capture) apparatus (García *et al.*, 2011). It has been suggested that the model may allow for estimating the root, leaf, and branch biomass of stands (García *et al.*, 2011), thus providing both timber growth estimates, and a standing biomass estimate for forests. It is also suggested that the model productivity may be modulated by climate and nutrient parameters,

allowing for predictions in a changing climate (García *et al.*, 2011). However, neither the standing carbon nor climate change predictions have been tested yet. Additionally, unlike 3PG there has been no work on integrating the model with routines of soil carbon dynamics (Xenakis *et al.*, 2008), which are an important component of the forest carbon cycle (Jandl *et al.*, 2007).

While there can be no 'perfect model', certain models will lend themselves better than others to certain tasks. Here we do not aim to determine a perfect model, but instead compare model utility for different tasks. This paper has two objectives. Firstly, we introduce the use of the SLeDG approach in UK forests. The model is described and parameterized for Scots pine (*Pinus sylvestris* L.). Scots pine is the most abundant native conifer in the UK, and the second most abundant overall species - occupying over 17% of the UK forest area (Forestry Commission, 2011). With current forest strategy requiring afforestation with native species, Scots pine's importance in UK forestry looks set to increase (Woodland Expansion Advisory Group, 2012). Timber outputs, as well as standing carbon outputs are estimated and reported for the first time with a SLeDG model.

Secondly, forecasts of forest growth and standing carbon estimates of the SLeDG model are compared with those of the ForestYield package and the 3PGN model. Although versions of 3PG have previously been compared with other growth models (Weiskittel *et al.*, 2007; Pinjuv *et al.*, 2006), the ForestYield model has not previously been compared to alternative modelling methods for forest carbon accounting. This, therefore, allows for a comparison of the outputs of these forest growth models, as well as identifying the potential for improving the current methodology for stand level forest growth and carbon reporting estimations.

2.2 Methods

2.2.1 Data

The data for the parameterisation of the models were provided by the Forest Research Forest Mensuration, Modelling and Forecasting Group, consisting of 51 PSPs across Scotland. The measurement statistics taken from these PSPs are summarised by age group in Table 2.1. These plots were planted with Scots pine between 1878 and 1965. Measurements were taken from stands ranging in age between 14 and 125 years, with at least two mensurational surveys per plot. Plots varied in their management with a variety of thinnings undertaken. Thirteen plots were unthinned controls. Four soil types were selected by Ecological Site Classification (Pyatt *et al.*, 2001): podzol, brown earth, sand and podzol/brown earth mixture; and 45 soil sample plots were collected as part of an earlier study (Xenakis, 2007). The elevation of both PSP and soil plots ranged from 3 to 364 m a.s.l., and were located between latitude 56°63.1' and 57°69.3'N and longitude 5°19.7' and 3°07.0'W. Tree volume measurements were provided by the Forestry Commission's tree pulling database, which contains measurements from 17 stands of Scots pine across the UK aged between 27 and 44 years.

2.2.2 Model definitions

SLeDG

This version of the SLeDG model is an adaptation of the model by García *et al.* (2011), which is an evolution of the model first suggested by García (1979). This family of models uses a state-space approach to forecast the stand development based on a description of stands using four state variables: top height, number

Table 2.1: Summary of individual measurements from the 51 permanent sample plots by age group.

	Mean	SD	Minimum	1st Quartile	Median	3rd Quartile	Maximum
Young plots (Age <40 years, $n = 88$)							
Age	31.2	6.42	14.0	28.0	32.0	37.0	39.0
Top height (m)	12.6	2.11	6.80	11.1	12.6	14.1	16.6
Stems ha^{-1}	2059	1150	608	1212	1755	2606	6125
Basal area (m^2)	31.4	8.26	16.9	26.5	29.9	34.9	53.5
Volume (m^3)	168	65.2	45.9	118	175	209	290
Yield Class (m^{3}ha$^-$1yr$^-$1)	10.2	1.68	7.0	9.0	10.0	11.0	14.0
Initial Spacing (m)	1.50	0.48	0.90	1.20	1.40	1.80	2.40
Middle-aged plots (40 $\geq$ Age <70 years, $n = 140$)							
Age	53.1	7.75	40.0	46.0	51.0	60.0	69.0
Top height (m)	18.1	2.48	12.0	16.5	18.3	19.8	23.9
Stems ha$^-$1	1196	792	792	561	934	1703	3948
Basal area (m^2)	40.1	9.64	23.7	32.1	37.75	49.0	63.9
Volume (m^3)	304	78.5	165	245	295	354	553
Yield Class (m^{3}ha$^-$1yr$^-$1)	9.67	1.66	4.0	9.0	10.0	10.0	14.0
Initial Spacing (m)	1.45	0.47	0.90	1.20	1.40	1.80	2.40
Old plots (Age $\geq$ 70 years, $n = 38$)							
Age	87.37	11.8	71.0	79.0	87.0	94.8	115
Top height (m)	21.26	4.12	13.0	19.3	21.7	24.2	27.9
Stems ha$^-$1	631	337	259	368	496	787	1473
Basal area (m^2)	43.9	13.2	25.1	32.1	41.0	55.7	68.4
Volume (m^3)	397	144	173	294	385	502	487
Yield Class (m^{3}ha^{-1}yr^{-1})	8.0	2.27	4.0	8.0	8.0	9.0	12.0
Initial Spacing (m)	1.02	0.22	0.90	0.90	0.90	0.90	1.40

of stems per hectare, tubular volume (the product of basal area and top height), and occupancy. Occupancy is analogous to an interception efficiency: an index of the rate of gross photosynthesis versus a maximum potential rate, where a stand has enough leaves to intercept all photosynthetically active radiation (PAR) (Monteith, 1972).

Changes in the state variables through time are represented by differential functions. The model variables are listed in Table 2.2. The SLeDG model was parameterised for Scots pine in three stages similar to García *et al.* (2011): height (a site index model), mortality, and basal area with occupancy. Additionally, model outputs for merchantable volume were also parameterised. The biomass expansion factors (BEF) and root:shoot ratios of Levy *et al.* (2004) were used to provide standing biomass outputs based on the merchantable volume. Details of the model structure and parameterisation are available in Appendix A.

Table 2.2: SLeDG model variables and units

Variable	Units	Definition
H	m	Top height
N	stems ha^{-1}	Number of stems (per hectare)
W	m^3 ha^{-1}	Tubular volume; product of B and H
Ω	-	Occupancy
H_s	m	Site index (Index age 50 years)
B	m^2 ha^{-1}	Basal area
R	-	Relative closure
V	m^3 ha^{-1}	Merchantable volume (stem to 7cm dia.)

Model statistics were calculated to provide an initial benchmark of the model fit to the data. As the dataset was small the statistics were only calculated with the PSP data used in model calibration, i.e. no independent data were used. Therefore a bootstrap analysis was used to provide a validation of the model as suggested by Vanclay and Skovsgaard (1997). One thousand bootstraps were run for each part of the model parameterisation resulting in confidence intervals for

calibrated parameters. Variance inflation factors were calculated for each part of the model to assess multicollinearity among state variables. Mean absolute difference; percent mean absolute difference; and the modelling efficiency were also calculated. Mean absolute difference is simply the average of all deviations of PSP data points from the model, which can also be expressed as a percentage. Modelling efficiency is described by Vanclay and Skovsgaard (1997). It provides a statistic analogous to R^2, whereby 1.00 represents 'perfect' fit between model and measured data, and 0.00 represents a poor fit (negative values indicate very poor fit).

3PGN

The 3PGN model is described in Xenakis *et al.* (2008) as a process based model structure coupling the 3PG model (Landsberg and Waring, 1997) with the introductory soil carbon balance model (ICBM) (Andrén and Kätterer, 1997).

The 3PG model can be broadly separated into three parts. The first part deals with the derivation of the primary production: Gross primary production is calculated using photosynthetically active radiation. The photosynthetically active radiation is estimated as half of incoming shortwave radiation (Landsberg and Waring, 1997), or may be estimated using empirical relationships based on monthly maximum and minimum temperatures in the absence of direct radiation measurements, as per Coops and Waring (2001). Photosynthetically active radiation is adjusted to available photosynthetically active radiation, scaled by a function of Leaf Area Index. Dimensionless modifiers for vapour pressure deficit, soil water, temperature and age determine the utilisable available photosynthetically active radiation. Gross primary production is calculated by multiplying the utilisable available photosynthetically active radiation by an apparent quantum efficiency which is usually assigned the value of 0.03 mol C

(mol photon)$^{-1}$ (cf. review of published literature by Landsberg and Waring (1997)). Finally, gross primary production is simply scaled by 0.48 to give net primary production.

The second part determines the partitioning of the production to above and below ground portions (Landsberg *et al.*, 2003). The production may be allocated to either the roots, stem, or foliage of a stand. Changes in biomass in the roots, stem, and foliage are therefore the balance of the production allocated to each minus root dieback, stem mortality, and litterfall. The below ground portion of carbon allocation (η_r) is determined by a fertility rating (a percentage site productivity rating), water content, and stand age. The above ground allocation of carbon is divided between stem and foliage using a ratio determined by basal area.

The third part produces outputs from the model such as stand volume, stem number, and basal area which may be of use to managers. Stem number change (mortality) is estimated by a version of the -3/2 self-thinning rule (Yoda, 1963). Increases in stem mass (dw_s) are used to calculate increases in stem diameter, and an allometric relationship is used to scale this to stand volume for output.

The Introductory Soil Carbon Balance Model (ICBM) (Andrén and Kätterer, 1997) is incorporated by including three carbon and three nitrogen pools for soil carbon. Each pool has different rates of decomposition, which may be further modulated by environmental conditions. Litterfall, root turnover and natural mortality calculated by 3PG are used as inputs to the soil carbon pools.

A previous calibration of 3PGN parameters for Scots pine (Xenakis *et al.*, 2008) was used for this study. This used the same 51 plot dataset as the SLeDG parameterisation. The calibration was performed using an application of the Bayesian theorem with the implementation of a Monte Carlo Markov

Chain. Calibration was performed for all plots and a mean parameter vector was extracted. For more details see Xenakis *et al.* (2008).

Average climatic and site conditions for each yield class (YC) were estimated based on mean climate for each yield class and a mean soil type estimated from 45 soil samples collected by Xenakis *et al.* (2012) from across Scotland. Solar radiation was estimated from temperature, humidity and site information using the algorithm given by Xenakis *et al.* (2008).

Thinning in 3PGN is represented as a fraction of the biomass of foliage, wood and root of the mean tree removed in each intervention. The fractions removed for each yield class in thinnings were based on outputs from the tables of Edwards and Christie (1981). The biomass of the three structural pools before and after thinnings were calculated using the allometric equations developed by Xenakis *et al.* (2012). Thus the ratio of the biomass removed from thinnings to the biomass before thinnings was estimated. Model outputs were calculated with and without thinnings.

ForestYield

ForestYield (Forest Research, 2001) is a computerised version of the yield tables of Edwards and Christie (1981). It outputs top height, basal area, stem number, and volume for stands of given planting density, site quality (YC), and thinning regime. The equations used to calculate the yield tables are not utilised in ForestYield. Instead, it includes the data from the yield tables, and points in between table cells are estimated by linear interpolation. Stands that do not match these predetermined YCs, planting, and thinning regimes, are estimated by using the closest regime. To estimate stand whole tree biomass, ForestYield outputs were expanded with the biomass expansion factors estimates of Levy *et al.*

(2004) as is performed in the land use, land use change and forestry (LULUCF) reporting in the UK (Dyson *et al.*, 2009), and in a similar manner to the SLeDG model.

2.2.3 Model comparison and initiation

Such different models are not easily compared statistically. Previous model comparisons have looked at errors when models have been validated against common data (Weiskittel *et al.*, 2007; Pinjuv *et al.*, 2006). However, as all available Scots pine data were utilised in parameterisation of SLeDG and 3PGN, a similar comparison was not possible.

Instead, all three models were compared by looking at how each predicts growth over the typical range of productivity classes (defined by YC) for one rotation of one hundred years. These represented hypothetical stands, rather than looking at specific stands which have been measured.

In order to compare the models' predictions of stands through time, a standard of site quality is needed. ForestYield utilises yield class (YC) as its measure of site quality, however 3PGN and SLeDG require a conversion between their site quality measures and YC. In this study, even YCs ranging between 4 and 14 $m^3ha^{-1}yr^{-1}$ were used. The YC is the estimated mean annual increment of a stand of trees which occurs at the intersection between the idealized curves for mean annual increment and current annual increment plotted against stand age (Edwards and Christie, 1981).

In the SLeDG model, site index (H_s) is used as a measure of site quality. The relationship between YC and H_s is given as:

$$\mathrm{YC} = \alpha_1 + \alpha_2 H_s \tag{2.1}$$

With a reference age of 50: $\alpha_1 = -5.507$, and $\alpha_2 = 0.867$ (RMSE=0.428, R^2=0.981), for Scots pine (Fonweban, 2012, pers. comm.).

In 3PGN, site quality is represented by the fertility rating. The link between 3PG and ICBM, which calculated the fertility rating parameter from ICBM's output, was removed and so fertility rating was re-introduced as a parameter (cf. Minunno *et al.* (2010)).

The model was run using the parameter set of Xenakis *et al.* (2008) (fit to the same 51 PSPs) for each soil type. The fertility rating parameter was calibrated manually to achieve the closest fit of predicted against observed diameter at breast-height (dbh). The calibrated values of fertility rating were assigned to the different yield classes based on mean YC for a given soil type. For two YC (8 & 10) values for fertility rating were interpolated between the fitted fertility ratings due to lack of stand data.

Initial planting density was fixed at 5000 stems ha^{-1}; a previous average for Scots pine planting in the UK (Forestry Commission, *Pers.Comm.*) and previously used in 3PGN forecasts by Xenakis (2007). It should be noted however that current grant applications for Scots pine forest establishment in Scotland requires a density of 3000 stems ha^{-1} at establishment (Scottish Executive, 2012). Assuming a constant initial planting density across modelling platforms provides a common starting point for forecasting hypothetical stand growth.

Differences in outputs of top height, basal area, stem numbers, volume, and whole tree biomass were compared graphically over the range of productivity commonly seen in the UK: between YC 4 $m^3ha^{-1}yr^{-1}$ and 14 $m^3ha^{-1}yr^{-1}$. Similarities and differences in how the models forecast growth were considered and potential

causes discussed. Additionally, the requirements of the models were compared: what parameters and variables are required in order to run a simulation of a stand, and how that relates to model purpose and utility.

2.3 Results

2.3.1 SLeDG parameterisation

The fitted parameters, their error, and bootstrap derived confidence intervals for the height-age and mortality sub-models are given in Table 2.3. The fit of these sub-models to the PSP data is shown in Figures 2.1 & 2.2.

Figure 2.1: Model-data comparison figure for top height growth in Scots pine permanent sample plots . SLeDG modelled top height growth (dashed lines) for even site indices 10 - 22 (age 50) based on Scots pine PSP (permanent sample plot) data.

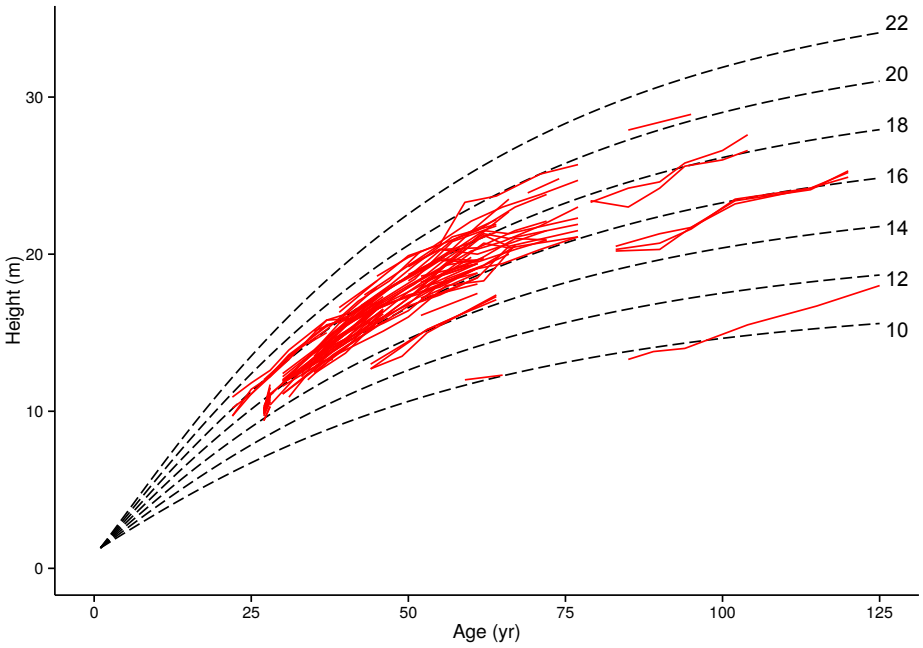

In the parameterisation for basal area and occupancy, the values for loblolly pine relating to occupancy and relative size of mortality loss ($b_9 = 0.4$, $b_{10} = 2.4$,

Figure 2.2: SLeDG model-data comparison figure for natural mortality in Scots pine permanent sample plots . Mortality of stands as top height increases for different initial planting densities. PSP (permanent sample plot) data is shown with the fitted model (dashed lines).

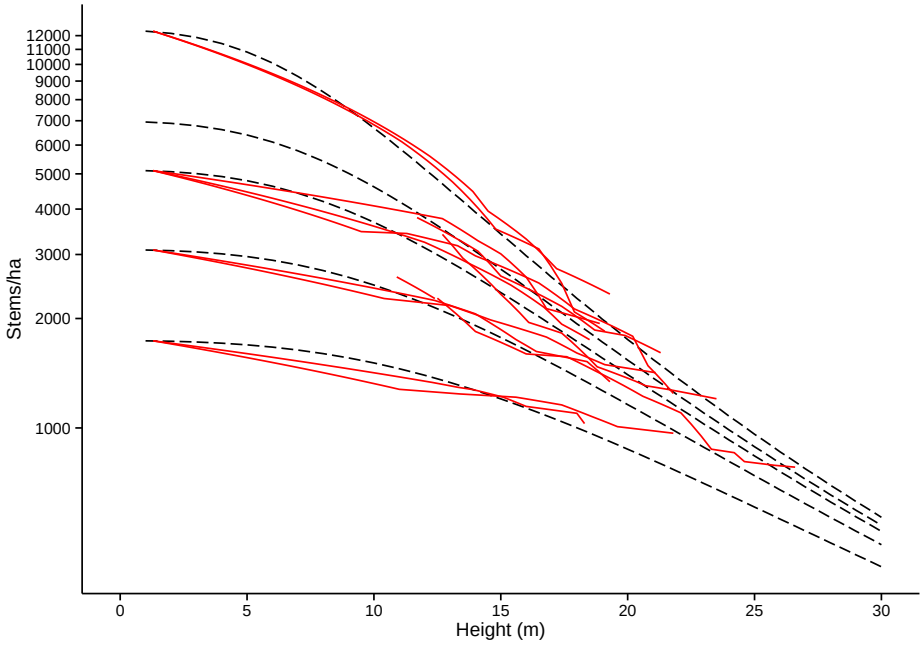

Figure 2.3: Error in basal area predictions using estimated parameters for SLeDG. Dashed line indicates a linear model fitted to the residuals.

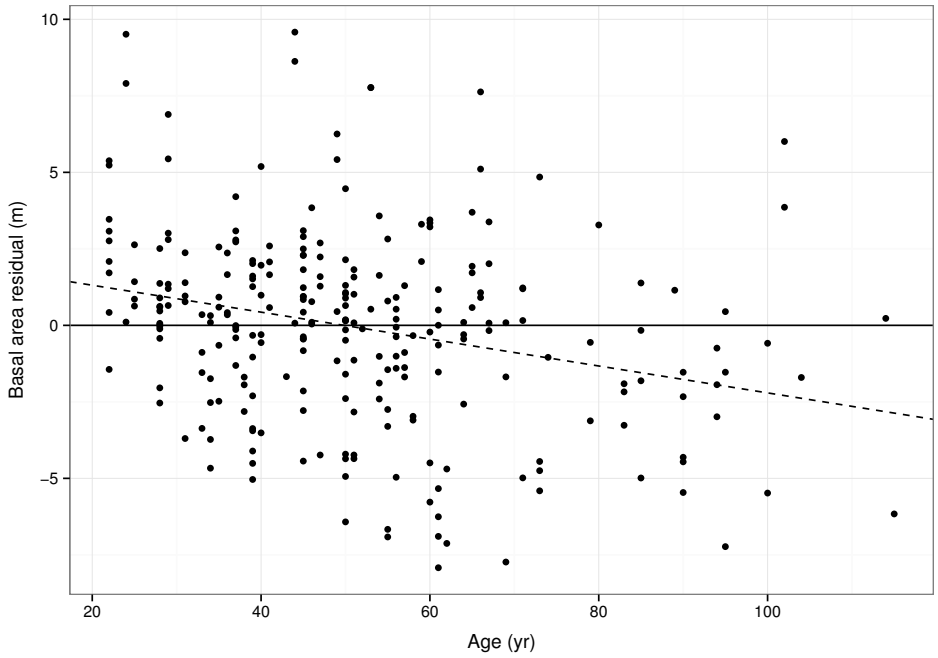

$b_{12} = 2.778 \times 10^4$) (García *et al.*, 2011) performed well due to the similarities in shade tolerance and thus self thinning between the pine species. Thus values for b_9, b_{10} and b_{12} were fixed in the parameterisations, as preliminary investigations showed no statistical improvement when these parameters were allowed to vary. These fixed values and the other estimated values for all parameters relating to basal area and occupancy are given in Table 2.3. The errors are estimated from the Hessian calculated in the parameterisation, and confidence intervals are based on the bootstrap analysis.

The errors in the predicted value of basal area (B) over the range of ages is given in Fig. 2.3. The linear model fitted to the errors has a slope significantly different from zero (P = 2.13 $\times 10^{-4}$), indicating consistent overestimation in the first 50 years and underestimation in years after.

The estimates of the coefficients from a linear regression of merchantable volume (V) on tubular volume (W) using aggregated data from the tree pulling database were $\beta_v = 0.394$ and $c_v = 11.01$. The regression had a R^2 value of 0.978.

The model for projecting forest stands can be summarised by the following equations:

$$\frac{dH}{dt} = 0.0232\left[(q/H)^{0.859} - H\right] \tag{2.2a}$$

$$\frac{dN}{dH} = 7.57 \times 10^{-7} H^{1.83} N^{1.86} \tag{2.2b}$$

$$\frac{d\Omega}{dH} = 0.105 H^{1.04}(1 - \Omega) \tag{2.2c}$$

$$\frac{dW}{dH} = 0.249 \Omega H^{1.04} N^{0.4} - 0.4 \frac{W}{N}\frac{dN}{dH} \tag{2.2d}$$

Where H, N, W, and Ω are top height, number of stems per hectare, product of

basal area and top height, and occupancy respectively. The local (site specific) productivity is defined by the parameter q which can be derrived from the site index (see Appendix A). The latter three equations may be multiplied by the first equation to express the variablility in N, Ω, and W in terms of dt instead of dH and (2.2b) may be substituted in to (2.2d) for a more standard form.

All variance inflation factors in the model were less than 5 with the exception of top height in the stem wood accumulation function (Equation 2.2d) which had a value of 7.40. This value is still below the threshold value of 10 suggested as a sign of high collinearity by Kutner *et al.* (2004). The statistics of model fit for SLeDG are given in Table 2.4 for H, N, and B. As Ω is not observable, no model fit is given. Overall there is high modelling efficiency for all three variables, indicating a good agreement between observed and estimated values. Although the lowest modelling efficiency is seen in B, it has a lower percentage mean absolute difference than N. Predictions of H show the best agreement between observed and estimated values, with high modelling efficiency and the smallest percentage mean absolute difference.

2.3.2 3PGN Calibration

All of the parameters bar one used in this instance for 3PGN can be found in the calibration for Scots pine by Xenakis *et al.* (2008) and Xenakis (2007). The only difference here is in the values of fertility rating. The range of fertility rating for given YC (and associated soil type) is given in Table 2.5. The proportion of explained variance by the regression of measured versus predicted dbh was always greater than 0.7 for all YCs which had direct measurements of dbh.

Table 2.3: Stand Level Dynamic Growth (SLeDG) model parameter estimates, errors, and confidence intervals calculated from bootstrap analysis for Scots pine.

Parameter	Value	Standard Error	95% Confidence Interval	Definition
b_1	q	-	-	Height parameters
b_2	0.0200	1.31×10^{-3}	0.0121 — 0.0227	
b_3	0.859	2.98×10^{-2}	0.804 — 0.901	
q	-	-	-	Site quality measure
b_4	7.57×10^{-7}	4.61×10^{-7}	-1.43×10^{-6}—1.46×10^{-4}	Mortality parameters
b_5	1.83	0.32	0.151 — 2.36	
b_6	1.86	0.17	1.13 — 2.34	
b_7	0.249	0.464	0.142 — 0.274	Gross increment parameters
b_8	1.04	0.72	0.965 — 1.24	
b_9	0.4†	-	-	
b_{10}	2.4†	-	-	Occupancy exponent
b_{11}	0.105	0.368	-2.79 — 0.943	Occupancy scalar
b_{12}	2.778×10^4†	-	-	Planting density for full closure at planting
β_v	0.394	2.84×10^{-3}	-	Merchantable volume scalar
c_v	11.0	1.94	-	Merchantable volume intercept

†Indicates fixed parameters (that were not adjusted in parameterisation).

Table 2.4: Statistical measures of model fit in calibration against permanent sample plot (PSP) data

Variable	Top Height (m)	Stems ha^{-1}	Basal area (m^2)
Mean absolute difference	0.3521	130.1	2.551
% Mean absolute difference	2.128	11.83	7.317
Modelling efficiency	0.9875	0.9334	0.9092

Table 2.5: Fertility rating values for given soils and associated yield class (YC) based on regression between modelled and observed diameter at breast-height (dbh)

Soil type	YC	Fertility rating	Adjusted R^2
Podzol	4	0.100	0.898
Regosol	6	0.265	0.747
Gley	8	0.300 ‡	-
Humic gley	10	0.335 ‡	-
Podzol/Brown earth	12	0.370	0.928
Brown earth	14	0.550	0.971

‡Indicates interpolated values

Model predictions

The variable output for unthinned and thinned stands for all three models can be seen in Figure 2.4. The range of productivity between YC 4 - 14 is represented for each model by a different coloured ribbon. As ForestYield predictions only begin at age 40 years for YC 4 stands, the ribbon representing ForestYield was truncated. Height and average dbh show similar trajectories over the range of productivities for all three models, in both thinned and unthinned stands.

There was no early mortality predicted by 3PGN until the age of 25 years or even later in less productive stands. As previously noted, ForestYield does not produce any mortality predictions before 40 years in YC 4. ForestYield does produce mortality predictions for higher productivity stands younger than 40 years, though the earliest mortality is predicted at 25 years in YC 14 (Edwards and Christie, 1981). Only SLeDG was able to predict early stand mortality (Figs. 2.4c & h). In the unthinned stand simulation, 3PGN and ForestYield

show reasonable agreement, with less than 1000 stems difference between most and least productive stands. The SLeDG model predicts a much wider difference in stem numbers between most and least productive YCs. When the thinned stands are simulated, there is better agreement between models (Fig. 2.4h).

Although 3PGN predicts on average a greater volume than SLeDG over the period of an unthinned rotation (Fig 2.4d), it also predicts the lowest biomass of the three models, with the exception of the lowest productivity stands predicted by ForestYield (Fig. 2.4e). Although 3PGN predicts much higher volume growth than SLeDG for thinned stands, its biomass prediction follows a different trajectory, with either lower or comparable biomass relative to SLeDG. ForestYield shows the largest difference between highest and lowest YC in its prediction of volume and biomass. It also predicts a much greater volume and biomass in higher yield class stands than both SLeDG and 3PGN.

2.4 Discussion and conclusions

2.4.1 SLeDG parameterisation

The SLeDG model as summarised by Equation (2.2) provides an alternative method for yield prediction in British stands of Scots pine. Although parameterised with a small dataset, the model provides reasonable forecasts of Scots pine growth throughout the range of productivity observed in the UK.

Simultaneous parameter estimation has previously been identified as the best way to minimize model errors (Soares *et al.*, 1995; Vanclay and Skovsgaard, 1997). The three stage fitting of SLeDG could therefore introduce additional error compared to a simultaneous fitting operation. The next chapter investigates the use of

Figure 2.4: Plots of SLeDG, 3PGN, and ForestYield thinned and unthinned stand predictions through time. Ribbons indicate range of productivity equivalent to YC 4 to 14. DBH denotes diameter at breast-height

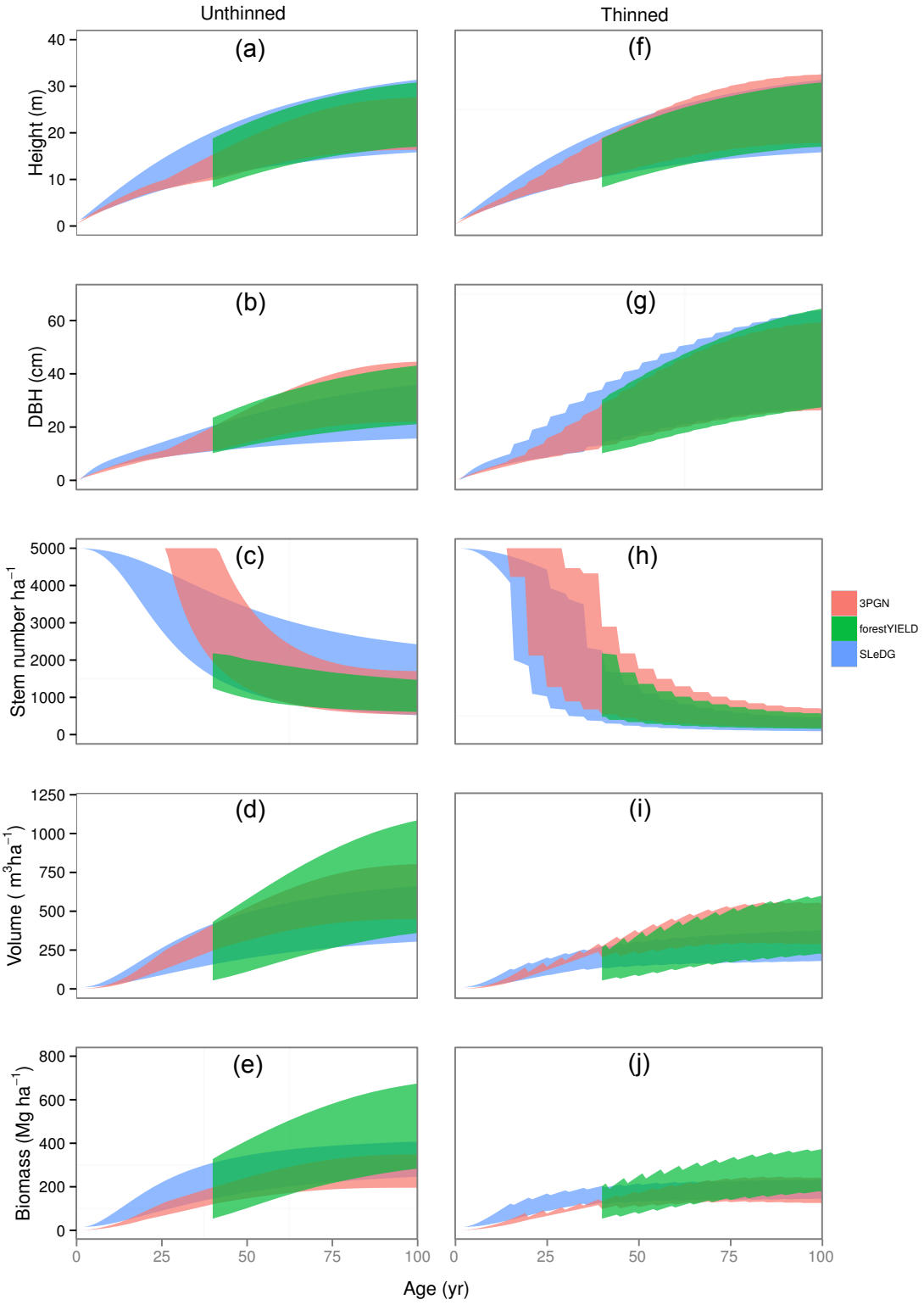

Bayesian methods of simultaneous parameter estimation, which were not used here in order that the author could become familiar with how SLeDG style models had previously been parameterised. However, by using the three stage fitting procedure, height growth and then mortality is modelled as best as possible before modelling basal area. In a simultaneous estimation the accuracy of basal area would be increased at the cost of reducing accuracy in top height and mortality (assuming simultaneous fitting would weight the accuracy of all variables equally). As the SLeDG model uses an assumption that stand development is driven by an increase in height (García, 2010), optimising the height growth part of the model above other model variables may be desirable.

The site index model selected in the parameterisation produces an anamorphic set of curves (Fig. 2.1). Anamorphic curves share the same shape and form between site indices, and can be referred to as time scaled curves. While anamorphic height growth curves have been criticized in the past for their single point productivity classification (Zeide, 1978), the selection versus alternative curve forms in the parameterisation (see Appendix A) indicates that this simple function is sufficient. Anamorphic curves have also been shown to be useful for UK Sitka spruce stands (Rennolls, 1995).

The mortality section of the SLeDG model (Fig. 2.2) is an example of a self-thinning 'law' as explained by García (2009). Thus, like other self-thinning laws there is a maximum stem number for a stand of a given height. However, the trajectory of mortality for most stands is not dependent on this self-thinning line until greater heights are reached. This can be seen in Figure 2.2 as the point when the models mortality projections come close together past stand heights of 20m.

Occupancy is an implicit (or latent) variable in this model as in previous parameterisations of SLeDG for other species (García *et al.*, 2011). As such the

values predicted by the model cannot be benchmarked against empirical data. Despite the fact that it is not a direct physical measure, occupancy is useful to provide a physiological limitation on stand productivity, similar to the PAR modulation by LAI in 3PGN, taking into account reductions in productivity at initial planting or following thinnings. In the future, it may be possible to estimate occupancy based on relative stand closure using light detection and ranging (LiDAR) measurements. Alternatively, a method similar to that of Duursma *et al.* (2012) for estimating light use efficiency in woody plants might estimate occupancy directly. This method uses just two parameters: crown density (the ratio of leaf area to total crown surface area) and leaf dispersion (a measure of the degree of aggregation of leaves) to model light use efficiency. This may be scaled from individual plants to stand scale using LiDAR measurements to identify the aggregation of trees and the crown density within a stand.

Although the linear model fitted to the basal area residuals indicates a consistent bias which is a function of stand age, the linear model is likely to be affected by the few oldest plots (> 70 years) in the dataset. The measurements of older plots in the PSP dataset tend to be in less productive plots (Table 2.1.), with more productive plots having been harvested. Thus the dataset is not representative of all productivity classes over the range of ages. As lower productivity stands are expected to have lower basal area in earlier stages of growth, this trend is likely to continue in later stages of the model, hence the potential for underestimation of basal area in older stands. Ideally PSP data from more productive, older stands would be included in a future parameterisation to remedy this.

The statistical tests to benchmark SLeDG (Table 2.4.) reveal an excellent fit between the data and the model that has been fit to the data. A modelling efficiency so close to 1.0 is consistent with a graphical assessment of the model as can be seen in Figures 2.1. and 2.2.; where the model follows closely the measured values. Ideally independent data would have been used in a benchmark

analysis. However, because of the small size of the PSP dataset, the decision was made to use all data in parameterisation. Bootstrap simulations are suggested as an alternative to independent validation in cases of data scarcity (Vanclay and Skovsgaard, 1997). Results of the bootstrap analysis were mostly consistent with the parameter estimates (Table 2.3.). However, the appearance of negative values in the confidence intervals of b_4 and b_{11} suggest issues with the parameterisation method, as it should not be possible for the model to increase the number of stems or decrease occupancy (see Equations 2.2b and 2.2c). Given more time this could have been investigated further. The parameter estimates for b_7 and b_8 do not sit in the middle of the bootstrap confidence intervals, which could be a result of bias in sampling of the bootstrap. Non-overlapping time intervals used in the parameterisation are assumed independent. However, plots with more measurements are more likely to be sampled repeatedly in the bootstrap which uses sampling with replacement.

Further improvements to SLeDG may include modulating the site index part of the model by a climate index (similar to the climate variables used in 3PGN) to allow for predictions in a changing climate. Equally, a soil model may be integrated with the model as in 3PGN with a variable similar to fertility rating modulating the site index, and the occupancy providing values for fine root turnover and litter production. With this a measure of soil carbon accumulation may be obtainable.

2.4.2 Model comparison

Despite their differences in structure, the three models show reasonable agreement in variables and outputs over the years predicted. This is especially true in the thinned stand projections. The main differences occured in the predicted volume and biomass forecasts. The higher biomass estimates of SLeDG compared to

3PGN in unthinned stands (Fig. 2.4e.) may be similar to overestimates of biomass seen when using BEF based on only one variable (Lehtonen *et al.*, 2004), as the BEF is only based on top height (Levy *et al.*, 2004). Additionally, this discrepancy may be explained by the underestimation in biomass previously observed when using 3PGN to estimate Scots pine growth, due to an underestimated foliage biomass pool (Xenakis *et al.*, 2008). As before, the cause of the underestimate of 3PGN may be better understood given a more complete dataset with foliage and root carbon storage in chronosequences. Regardless of the cause, both models forecast a smaller range of volumes and biomass than ForestYield. It is possible that the lower variation in stem numbers observed in ForestYield (Figs. 2.4c. & 2.4h.) does not represent the variation one might expect between very high and low productivity sites. If lower fertility sites had a higher stem number for a given height, the range in stand volume may be reduced to a range similar to that observed in the other two models.

In thinned stands, SLeDG and 3PGN arrive at a similar biomass estimate across the range of YC, despite an earlier biomass accumulation predicted by SLeDG. However, SLeDG still predicts lower volumes in thinned stands. This may also be a symptom of the low number of older high productivity stands in the PSP dataset (Table 2.1).

Given the limited PSP data available for Scots pine in the UK the benefit of using the SLeDG approach is that despite the limited dataset it still provides a reasonable forecast of stand growth across a range of sites. There is a reduction in time and effort required to parameterise SLeDG versus 3PGN, which requires 50 parameters to be estimated (Xenakis *et al.*, 2008) compared to the 13 in this parameterisation of SLeDG. Additionally, climatic variables including maximum and minimum monthly temperatures and precipitation may not be easily obtained: being dependent on the nearest weather station. However, improved data availability reduces this advantage of SLeDG over 3PGN. With

increasing data availability from remote sensing sources, 3PGN may incorporate inputs in a similar way to Physiological Principles Predicting Growth (3PG) Spatial (3PGS) (Coops *et al.*, 1998): using satellite data to estimate the leaf area density, chlorophyll content in canopies, maximum photosynthetic capacity and biomass for 3PG model calibration. Thus, the potential for using 3PGN in UK forests can only increase. Indeed, a potential benefit of 3PGN is that it may utilise a wider range of data for calibration should it become available. Both forest growth variables and carbon fluxes may be utilised by 3PGN for calibration and validation (Minunno *et al.*, 2010).

In this model comparison, we provide no indication of the uncertainty in model predictions. Both SLeDG and 3PGN provide parameter error values, which may be propagated to the state variables and model outputs. ForestYield does not provide any uncertainty in its parameters, and the yield tables that it is based on also provide no error values (Edwards and Christie, 1981). In financial terms, a measure of uncertainty is highly desirable for estimating optimum harvest (Lohmander, 1988). Equally for carbon storage, a measure of uncertainty is important for both policy makers and managers, with uncertainty in parameters identifying parts of models requiring further attention (Smith and Heath, 2001). Indeed, quantification of uncertainties features heavily in the guide for LULUCF reporting (IPCC, 2003). Bayesian approaches to forest model calibration such as those of van Oijen *et al.* (2013), Patenaude *et al.* (2008), and Xenakis *et al.* (2008) are one approach which could lead to better understanding of model uncertainty, and future work on models for stand level development should consider this as an option. More generally: greater transparency in the relationships, assumptions and limitations of empirical yield models used for timber estimation and as drivers for other models (e.g carbon reporting (Milne *et al.*, 1998) and wind risk estimation (Gardiner *et al.*, 2004)), can lead to wider utility and application.

While this paper has concentrated on Scots pine in particular, the calibration of

both SLeDG and 3PGN of other species both in the UK and beyond is possible. Both models are aimed at forecasting even-age monocultures, reducing ease of application in more complex forest stand structures. As a counterpoint, both models forecast stands based on the current state of the system without requiring historical measurements to estimate productivity, particularly useful in countries where details of forest establishment are not widely known. With hybrid models it is possible to allow for a greater range of forest management strategies than static tables. Forecasts can be based on the current state of a forest stand, rather than fitting a given stand to a predetermined growth trajectory. Thus, improved estimates of forest stand-level metrics in the UK should allow for flexibility in predictions following any alterations in forest management; the ability to utilise as many data as possible whilst being robust enough to be able to run efficiently with minimal data available; and also be fully documented in order that various sources of error may be accounted for. None of the models considered here reach such lofty goals. However, it seems of benefit to move towards dynamic models of forest growth for carbon stock estimation. With current data availability a dynamic model such as SLeDG, can account for changes in forest management. Replacing the static yield table approach currently used in C-FLOW with growth predictions from a dynamic statistical model could provide growth estimates for forest management in cases where management has deviated from the traditional schemes included in the tables of Edwards and Christie (1981). In addition it is then possible to run model based scenarios of alternative management approaches to inform management. In the future, when data from multiple sources (for example remote sensing, and sensor networks) become more available, models such as 3PGN may become more appropriate, providing both forecasts and insight into the underlying processes driving changes in forest growth. Indeed it may be most appropriate to consider the use of both SLeDG and 3PGN in concert to provide forest growth forecasts in the future. Such an approach allows the ensemble of

models to continue to benchmark each other, whilst providing more information about the uncertainty of predictions.

Chapter 3

Bayesian calibration and Bayesian model comparison of a stand level dynamic growth model for Sitka spruce and Scots pine

J. Lonsdale[1], F. Minunno[2], M. Perks[3], M. Mencuccini[1,4]

[1]School of Geosciences, University of Edinburgh, Edinburgh, EH9 3JN, UK

[2]Department of Forest Sciences, University of Helsinki, Yliopistonkatu 4, 00100 Helsinki, Finland

[3]Forest Research, NRS, Roslin, Midlothian, EH25 9SY, UK

[4]ICREA at CREAF, Cerdanyola del Valles, Barcelona, Spain

(Submitted to *Forestry*)

Abstract

Growth models continue to be of importance in modern multi-functional forestry to provide forecasts. Bayesian calibrations allow both model structure and parameters to be assessed simultaneously in a probabilistic framework, providing a model with which forecasts and their uncertainty can be better understood and quantified using posterior probability distributions. A Bayesian calibration of a Stand Level Dynamic Growth (SLeDG) model is carried out for both Sitka spruce and Scots pine in the UK for the first time. The calibration used the Differential Evolution Markov-Chain method to reduce the required number of iterations for inference. Two different model structures were considered for estimating local stand productivity: one using the measured height-age relationship, and one using estimated site yield class. The height-age relationship was shown to be more probable for both species in a Bayesian Model Comparison (Total model probability = 0.64 and 0.58 for Sitka spruce and Scots pine respectively), although metrics of model performance were similar for both model structures ($R^2 \geq 0.88$ in all variables). A complete calibration (using all data) of the more probable model structure was then completed, and excellent model fit was observed ($R^2 > 0.95$ for all variables in the case of both species). Forecasts of forest growth using parameter distributions from the calibration were demonstrated, and are compatible with existing yield tables for both species. This method could be applied to other species or other model structures in the future.

3.1 Introduction

Due to the time scales involved in a forest rotation, modern multi-purpose forestry continues to require robust forest growth models to forecast timber, carbon storage, and even time to maturity for recreational uses. Current computing power and availability has resulted in a marked increase in the use of Bayesian approaches when calibrating models across a range of fields. For the parameterisation of forestry models Bayesian approaches have been shown to produce outputs comparable to maximum likelihood approaches (Li *et al.*, 2011; Laloy and Vrugt, 2012), but with the added benefit of a full posterior distribution of parameters, thereby facilitating a more thorough understanding of areas of uncertainty within a model. It is also relatively simple to use the Bayesian method to investigate uncertainty in model structure through Bayesian Model Comparison (BMC) (van Oijen *et al.*, 2013). While Bayesian approaches are becoming more prevalent for forest ecosystem modelling, particularly for calibration of process-based models (van Oijen *et al.*, 2013; Minunno *et al.*, 2013), they have not seen wide application in forest growth and yield modelling. Site index (Li *et al.*, 2011), tree mortality (Metcalf *et al.*, 2009), diameter distribution (Bullock and Boone, 2007), and yield models (Green and Strawderman, 1996) have all used Bayesian approaches, however a complete calibration of an empirical stand level growth model has not yet been done using a Bayesian approach.

Stand Level Dynamic Growth (SLeDG) models, based on the initial work of García (1979), have been developed for a variety of tree species around the world: most recently trembling aspen (*Populus tremuloides* Michx.) in British Columbia (García, 2013) and Scots pine in the UK (Lonsdale *et al.*, 2015). SLeDG models use differential equations to forecast a state vector composed of common stand level forest inventory measures (top height, number of stems, and basal area). Their strength lies in that they are able to provide robust predictions from any

point in state space after calibration with even small datasets (Lonsdale *et al.*, 2015). It should be noted that while some process-based models may also be stand level, dynamic growth models, here SLeDG models specifically refer to models of the form suggested by García (1979) as a convenient acronym.

The prevalent methodology for parameterising SLeDG models is to use a combination of the values of maximum likelihood to estimate the top height growth parameters (Hu and García, 2010), non-linear least-squares to estimate mortality parameters (García, 2009), and basal area growth parameters (García *et al.*, 2011). While using these methods of parameter estimation to successively parameterise a model undoubtedly produce acceptable results, it is often difficult to identify suitable starting points for parameter calibrations, and the differential equations strong non-linearity can lead to algorithms reaching false optimisation maxima in the state space. It is also suggested that simultaneous parameter estimation may reduce model errors (Vanclay and Skovsgaard, 1997), thus improving forecasts. Over 30 years ago, Garcia (1983) suggested Bayesian methods could be used in the place of maximum likelihood for parameter estimation in Stand Level Dynamic Growth (SLeDG) models; however, to date there appears to have been no published attempts to calibrate SLeDG models using Bayesian methods.

Thus, here we demonstrate the use of Bayesian methods to parameterise dynamic forest growth models. We have completed two Bayesian calibrations of a SLeDG model for the two most important conifer species in the UK: Sitka spruce (*Picea sitchensis*) and Scots pine (*Pinus sylvestris*). Together they make up 68% of British conifer forests (Forestry Commission, 2011). Markov Chain Monte Carlo (MCMC) methods are often used in Bayesian calibrations for posterior inference (e.g. van Oijen *et al.* (2013)) and here we use a recent development of this method: Differential Evolution Markov Chain (DE-MC) (ter Braak, 2006). The DE-MC is detailed in the methods section, but it most importantly provides a method of accelerating chain convergence.

Here we provide a brief description of the SLeDG model, as well as the theory of the DE-MC. Then two different ways of including an estimate of local site productivity are compared using a BMC. Finally we provide parameterisations, validation and uncertainty measures for the optimal models selected by BMC for both species, and provide an example growth forecast based on the parameterisation. We conclude by discussing the most important implications of this work for future uses of Bayesian calibration of forest growth models.

3.2 Methods

3.2.1 Overview

The data for the calibrations were provided by the Forest Research Forest Mensuration, Modelling and Forecasting Group and comprised permanent sample plot (PSP) measurements from 171 Sitka spruce plots and 134 Scots pine plots located throughout the UK. The main characteristics of the plots are summarised in Table 3.1. To capture the shape of growth trajectories, stand conditions at planting were added to the measurements based on the recorded initial spacings (ranging from 0.9 m to 2.4 m square spacing for both species), and assumed planted trees were breast height (1.3 m).

The data for each species were initially split in half ($n/2$), fully randomly to provide a cross-validation for the model comparison with separate calibration and validation datasets. Bayesian calibrations using DE-MC were performed for each species using the calibration data. Two different model structures for estimating local site productivity were calibrated (detailed below). A BMC was then performed using the validation dataset to identify the preferred model structure. Finally a model calibration of the preferred structure was run using

the whole dataset to provide posterior parameter distribution estimates which also indicate uncertainty.

3.2.2 SLeDG model

Stand Level Dynamic Growth (SLeDG) style models are based on the modelling approach first suggested by García (1979). This family of models is biologically based and uses a state-space approach to forecast the stand development. Stands are described using a state vector of common forest inventory measures. A more detailed explanation of SLeDG models can be obtained in the supplementary information of Lonsdale *et al.* (2015) or García *et al.* (2011). In this instance three variables make up the state vector: top height (H), number of stems per hectare (N), and the product of basal area and top height ($B \times H = W$), for convenience henceforth referred to as tubular stem. This variable is highly correlated with merchantable volume and biomass, and behaves more simply than basal area alone.

Changes in the state vector are forecast as a function of itself ($\mathrm{d}X/\mathrm{d}t = \mathrm{f}(X)$) with an equation for each part of the state vector:

$$\frac{dH}{dt} = b_1 \left[(b_2/H)^{b_3} - H \right] \tag{3.1a}$$

$$\frac{dN}{dH} = -b_4 H^{b_5} N^{b_6} \tag{3.1b}$$

$$\frac{dW}{dH} = b_7 H^{b_8} N^{b_9} - b_9 \frac{W}{N} \frac{dN}{dH} \tag{3.1c}$$

Where b_i are parameters to be estimated. Equation 3.1a is a form of the von Bertalanffy model commonly used in growth models for both plants and animals. A measure of site-specific productivity was included by setting b_1 as a site specific parameter, which results in anamorphic height growth curves of consistent shape

Table 3.1: Summary statistics for permanent sample plot (PSP) stands used

	Mean	SD	Minimum	Quartile 1	Median	Quartile 3	Maximum
Sitka spruce ($n = 171$)							
yield class (YC) ($m^3ha^{-1}yr^{-1}$)	18.10	4.58	5.00	15.00	17.00	21.00	32.00
Age (yr)	34.34	12.94	12.00	23.00	34.00	42.00	87.00
Top height (m)	18.92	6.71	5.20	13.6	18.3	22.8	41.3
Trees ha^{-1}	1660.2	1135.6	119.0	737.5	1413.5	2320.5	7769.0
Basal area (m^2 ha^{-1})	43.56	15.95	4.36	31.66	41.03	55.01	93.41
Scots pine ($n = 134$)							
YC ($m^3ha^{-1}yr^{-1}$)	9.61	2.08	5.00	8.00	9.00	11.00	18.00
Age (yr)	45.59	19.90	14.00	30.0	43.0	57.0	123.0
Top height (m)	16.27	4.81	5.80	12.60	15.90	20.0	28.90
Trees ha^{-1}	1460.8	1192.6	78.0	618.8	1073.5	1939.0	6415.0
Basal area (m^2 ha^{-1})	32.71	11.50	3.23	24.54	30.50	38.96	75.26

SD = Standard deviation, YC = Yield Class

Number of available permanent sample plots are given in brackets after each species' name.

with height scaled by the site specific parameter. Anamorphic height growth curves have been previously used for both Sitka spruce and Scots pine in the UK (Lonsdale *et al.*, 2015; Rennolls, 1995).

Both changes in stem number and tubular stem (Equations 3.1b and 3.1c) are for given changes in height rather than time, as such changes are likely to be better predicted by a physiological change (such as height) rather than temporal change (García, 2010).

3.2.3 Bayesian Calibration with Differential Evolution Markov Chain

Bayes' formula states that the probability of the parameter values (θ), given data (D), in a model is proportional to the current uncertainty in parameter values ($\mathrm{P}(\theta)$) multiplied by a likelihood function ($\mathrm{P}(D|\theta)$): a measure of fit between the model and the data, given the parameters. Thus,

$$\mathrm{P}(\theta|D) \propto \mathrm{P}(\theta)\mathrm{P}(D|\theta) \tag{3.2}$$

These three terms are usually referred to as the posterior, the prior, and the likelihood, respectively. Bayesian calibration begins with the specification of a prior uncertainty in the set of parameter values as a multivariate probability distribution. The likelihood function is then determined using the model's ability to match the data (D) with given candidate parameter values θ (van Oijen *et al.*, 2005). The common assumption that measurement errors were Gaussian and uncorrelated was used here. Thus, likelihood was calculated for each data point D_j compared with the corresponding model output $\mathrm{f}_j(\theta)$ for all η data points in

the data sample:

$$\mathrm{P}(D|\theta) = \prod_{j}^{\eta} \phi(D_i - \mathrm{f}_j(\theta); 0, SD_j) \tag{3.3}$$

Where ϕ represents a Gaussian function with mean 0, and standard deviation SD_j.

To perform the calibration an iterative process which explores parameter space is often used to simulate the distributions of Equation 3.2. The most common and general of these is the Metropolis algorithm (Metropolis *et al.*, 1953). In this method, a proposal of new parameters (θ_x^*) is suggested by adding a random shift (ϵ)to the existing parameter values (θ_x):

$$\theta_x^* = \theta_x + \epsilon \tag{3.4}$$

The ratio between the proposal posterior and the existing posterior is calculated (known as the Metropolis ratio (β)):

$$\beta = \frac{\mathrm{p}(\theta_x|D)}{\mathrm{p}(\theta_{x-1}|D)} \tag{3.5}$$

The proposal is accepted with a probability equal to this ratio (β) and the chain of iterations moves forward from that point in parameter space. If the proposal is rejected the chain of iterations returns to θ_x for another random shift (van Oijen *et al.*, 2013). The difficulty in this method lies in trying to balance between making sufficiently large shifts to progress through the parameter space, while still accepting enough proposed parameter values.

More recent developments have suggested improvements in this random-walk method, allowing for more directed exploration of parameter space. In this study the DE-MC with snooker updater is used. The standard DE-MC method was

developed by ter Braak (2006) and further refined by ter Braak and Vrugt (2008). It aims to improve the scale and orientation of jumps in the MCMC method. This is achieved by using a number of iterative chains of parameters, n. Each parameter vector x_i (where $i = 1 : n$), or chain state, is updated using a proposal x_i based on the difference between the parameter position of two other chains' states. Thus a given chain's proposal (x_i^*) is given by:

$$\boldsymbol{x_i^* = x_i + \gamma(x_{R1} - x_{R2}) + \varepsilon} \tag{3.6}$$

Where γ is a user-defined scalar, ε is a random vector with a small variance compared to the posterior, and x_{Ri} are drawn from other chains' states x_{-i}. Earlier versions of the DE-MC required a number of chains greater than the dimensionality of the parameters (ter Braak, 2006), however by sampling difference vectors from previous points in the chains the number of chains that must be run is reduced (ter Braak and Vrugt, 2008). Thus θ_{Ri} is sampled from the present state of other chains as well as the previous states back to a user-defined previous number of states (M_0). A further enhancement used in this analysis is the snooker updater which instead of a simple vector difference (Equation 3.6.) uses the difference of the orthogonal projection of two other chain states (from past or present) onto a line between the chain state being updated and another random chain state, $\mathbf{z}$. The proposed update is given by:

$$\theta_i^* = \theta_i + \gamma(\mathbf{z_{P1}} - \mathbf{z_{P2}}) \tag{3.7}$$

Where $\mathbf{z_{Pi}}$ is the orthogonal projected position of other chains onto the line $\theta_i - \mathbf{z}$, and γ is again a user-defined scalar. The proposed update is accepted with probability equal to the Metropolis ratio (ter Braak and Vrugt, 2008).

Relatively uninformative uniform priors were used for each of the parameters (b_i) (Table 3.3). The parameters do not represent any physical value (such as is the case in process-based models), and thus theoretically do not have limits. However, to ensure convergence in a reasonable number of iterations all other parameters were loosely constrained with uniform priors based on previous estimates of parameters for SLeDG models with similar structure (e.g Lonsdale *et al.* (2015),García *et al.* (2011),Broad and Lynch (2006)). Parameters were not allowed to go below zero, as values below zero would result in negative growth (e.g. b_1, b_2, b_7), or increases in stem numbers (e.g. b_4) (See Equations 4.1a. 4.1b. 4.1c.). Additionally no previous parameterisations of a SLeDG style model have found negative parameters. Measurement uncertainty was not provided in the PSP dataset and so it was assumed that top height had 10% measurement uncertainty, number of stems 20% uncertainty, and tubular volume 30% uncertainty (as it also includes the uncertainty in top height). Only unthinned stands were used in the calibration of the mortality part of the model (Equation 4.1b), and it was assumed that basal area should always be increasing as negative basal area is indicative of disturbance events (García, 2013) such as windthrow which are not accounted for in this model. Alternative forms for predicting basal area growth may accommodate negative growth in the future, however it is also possible that observed negative growth is a result of the difficulty in measuring diameter (Clark *et al.*, 2007), which is required to estimate basal area. Thus stands where basal area decreased were excluded from the calibrations. For each model considered in this study, three million iterations split between three chains were run to determine the probability density functions for parameters b_i. The first half of these iterations were discarded as burn-in (iterations where the chain is yet to reach the area of high posterior probability). Chain convergence was assessed visually and the Gelman-Rubin diagnostic (Gelman and Rubin, 1992) was calculated and checked to have a value less than 1.1 for all parameters.

3.2.4 Bayesian model comparison

BMC follows logically from Bayesian calibration, but instead of model parameters being informed by data, it is the model selection. Thus the probability of a model given data P($M|D$) is proportional to the product of the prior probability of a model P(M) and an integrated likelihood, P($D|M$). By splitting the data (D) in half to give calibration data (D_c) (which has been used to estimate the prior parameter distribution P($\theta|D_c$)) and validation data (D_v) the integrated likelihood can be calculated using the law of total probability as:

$$\mathrm{P}(D_v|M, D_c) = \int \mathrm{P}(D_v|M(\theta))\mathrm{P}(\theta|D_c)d\theta \tag{3.8}$$

The integrated likelihood was estimated using the validation dataset for each species, with the prior distributions estimated by a calibration of the model with the calibration dataset. This used a sample of 1000 parameter sets from the prior distributions. Each model's probability was calculated as its integrated likelihood divided by the sum of all integrated likelihoods.

The advantage of BMC versus frequentist model comparison indices such as Akaike information criterion (AIC) is that parameter uncertainty determines a models' probability rather than a single parameter vector (Tuomi *et al.*, 2008).

Two approaches to estimating site specific productivity were compared using the Bayesian model comparison. The first method (Model 1) used an integrated form of Equation 3.1a to estimate the site productivity given a fixed origin $[t_1, H_1] =$ [0,0], the height at time t_x being given as:

$$H_x = b_1(1 - e^{-b_2 t_x})^{1/b_3} \tag{3.9}$$

This equation can then be solved for b_1 giving a site specific productivity. The second method (Model 2) of including an estimate of site productivity used the Forestry Commission determined YC. A simple relationship between YC and a site index (SI) at age 50 (H_{50}) is given as:

$$H_{50} = \alpha_1 + \alpha_2 \mathrm{YC} \tag{3.10}$$

The estimated H_{50} can then be substituted into Equation 3.9 with $t_x = 50$, and the local parameter calculated as for the first method. The parameters α_i are estimated as part of the calibration, constrained by uniform priors of -50 – 50.

The model comparison used the half of the dataset not used for the initial Bayesian calibration. Model probabilities for determining each of the state variables (H,N, and W) as well as for the model as a whole were compared to identify the most suitable model structure.

3.3 Results

3.3.1 Initial calibrations

All initial calibrations (for both Sitka spruce and Scots pine) using the calibration data for both Models 1 and 2 reached convergence after one million iterations with Gelman-Rubin statistic < 1.1. Graphical inspection of the chains confirmed convergence. The one million iterations took approximately 15 minutes to complete for the Sitka spruce calibration data in both Models 1 and 2, and approximately 12 minutes for both models in the case of Scots pine (all computations performed on 1.6 Ghz Intel Core i5-2467M CPU).

3.3.2 Bayesian model comparison

The results from the comparison of the two alternative model structures employed to include site quality when predicting the validation dataset are given in Table 3.2. When predicting the validation half of the data with the highest probability parameter vector (given by the more commonly used measures of model performance (root mean standard error (RMSE) and R^2) the model using existing site YC as a measure of productivity (Model 2) performs better than the alternative model, especially for Scots pine due to lower RMSE and R^2 values closer to 1. Conversely, the BMC results indicate the model structure that uses the current state to estimate productivity (Model 1) has a higher probability for both species. Interestingly, the total model probability for Model 1 is lower than the highest variable specific measure probability (height in both species). It should be noted that the differences in performance are small between the two models according to all of the benchmarking statistics used here. Nonetheless, as the full calibration uses Bayesian methods, the decision was made to perform calibrations for both species using the Model 1 structure, which showed the highest probability over all variables and in total according to the BMC.

3.3.3 Model calibration

For both species the full calibration reached convergence after the three million iterations with Gelman-Rubin statistics < 1.1 and convergence observed in a graphical assessment of the Markov Chain. Three million iterations took 50 minutes for Scots pine and 60 minutes for Sitka spruce. The most probable parameter vector is found in the Markov chain as the highest product of likelihood and prior probability density. The most probable parameter estimates and their credible intervals for both species are given in Table 3.3.

Table 3.2: Model probability and fit statistics of validation data to model runs using most probable parameter vectors for each state variable for both Sitka spruce and Scots pine. Model 1 refers to the model that uses current state to estimate site productivity. Model 2 refers to the model that uses estimated yield class (YC) to define site productivity.

Model	Top height, H (m)			Stem density, N (stems ha^{-1})			Tubular volume, W (m^3)			Total model
	Probability	RMSE	R^2	Probability	RMSE	R^2	Probability	RMSE	R^2	Probability
Sitka spruce										
1	0.73	1.56	0.89	0.53	427	0.88	0.51	128	0.88	0.64
2	0.27	1.09	0.95	0.47	361	0.89	0.49	106	0.93	0.36
Scots pine										
1	0.69	0.64	0.98	0.51	173	0.98	0.50	65.0	0.95	0.58
2	0.31	0.59	0.98	0.50	151	0.98	0.50	83.9	0.90	0.42

Table 3.3: Uniform prior bounds and posterior parameter estimates for Sitka spruce and Scots pine. Most probable parameters are those that had the highest product of likelihood and prior vector in the Markov chain. There is no distribution for b_1 as it is a local parameter calculated as a function of b_2, b_3, and stand height at measured time.

	Priors:		**Posteriors:**			95% credible interval	
	Min	Max	Mean	Standard deviation	Most probable	Min	Max
Sitka spruce							
b_2	0.00	1.00	0.0115	3.42×10^{-4}	0.0118	0.0112	0.0124
b_3	0.00	1.00	0.863	0.00126	0.863	0.86	0.865
b_4	0.00	1.00	3.64×10^{-5}	1.57×10^{-5}	2.19×10^{-5}	1.71×10^{-5}	8.07×10^{-5}
b_5	0.00	10.0	0.704	0.0339	0.727	0.638	0.769
b_6	0.00	10.0	1.76	0.0455	1.81	1.66	1.84
b_7	0.00	50.0	9.71	3.99	7.95	3.38	18.6
b_8	0.00	100	0.0584	0.0566	2.80×10^{-3}	2.09×10^{-3}	0.21
b_9	0.00	1.00	0.375	0.0738	0.408	0.24	0.536
Scots pine							
b_2	0.00	1.00	0.129	5.06×10^{-4}	0.0125	0.0124	0.0143
b_3	0.00	1.00	0.818	2.47×10^{-3}	0.819	0.812	0.822
b_4	0.00	1.00	8.70×10^{-3}	8.24×10^{-3}	1.56×10^{-3}	1.62×10^{-3}	0.0297
b_5	0.00	10.0	0.587	0.0698	0.687	0.446	0.711
b_6	0.00	10.0	1.21	0.0812	1.36	1.04	1.35
b_7	0.00	50.0	18.2	10.9	21.6	3.39	44.0
b_8	0.00	100	0.206	0.154	0.466	0.0104	0.581
b_9	0.00	1.00	0.184	0.122	6.49×10^{-4}	9.99×10^{-3}	0.458

The result of using the most probable parameter vector (see Table 3.3) to predict the observations in the full dataset can be seen in Figure 3.1. The state variable fit statistics using the full dataset for each species are given in Table 3.4. The model closely fits observations for both species in all state variables indicated by the R^2 values. However, slopes significantly different from 1 indicate that in Scots pine predictions of top height and number of stems tend to be overestimated, while tubular volume has a tendency to be underestimated for both species.

Table 3.4: State variable fit statistics for Scots pine and Sitka spruce models using the most probable parameter vector against the full datasets. Parameter vectors were estimated using a full dataset calibration.

	Top height (m)	Stems ha^{-1}	Tubular volume (m^3)
Sitka spruce			
RMSE	0.916	206	93.8
R^2	0.981	0.964	0.970
Slope	0.997	0.964	0.967*
Scots pine			
RMSE	0.596	137	42.1
R^2	0.983	0.978	0.982
Slope	1.02*	1.04*	0.955*

* indicates slopes significantly different to 1 ($P<0.01$)

Example forecasts over a range of productivity classes using the estimated parameters with their uncertainty are given in Figures 3.2 and 3.3. The forecasts are made using a draw of 5000 parameter vectors from the Markov Chain. The plots illustrate forecasts from the last measurement of a randomly selected stand from the dataset until the stand reaches 120 years. It is possible to see the skew in probable predictions in the location of the most probable predictions (dashed lines) differing from the center of the shaded probability intervals. The predictions are mostly consistent with the existing yield tables of Edwards and Christie (1981) (dotted lines) which are commonly used for growth predictions in UK forests. The yield tables do not agree particularly well with stem number and tubular volume measurements in the case of Scots pine (Fig. 3.3).

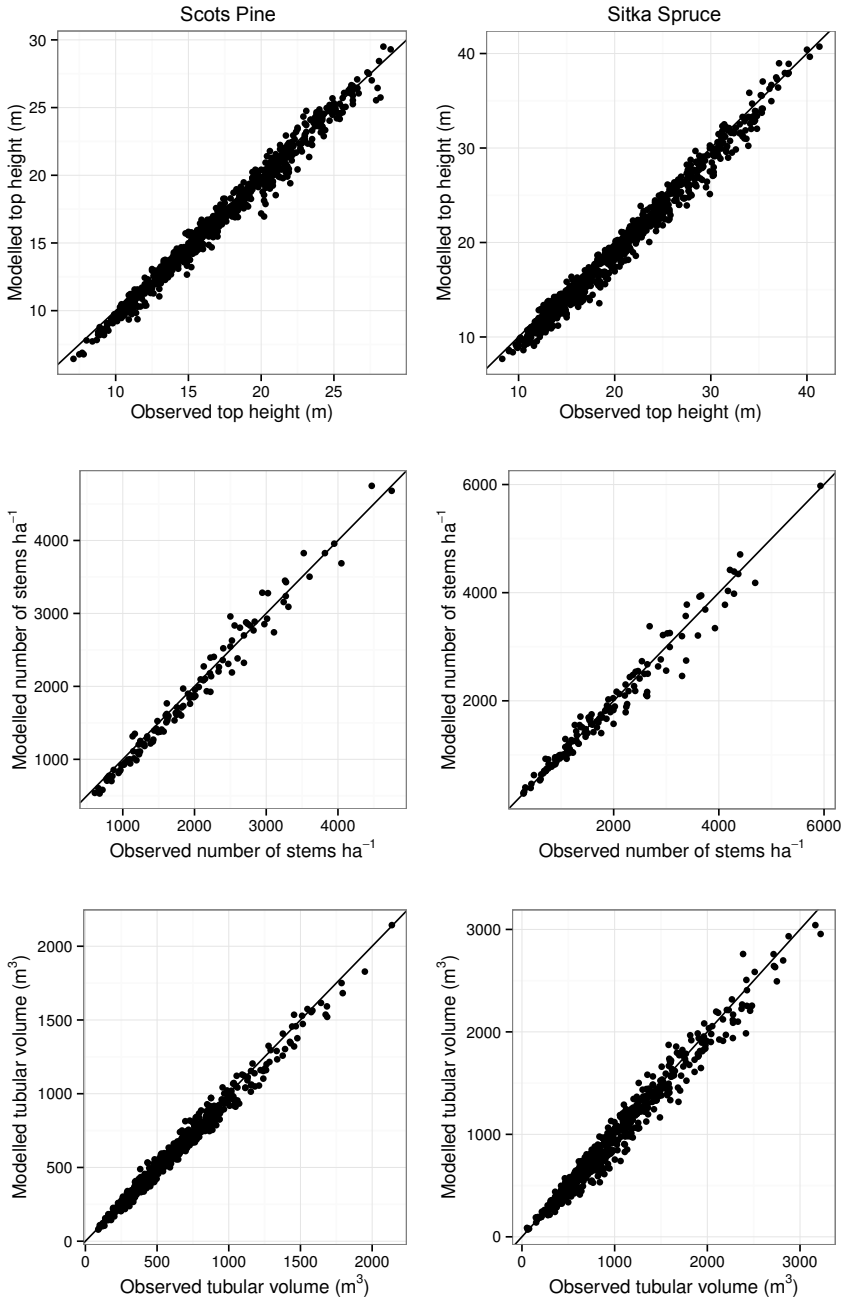

Figure 3.1: Model fit for both Scots pine and Sitka spruce SLeDG models using the most probable parameter vector given by the DE-MC calibration.

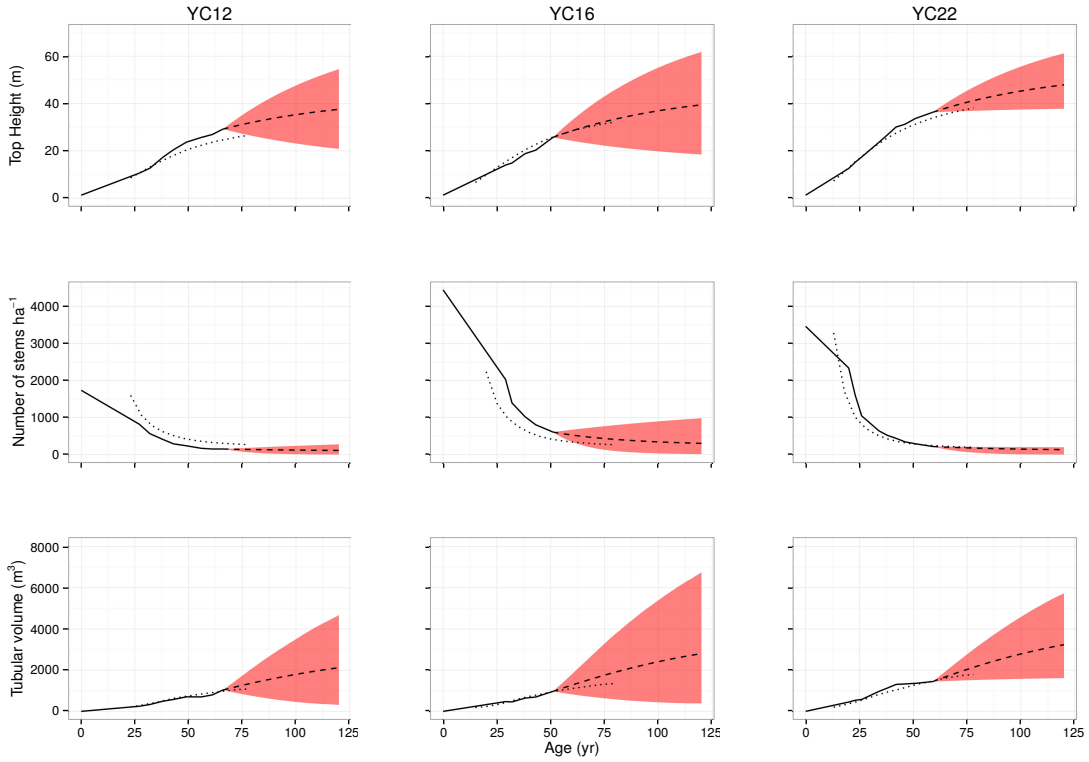

Figure 3.2: Example forecasts of state variables (continuous line) for 3 randomly selected Sitka spruce stands (Yield Classes 12,16 & 22) using 5000 parameter draws from the Markov chain. Dashed line indicates most probable parameter vector prediction, and shaded area indicates 95% probable interval. Dotted line indicates forecast based on the yield tables of Edwards and Christie (1981) for the given yield class.

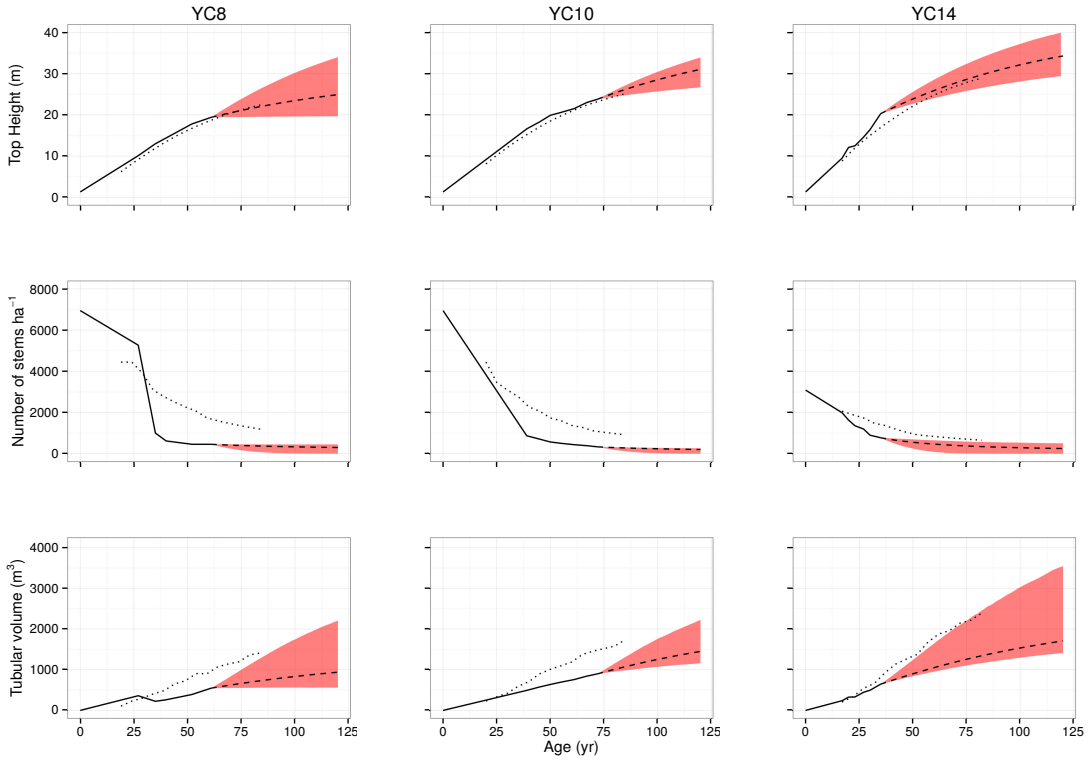

Figure 3.3: Example forecasts of state variables (continuous line) for 3 randomly selected Scots pine stands (Yield Classes 8,10 & 14) using 5000 parameter draws from the Markov chain. Dashed line indicates most probable parameter vector prediction, and shaded area indicates 95% probable interval. Dotted line indicates forecast based the yield tables of Edwards and Christie (1981) for the given yield class.

3.4 Discussion

The results presented here demonstrate that Bayesian calibration provides a way to calibrate dynamic forest models based on complete posterior distributions of model parameters and any model outputs of interest. Similarly to Li *et al.* (2011), we would not suggest that Bayesian methods replace frequentist methods, which have been shown to be adequate for parameterising SLeDG models (e.g. Lonsdale *et al.* (2015); García (2013)). However, there are several advantages in the Bayesian approach when considering model uncertainty. The posterior parameter distributions provide a much better understanding of parameter uncertainty resulting in a better illustration of prediction uncertainty as can be seen in Figures 3.2 and 3.3. Performing model comparisons by using the posterior probability distributions is useful when considering model structural uncertainty (Kass and Raftery, 1995).

Here, the two different model structures could be considered demonstrations of 'stand site index' versus 'site site index' as described by García (2006). Model 1, which assumes the productivity is defined by the current state of a stand growing on a site is an example of stand site index. Conversely, Model 2, which has a fixed productivity throughout a rotation predefined by a site's estimated YC, thus a property of the site itself (not the trees growing on the site), is an example of site site index. The BMC results suggest better performance of Model 1 with the potential to reduce uncertainty, however the RMSE and R^2 values from the validation show close to equal performance of the models. This suggests that the two additional parameters in Model 2 (α_i) are what cause the reduced model probability, equivalent to the penalisation imposed by increased number of parameters in AIC-based approaches.

The fact that the total model probability in Model 1 for both species is lower than the highest variable specific probability (Table 3.2) could mean that the

parameter sets that contribute to increasing the probability of Model 1 for estimating height (H), reduce probability of Model 1 for estimating number of stems (N) and tubular volume (W). Thus the mean log-likelihood is lower than if drawn parameter sets led to increased probability across all variable specific probabilities.

Values of YC for the vast majority of forests in the UK are available in the Forestry Commission's sub-compartment database (SCDB) and thus Model 2 provides a method to spatialise predictions across the UK. However, while measures such as local yield class (Edwards and Christie, 1981) may go some way to adjusting site quality measured over a rotation, only limited measurements of site productivity may be available due to cost of providing repeated stand measurements. The increased prevalence of remote sensing techniques such as light detection and ranging (LiDAR) may reduce this cost, making Model 2 a favorable approach. Indeed, additional data provided by LiDAR measurements could be added to the existing dataset to further refine the growth model in a form of data assimilation similar to Patenaude *et al.* (2008), potentially further reducing parameter uncertainty. Overall, consideration of scale and data availability will also be of importance when selecting a model for making predictions. Large scale prediction using Model 1 requires further data collection and processing for productivity estimation whereas Model 2 may be applied at the UK scale using the currently available data, although with increased uncertainty.

The final model calibrations for both species showed excellent fit between the observed and most probable parameter vector based predictions for each of the state variables. To some extent this is to be expected as fits are shown for data with which the calibration was completed. However, one of the main arguments for the use of Bayesian calibrations is that both model and dataset may be fully utilised. The under and over prediction seen in certain state variables are small (Table 3.4), but may be improved by changing the structure of the sub-models

(Equations 4.1a, 4.1b, 4.1c). For example García and Ruiz (2003) used a simpler mortality model than presented here, and alternative forms of the von Bertalanffy equation have been previously compared for site index (Li *et al.*, 2011). This would be straightforward to compare using a BMC, as previously suggested.

The broad prior distributions for the parameters allowed both species to converge on posterior parameter distributions within three million iterations. Accordingly, the same prior distributions could be employed to obtain posterior distributions and thus parameter estimates for other species in other regions given comparable PSP data. The prior distribution provided an adequate balance between exploring parameter space and time to compute the Markov chain. A simpler Markov Chain method could have been used, but the number of iterations required to reach convergence would have been greater. Thus the DE-MC can be considered a computationally efficient approach to Bayesian calibration. Alternative Bayesian sampling methods could equally be used, such as Gibbs sampling (Gelman and Hill, 2007). The number of open source packages to perform such sampling are rapidly increasing (e.g JAGS (Plummer, 2013), STAN (Stan Development Team, 2014)) allowing for rapid development of forest models in a Bayesian framework.

3.5 Conclusions

This study has shown how Bayesian calibration can provide a flexible all-in-one framework for developing forest growth models, and calibrating their parameters. Both model structure and parameters can be simultaneously investigated and probabilities assigned to each. Additionally uncertainty estimates for both parameters and forecasts provided by posterior distributions enhance both model understanding and accounting efforts. The successful calibration of the SLeDG model demonstrated here could easily be adapted for other species, and it is

entirely possible to use this method to calibrate other forms of growth model. We would recommend this method for any future efforts in developing forest growth models.

Chapter 4

Combining a stand level dynamic growth model with LiDAR data to reduce uncertainty in forest growth estimates

J. Lonsdale[1,*], M. Perks[2], M. Mencuccini[1,3]

[1]School of Geosciences, University of Edinburgh, Edinburgh, EH9 3JN, UK

[2]Forest Research, NRS, Roslin, Midlothian, EH25 9SY, UK

[3]ICREA at CREAF, Cerdanyola del Valles, Barcelona, Spain

Abstract

Aerial light detection and ranging (LiDAR) is now often used to provide forest inventory data, due to the reduced cost of large scale surveys compared to ground measurements. However, aerial LiDAR is unable to provide a direct measurement of basal area or volume and usually relies on allometric relationships to estimate such variables. Data assimilation provides a method of combining a stand level dynamic growth model and its uncertainties with uncertain LiDAR observations to provide a potentially more accurate and precise assessment of a stand's state. LiDAR observations made at 4 times over 10 years were processed to provide estimates of forest stand-level (sub-compartment) height for Aberfoyle forest in Scotland. These top-height estimates were assimilated at the sub-compartment scale using an Ensemble Kalman Filter (EnKF) to investigate the potential for uncertainty reduction. Successive assimilations resulted in up to a 7.13 times reduction in state variable 50% uncertainty range at the forest scale. However, reductions were mixed at the sub-compartment scale. This is most likely a result of discrepancies between sub-compartment digital delineation and physical location. Sensitivity analysis of observation uncertainty indicated that if observational uncertainty could be reduced, the overall uncertainty following data assimilation could be reduced further.

4.1 Introduction

Difficulties with physical access and with the appropriateness of the spatial scale at which accurate forest inventory measurements can be conducted has led to increased usage of LiDAR technology instead of more labor intensive inventory practices (Evans *et al.*, 2006). Over the last decade a number of methods have been developed using light detection and ranging (LiDAR) data to estimate forest stand parameters such as stand and individual tree height; biomass and volume; Leaf Area Index; and even estimate parameters such as species composition. Comprehensive overviews of recent methods are given in van Leeuwen and Nieuwenhuis (2010) and Koch (2010). Estimates of individual tree and stand height have achieved high accuracy, for example RMSE of 0.23 m and 0.06 m respectively (Næsset and Økland, 2002). However, estimates for other stand parameters such as basal area and above ground biomass, which do not directly relate to LiDAR returns, may have much lower accuracy and precision: Anderson *et al.* (2008) achieved R^2 values of 0.16 and 0.27 for basal area and above ground biomass respectively.

One way of potentially improving estimates is to combine additional data sources with LiDAR data. This has commonly been performed using additional remote sensing data, for example with radar sensors (Hyde *et al.*, 2007), multi/hyperspectral sensors (Swatantran *et al.*, 2011; Anderson *et al.*, 2008; Popescu *et al.*, 2004), satellite imagery (St-Onge *et al.*, 2008; Hudak *et al.*, 2002; Lefsky *et al.*, 1999), and aerial photography (Suarez *et al.*, 2005).

Another way of improving forest inventory estimates is to use LiDAR estimates (and other remote sensing data) in the parameterisation of models which predict forest growth. Patenaude *et al.* (2008) used Bayesian calibrations to parameterise the Physiological Principles Predicting Growth (3PG) model (Landsberg and Waring, 1997) using a combination of hyperspectral, Radar, and LiDAR data.

The advantage of the Bayesian approach is that the uncertainty of the remote sensing estimates could be included in prior probability distribution functions of parameters. This results in a better overall understanding and representation of model and parameter uncertainty (van Oijen *et al.*, 2005). Indeed, Bayesian statistics have been used for a number of years in other fields of research to combine remote sensing data with models through a process of data assimilation. Examples exist in meteorology (Houtekamer and Mitchell, 2005, 2001), climatology (Annan *et al.*, 2005), oceanography (Haugen and Evensen, 2002; Evensen and Leeuwen, 1996), and hydrology (Moradkhani *et al.*, 2005), which all use the Ensemble Kalman Filter (EnKF) (Evensen, 1994) to perform the data assimilation. Data assimilation assumes that neither observations nor models provide a perfect description of a system, but combining them may provide the best estimate (Williams *et al.*, 2005).

The EnKF is based on the Kalman filter, which has been used for over 30 years in forest inventory (Walters *et al.*, 1991; Gertner, 1984; Dixon and Howitt, 1979). More recently, the Kalman filter has been used in the inventory of agricultural crops (De Wit and van Diepen, 2007), and in forest carbon accounting (Williams *et al.*, 2005). However, it has never seen widespread use in forest growth modelling, and has never been applied to combine forest LiDAR measurements with growth models, to the knowledge of the authors.

Here we present the first model-data fusion between a Stand Level Dynamic Growth (SLeDG) model and aerial LiDAR top height measurements to provide an adjusted uncertainty estimate of a forest inventory in a UK forest. We have combined a series of LiDAR measurements taken over 10 years in a Scottish forest with model estimates for stands of Sitka spruce (the most important timber species in the UK (Scottish Executive, 2012)) using an EnKF method.

4.2 Methods

4.2.1 Data

LiDAR measurements were collected from the area of Queen Elizabeth forest near Aberfoyle in the years 2002, 2006, 2008, and 2012. Each year covered a slightly different area and so the area for the analysis was reduced to the area which was covered in all years. The measurements cover an area from 56.12N -4.49E to 56.20N -4.31E. Details of the data capture are given in Table 4.1. Digital terrain models and canopy height models were provided with 1×1 m resolution, and percentile LiDAR returns were provided with 10×10 m resolution.

Table 4.1: LiDAR sensor summary for each year surveyed.

Parameter	Aberfoyle 2002	Aberfoyle 2006	Aberfoyle 2008	Aberfoyle 2012
Sensor	Optech ALTM2033	Optech ALTM2100	Optech ALTM2100	Optech Gemini 167 ALTM
Date of collection	19 Sept. 2002	31 May 2006	12 March 2008	31 March 2012
Laser pulse frequency	33,000 Hz	100,000 Hz	100,000 Hz	100,000 Hz
Flying altitude	1000 m	950 m	1000 m	1000 m
Scanning angle	20 degrees	10 degrees	20 degrees	10 degrees
Sampling intensity	3-4 hits m^{-2}	10-17 hits m^{-2}	1-3 hits m^{-2}	4-8 hits m^{-2}
Position accuracy	X,Y <40 cm	X,Y <40 cm	X,Y <40 cm	X,Y <40 cm
Elevation accuracy	Z <9- 15 cm	Z <9- 15 cm	Z <9- 15 cm	Z <9- 15 cm

Information on sub-compartment (stand) spatial data was obtained from the

Table 4.2: Mean statistics (and standard deviation) of ground data plots. Yield class is a measure of productivity estimated by maximum mean annual increment. DBH is diameter at breast height (1.3 m).

Plot	Age (yr)	Yield Class ($m^3ha^{-1}yr^{-1}$)	Tallest stem (m)	Mean DBH (cm)	Number of Stems
A111	29	18	21.6 ± 0.15	21.3 ± 7.68	6
A112	32	14	24.2 ± 0.12	27.8 ± 4.90	5
A1i	29	18	21.1 ± 0.33	24.9 ± 6.18	14
B111	39	20	25.6 ± 0.29	30.8 ± 4.46	4
B1b	31	20	27.7 ± 0.34	20.3 ± 6.16	15
B2f	43	20	21.6 ± 0.08	16.1 ± 5.34	14
C111	26	14	26.9 ± 0.65	35.0 ± 10.6	9
C112	41	20	31.6 ± 0.21	40.5 ± 9.68	6

freely available sub-compartment database (SCDB) GIS shapefiles (`http://www.forestry.gov.uk/datadownload`).

An additional eight ground measurements were used for benchmarking. They are summarised in Table 4.2. Locations were randomly assigned within the study area and are shown in Figure 4.1. These ground measurements were collected in March 2014 for timber quality assessment, and consist of 10×10 m plot measurements of diameter at breast-height (dbh) of all trees within the plot and the height of the tallest tree in the plot which provides an estimate of top height similar to that suggested by Hamilton (1975).

LiDAR Processing

In order to convert the LiDAR returns to stand level top height measurements, the 95th percentile returns were used: this is the height at which 95% of the laser pulses detected by the LiDAR sensor fall below in a given raster cell. The 95th percentile raster was multiplied by a scalar value of 1.1 which has previously been shown to estimate top height at a raster cell level with errors of only 5% (Juan Suarez, *Pers. Comm.*). The Zonal Statistics package in Quantum GIS (QGIS)

(QGIS Development Group, 2014) was used to calculate mean and standard deviation top height of each sub-compartment. This is achieved by calculating the mean and standard deviation for all raster cells within a given sub-compartment's geospatially defined area (often referred to as a sub-compartment polygon). This therefore includes a combination of measurement uncertainty and within stand variation in the observation uncertainty. Sub-compartments where the top height decreased between measurements were excluded from this analysis (removed sub-compartments $n = 103$), as insufficient information was available to determine the cause of a decrease in top height.

4.2.2 Stand level dynamic growth model

The SLeDG model is derived from the model first suggested by García (1979). Models of this style describe the forest stand by a state variable which is forecast using dynamic equations which are biologically based. In this instance the state variable was comprised of the commonly used forest variables top height (H), number of stems per hectare (N), and the product of basal area and top height ($B \times H = W$), henceforth referred to as tubular volume. Changes in state variables were forecast as a function of themselves as is the case in dynamical systems (Luenberger, 1979), and they are the same as have been previously used in Chapter 3. The equations are given below.

$$\frac{dH}{dt} = b_1 \left[(b_2/H)^{b_3} - H \right] \tag{4.1a}$$

$$\frac{dN}{dH} = -b_4 H^{b_5} N^{b_6} \tag{4.1b}$$

$$\frac{dW}{dH} = b_7 H^{b_8} N^{b_9} - b_9 \frac{W}{N} \frac{dN}{dH} \tag{4.1c}$$

In this instance b_1 is a stand specific parameter. Its value is estimated by substituting a site index derived from the Forestry Commissions productivity estimated yield class (YC) into equation 4.1a with an index age of 50 years. Site index is estimated from YC according to the equation:

$$H_{50} = \alpha_1 + \alpha_2 \mathrm{YC} \tag{4.2}$$

The values for α_i and the other parameters ($b_2 ... b_9$) have previously been estimated with the Bayesian calibration in Chapter 3 and are given in table 4.3.

Table 4.3: SLeDG parameter means and ranges for Sitka spruce. There is no distribution for b_1 as it is a local parameter estimated from the given yield class of each stand.

			95% credible interval	
	Mean	Standard deviation	Min	Max
α_1	15.7	4.01	8.56	24.1
α_2	1.36	0.232	0.922	1.85
b_2	0.0222	0.00647	0.0116	0.0355
b_3	0.560	0.219	0.105	0.923
b_4	0.00163	0.00331	1.02×10^{-5}	0.0102
b_5	0.217	0.173	7.68×10^{-3}	0.608
b_6	1.56	0.200	1.19	1.98
b_7	8.01	5.44	1.84	22.2
b_8	0.237	0.179	8.83×10^{-3}	0.658
b_9	0.253	0.128	0.0255	0.506

Greater detail of SLeDG models can be found in a number of other papers (e.g. Lonsdale *et al.* (2015); García (2013); García and Ruiz (2003)) which are beyond the scope of this paper.

4.2.3 Ensemble Kalman Filter

The EnKF is a development of the Kalman filter (Kalman, 1960). Overall error in a modelled system is minimised by combining model forecasts with measurements of the system. The impact of model versus measurement on the Kalman filter analysis is weighted by the error covariance of each (Evensen, 2009): In cases where measurement error is small the output approaches the measurement, however where there is larger error in the measurement (or the measurement is missing) there is larger weighting on the model predictions (Williams *et al.*, 2005). The original Kalman filter assumes Gaussian noise in both the system and measurements, and linear system dynamics; the EnKF uses an ensemble in order to estimate the covariance matrices which would either be unmanageably large or impossible to calculate with more complicated non-linear system dynamics. Instead of requiring an algebraic solution to forecast the state variable probability density, the probability density of the state variable is simulated using a large ensemble of forecasts which represents the best estimate of the state variable (Houtekamer and Mitchell, 2005) in a Markov Chain Monte Carlo (MCMC) method (Evensen, 2009).

Commonly this ensemble is generated by assuming that the model in equations (4.1a..c) contains model errors, and can be summarised as a stochastic differential equation:

$$d\psi = G(\psi)dt + m(\psi)dq \tag{4.3}$$

where ψ is the state vector $[H,N,W]$, G is equivalent to the model described in equations (4.1a..c), and $m(\psi)dq$ is a random stochastic forcing representing model errors using a Brownian motion process described here as dq. However, in this instance the ensemble is generated by drawing a sample of n parameter vectors (equal to the desired ensemble size) from the Markov chain generated in a previous model Bayesian calibration (detailed in the previous chapter). An ensemble of

state variables (e.g. $n = 100$) is forecast through time according to equation 4.3 using each parameter vector drawn, and then error covariances within the state vector are estimated for the model.

Error covariances for the state variable observations are then calculated by creating an ensemble of observations (d_j) of equal size to the ensemble forecast ($n = 100$) with Gaussian noise added to simulate measurement errors:

$$d_j = d + \epsilon_j \tag{4.4}$$

Here j is the ensemble instances from 1 to n, and ϵ is the simulated measurement error with a mean of zero and a variance equal to the observational uncertainty. The covariances in observations can then be estimated from this ensemble.

Once these have been calculated, an analysis step can be taken to combine the modelled and observed state variable according to the following equation:

$$\psi_j^a = \psi_j^f + K_e(d_j - M\psi_j^f) \tag{4.5}$$

where ψ^a is the analysed state variable estimate from the filter, ψ^f is the state variable forecast by the model. K_e is the Kalman gain and is a function of both model and measurement covariances estimated from both the observed and forecast ensembles. M is an operator that maps modelled variables to observed variables (as may be the case when state variables are not directly observed). In this instance $M = 1$ as the top height measurement directly relates to model output. $d_j - M\psi_j^f$ is the innovation vector, the difference between the observed ensemble (Equation 4.4) and the model forecast ensemble.

The EnKF was implemented using Python for this study. An adapted version

of the Pyda (`http://hickmank.github.io/pyda/index.html`) code was specifically developed that integrated with QGIS. Although faster Fortran implementations exist (e.g. Evensen (2003)), the ease of using python scripts with QGIS made Python preferable.

4.2.4 Workflow

For each sub-compartment, three ensemble forecasts of the state variables were calculated between stand establishment and a horizon of 100 years:

- Standard EnKF: An EnKF forecast assimilating the LiDAR top height observations aggregated to the sub-compartment level with observational uncertainty based on within sub-compartment variability.
- Reduced observational uncertainty EnKF: An EnKF forecast assimilating the LiDAR top height observations with a nominal 5% observational standard deviation.
- Model only forecast: A forecast made with only the SLeDG model. No assimilation.

In all cases an ensemble of $n = 100$ was used for each sub-compartment. Allen *et al.* (2003) suggested that an ensemble size of 100 members is usually sufficient, and this has been shown to be the case in a number of other studies (Gao *et al.*, 2011; De Wit and van Diepen, 2007). Additionally an ensemble of 100 members provides a reasonable computation time of 30 minutes to analyse the four observations over all 137 sub-compartments in this study. Initial stand conditions were set at an initial top height of 1.3 m, stand spacing and yield class as given in the SCDB, and basal area of zero.

In the two EnKF ensemble forecasts sub-compartment top height estimates from percentile returns of the LiDAR data were assimilated for each sub-compartment at the year when measurement occurred. This resulted in outputs of a series of analysis distributions of the state variable through time. The innovation vector was quantified for each sub-compartment at each LiDAR measurement point, calculated from the mean values of top height of both the model forecast ensemble and LiDAR estimated observation ensemble. The reduced observational uncertainty EnKF was run with 5% standard deviation to assess sensitivity to uncertainty in observations. This nominal value was selected as it has been suggested as the top height LiDAR error at the 10 $\times$ 10 m pixel level (J.Suarez, *Pers. Comm.*) and thus represents a 'best case' measurement uncertainty. Comparisons were made between the two different levels of observation for each sub-compartment.

The standard EnKF was also compared with the SLeDG model only forecast to demonstrate both the difference in state variable forecasts and uncertainty. The fit of both model only and standard EnKF predictions of top height to the LiDAR estimate were compared.

4.3 Results

4.3.1 Innovations due to EnKF

Innovation is the difference between the observation ensemble and the model forecast ensemble, thus only top height (H) innovation vectors could be considered. At the forest level (over all sub-compartments), the mean innovation vectors were non-significant in 2002, 2006, and 2008. Thus there was not a significant difference between the forecast ensemble and LiDAR observed top height. However, the

innovation vector in 2012 showed that observed LiDAR top height estimates were larger than ensemble forecast by 1.07 ±0.02 m. The top height innovation over LiDAR estimates in 2012 can be observed visually, by sub-compartment, in Figure 4.1. Innovation can be seen to vary between -8.00 to 8.00 at the sub-compartment level.

4.3.2 Uncertainty

State variable uncertainty was adjusted following each analysis step of the EnKF. An example of this can be seen in Figure 4.2. The 50% credible interval ranges in each sub-compartment were used to assess changes in uncertainty following the data assimilation. The difference between the forecast ensemble (ψ^f) uncertainty range and the analysed ensemble (ψ^a) uncertainty range is given in Table 4.4. In the first assimilation of 2002 LiDAR data the 50% uncertainty range increased significantly in all state variables (Table 4.4). This indicates a lack of overlap between the uncertainty ranges of the forecast ensemble and LiDAR derived observation, thus resulting in a stretched probability distribution across both uncertainty ranges. Reductions in uncertainty range occur for top height in 2006 and 2008, and in stem number uncertainty range in 2008. In both cases although statistically significant the size of reduction represented a nominal change (only centimeters or less than a single stem: Table 4.4).

Table 4.4: Changes between forecast ensemble 50% uncertainty range and analysed ensemble 50% uncertainty range after assimilating each years LiDAR data. Negative indicates a reduction in uncertainty range.

	2002	2006	2008	2012
Top height (m)	4.76*	-0.02*	-0.01*	-0.01
Stems ha^{-1}	256.53*	-0.46	-0.83*	-0.56
Tubular volume (m^3)	344.87*	0.36	0.32	-0.48

$*$ indicates significant change($P > 0.05$)

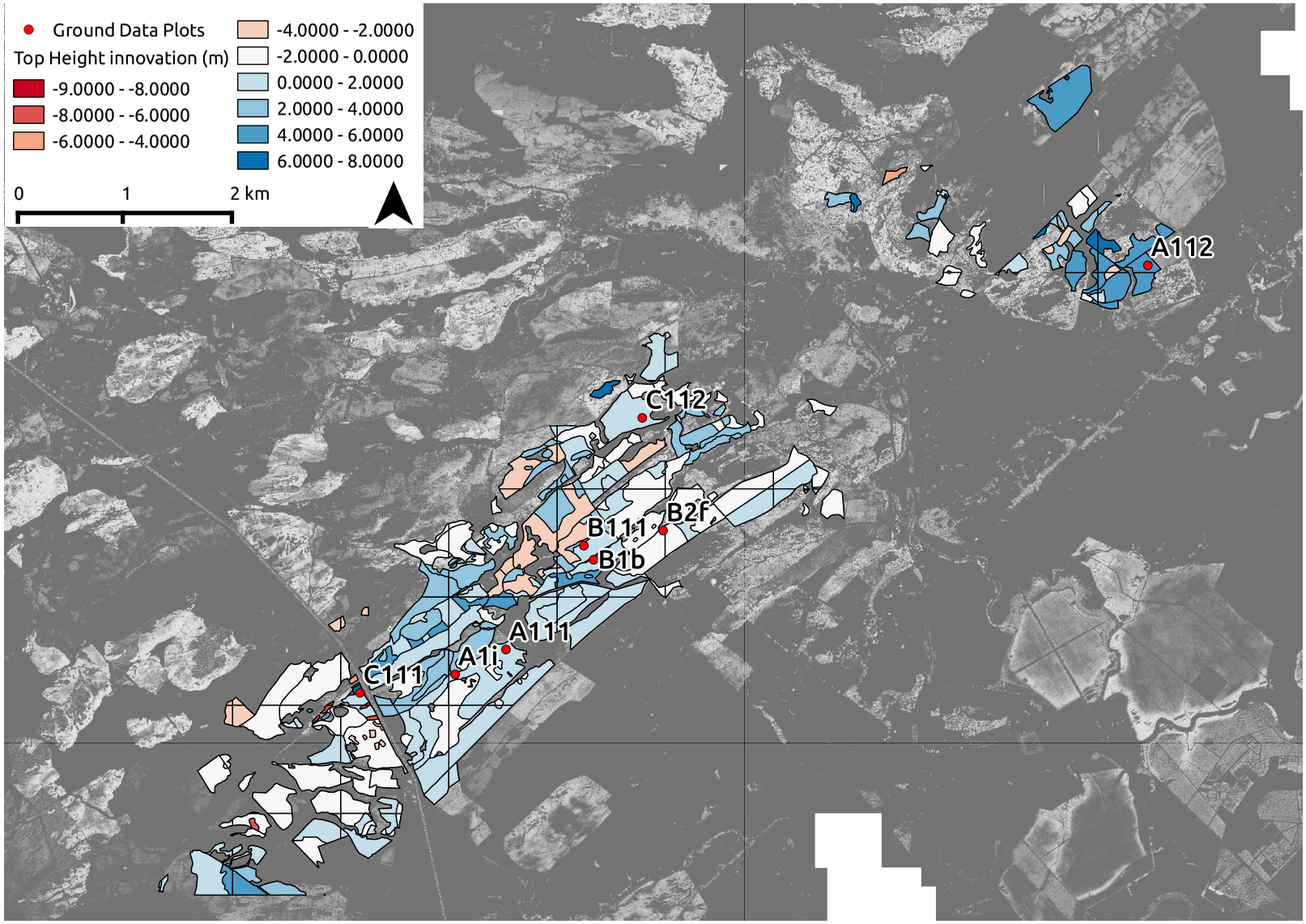

Figure 4.1: Top height innovation in 2012 where innovation is calculated as observation ensemble minus forecast ensemble. Points indicate ground measurement plot locations.

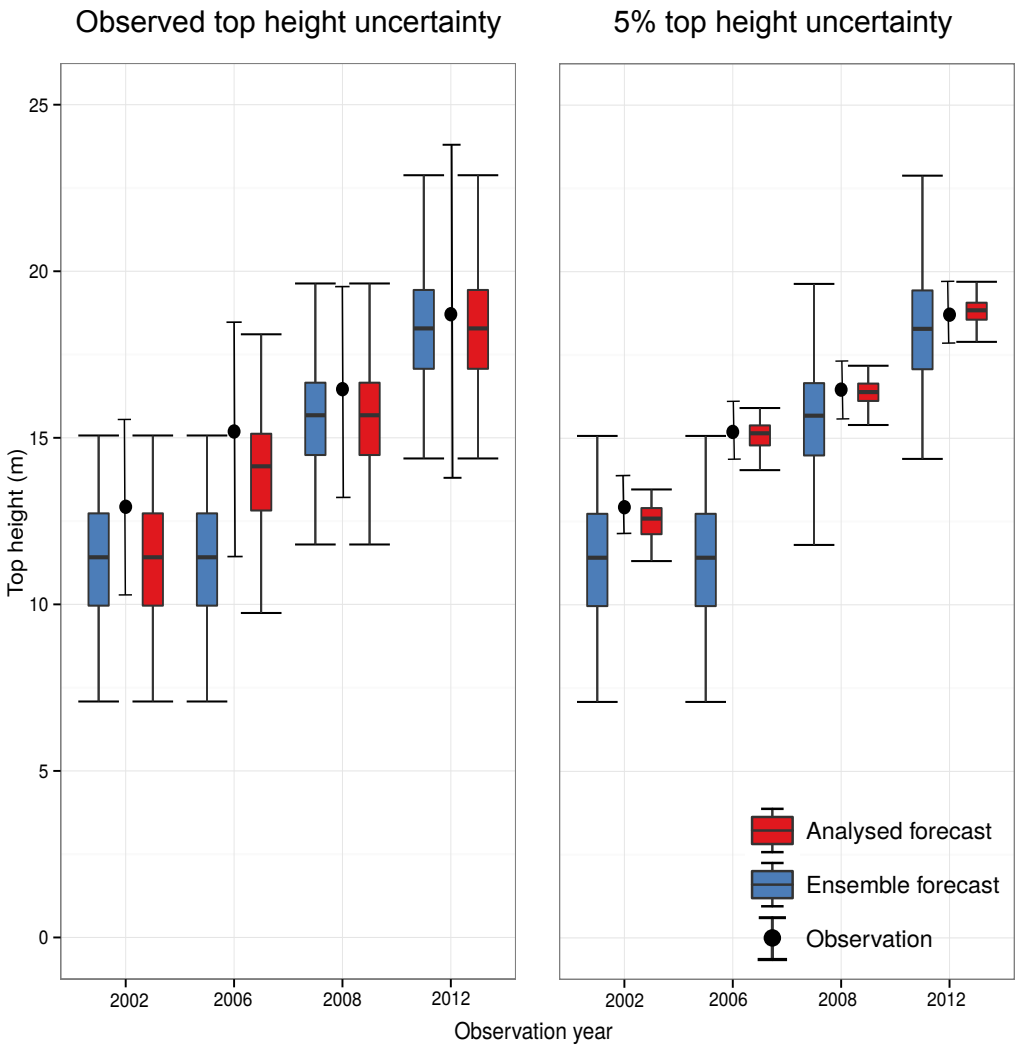

Figure 4.2: Randomly sampled sub-compartment illustrating analysed top height ensembles (ψ^a, in red) after assimilation of data (indicated a black point with standard deviation bars) versus original ensemble top height forecasts (ψ^f, in blue) at each LiDAR observation. Boxes indicated interquartile range, and whiskers the 95% credible range for height. The left-hand plot uses sub-compartment mean height with error estimated by within sub-compartment variability, the right-hand plot uses sub-compartment mean height with an assumed 5% error in that mean.

A summary of the 50% credible interval ranges for all sub-compartments, predicted both following the EnKF analysis step and with the SLeDG model only, are shown in Figure 4.3. The median of sub-compartment 50% credible interval ranges were reduced by 6.34, 7.36, and 6.11 times between the analysis in 2002 and 2012 for top height, number of stems per hectare, and tubular volume respectively. This can be seen in the light coloured boxplots in Figure 4.3. Although the median 50% credible interval range decreases overall following analysis between 2002 and 2012, it is interesting to note that there is an increase in median credible interval range between 2008 and 2012 for all state variables (see Fig. 4.3). This corresponds with the significant innovation vector for top height seen in 2012. All outliers in the analysis of the credible interval ranges derived from the EnKF analysis are from stands where the sub-compartment database shapefiles (polygons representing the spatial location of sub-compartments) did not match accurately with stand plantings (Figure 4.5). This issue is considered further in the discussion.

4.3.3 Sensitivity

Reducing the uncertainty in observations did not alter the mean values of analysed distributions, which is unsurprising as the mean values of the LiDAR observations were the same in both EnKF runs. However, uncertainty in the analysed distributions was affected as can be seen in Figure 4.2, where reduced observation uncertainty results in a tighter uncertainty range following analysis. The impact on uncertainty of reducing observation uncertainty was inconsistent. The top height 50% uncertainty range was reduced by a mean value of 0.20 m following the initial analysis in 2002. Subsequent assimilation steps showed an increase in the top height 50% range for 2006 and 2008, and an average increase in the 50% uncertainty range of 0.04 m in 2012, a nominal physical

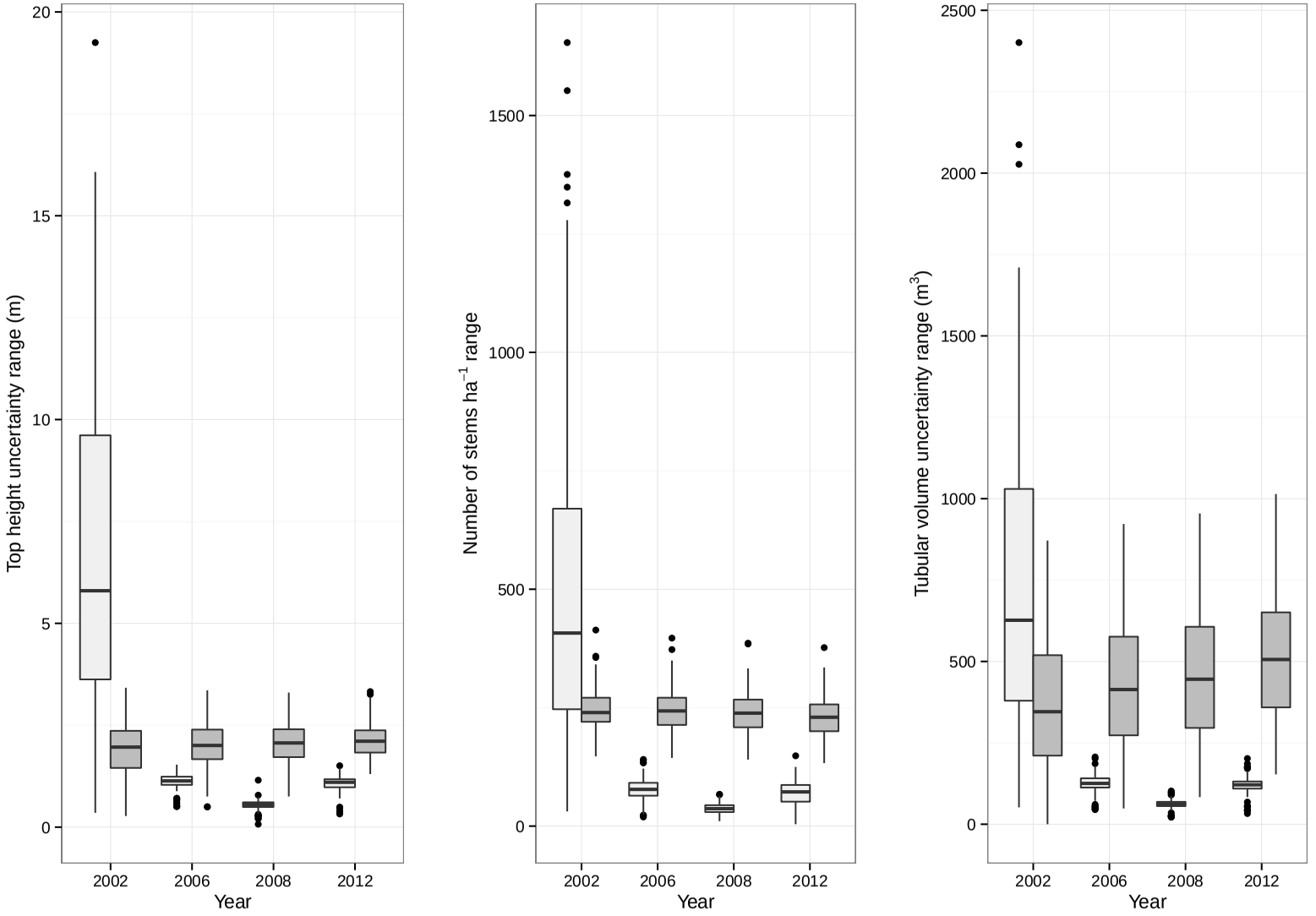

Figure 4.3: Variation in 50% credible interval range for state variables' probability distributions in all sub-compartments. Light boxes indicate ranges from Ensemble Kalman Filter (EnKF) analysis, dark boxes indicate ranges derived from model ensemble forecasts.

Table 4.5: Mean difference and confidence intervals (CI) between EnKF analysed predictions and model only prediction for state variables. Negative values indicate model over-estimates.

Year	Top height (m)		Stems ha^{-1}		Tubular volume (m^3)	
	Mean	95% CI	Mean	95% CI	Mean	95% CI
2002	-0.256	-0.421 – -0.0909	6.84	4.61 – 9.07	-8.54	-10.4 – -6.71
2006	-0.337	-0.546 – -0.128	7.70	5.01 – 10.4	-10.0	-12.8 – -7.32
2008	-0.352	-0.632 – -0.0728	7.75	4.67 – 10.8 6	-10.9	-14.3 – -7.37
2012	-0.316	-0.679 – 0.0464	6.84	3.25 – 10.4	-12.2	-17.2 – -7.17

value. Without observations of stems per hectare and tubular volume, there was no significant difference in their uncertainty based on a reduction in observed top height uncertainty alone.

4.3.4 Model comparison

In all cases the model consistently overestimated the height and volume, and underestimated the number of stems per hectare compared to the EnKF analysed predictions (Table 4.5).

Although median credible interval range in model only ensemble forecasts can be seen to change in all three state variables (Figure 4.3) there is no significant change ($P > 0.05$ in all cases) in the credible interval range according to an ANOVA. Thus uncertainty in model only predictions remains constant over the 10 years of observations. Outliers in model only ensemble range size were again a result of sub-compartment shapefile polygon mis-alignment.

4.3.5 Ground data

As the ground data consists at most of two plots within each sub-compartment it is not possible to draw any statistical conclusions regarding the fit of the models.

Instead, only a visual inspection can be made to indicate performance of the EnKF.

Here, the forecast of tubular volume is used with the ground data to show the performance of the data assimilation. Tubular volume increment is dependent on the state of all three state variables (Equation 4.1c.) thus allows a convenient proxy to consider all variables. As can be seen in Figure 4.4, for all but two plots (B111 & B2f), standard deviations of tubular volume overlap the 90% credible interval of predictions for the sub-compartment that they are located in.

4.4 Discussion

In this example of using the EnKF, a desirable reduction in forest stand variable uncertainty was not entirely achieved. Repeated assimilation of LiDAR data does reduce the uncertainty in state variables at the forest scale compared to model only predictions (Figure 4.3). At the sub-compartment scale the uncertainty reduction following each assimilation is often less obvious, with both large increases and minimal decreases in uncertainty range on average following each assimilation (Table 4.4). This is most likely a consequence of both initial sub-compartment conditions and the observational uncertainty, which in many cases appears to be greater than the model uncertainty.

Initial conditions are provided by the SCDB, and include the yield class which is used to establish site index in the SLeDG model (Equation 4.2). Yield class is often established based on a previous rotations growth (Forestry Commission, *Pers. Comm.*) and may not be representative of the current productivity of a sub-compartment. The result could be that the model running up to the initial assimilation vastly over- or under-estimates the top height, thus creating a greater disparity between the LiDAR observation and model. This increases the spread in

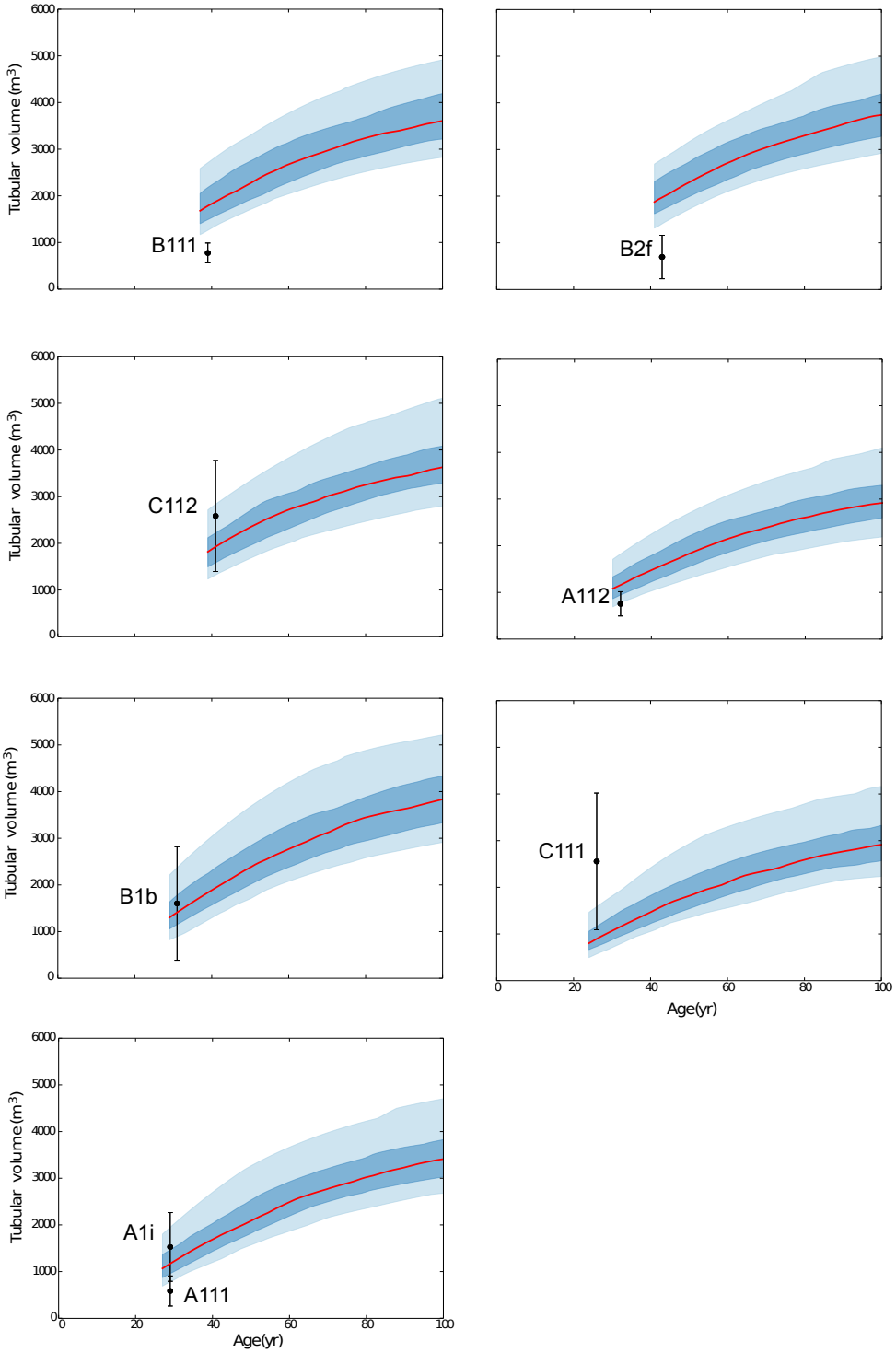

Figure 4.4: Stand tubular volume growth forecasts including median (red line), 90% (light blue area), and 50% (dark blue area) credible intevals following data assimilation in 2012. Ground data from 2014 is shown by the points with bars indicating standard deviation.

the analysed probability distribution. One way to ameliorate this is by allowing the yield class to be updated by the EnKF, although this would bring up the question of site-site index versus stand-site index raised in Chapter 3. Regardless, this initial condition affects both the assimilation and the model only predictions, and thus it may be appropriate to question the uncertainty range in model only predictions shown in Figure 4.3, which does not include yield class uncertainty. In future it may be most suitable to represent yield class with a probability distribution which is easy to implement in any Markov Chain predictive method: be it Bayesian calibration or EnKF.

Regarding observational uncertainty (in LiDAR measurements), the sensitivity analysis indicates that reducing the observational uncertainty could go some way to improving the benefits of the EnKF in reducing uncertainty (Figure 4.4). Therefore the issues of where the observational uncertainty comes from and how to reduce it in the future must be considered.

Kalman filters (including EnKFs) are not robust to large innovation due to outliers. Large innovations may affect the accuracy of the state predictions produced by the analysis (Roh *et al.*, 2013). Although at the forest level there was not significant innovation in the first three data assimilations, the sub-compartments showed a wide range of innovations with absolute values up to 8 m (Figure 4.1). Such innovations are likely a result of misaligned sub-compartment polygons (Figure 4.5). The mismatching of the sub-compartment polygons with observed forest stands seen in the LiDAR images, demonstrates what is referred to as representiveness errors (Koohkan and Bocquet, 2012). These occur where the scale of the model does not match the scale of observation. For example: in Figure 4.5 the central sub-compartment (labeled 310003076) mostly contains tall trees. However, smaller trees which should presumably belong to the surrounding sub-compartment (labeled 310003070) are also included. This should create greater uncertainty in the sub-compartment top height estimated

by aggregating the pixels, with a lower than expected mean top height. Instead, a bi-modal probability distribution function for top height is simplified to a normal distribution, and the observational uncertainty is underestimated. This results in a larger Kalman gain value (K_e), overweighting the innovation in the analysis step (Equation 4.5).

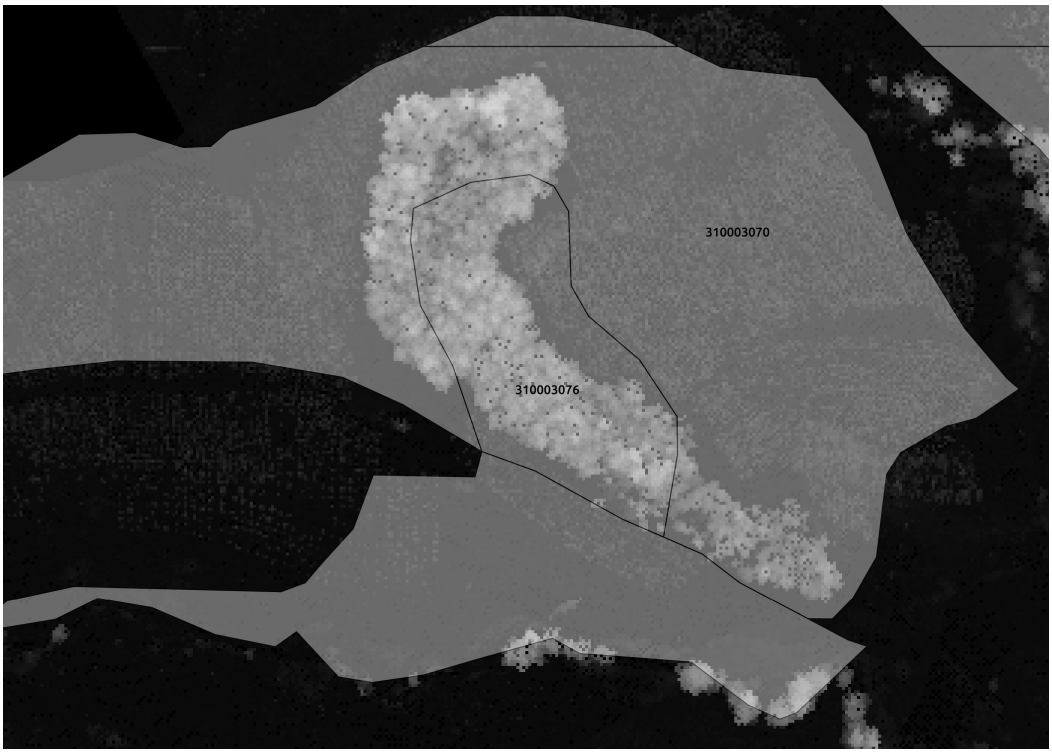

Figure 4.5: Demonstration of how sub-compartment shape definitions do not align with planting observed in LiDAR data.

It was not possible to estimate the scale of this issue, as attempts to define sub-compartments using unsupervised classifications based on LiDAR values were judged to be unsatisfactory in a visual assessment. However, in future it may be possible to combine the LiDAR observations with optical satellite data such as Landsat (e.g Lefsky *et al.* (1999)) to better define sub-compartments. Another potential improvement is to apply the EnKF at the pixels scale, thereby avoiding the representiveness error. Although initial conditions of each pixel would still be difficult to establish based on the inconsistency between observed stands and the sub-compartment polygons (Figure 4.5). It could be possible to run a within

sub-compartment pixel level height model similar to the sub-grid model suggested by Koohkan and Bocquet (2012) in dealing with representiveness errors. There are additional steps that can be taken within the EnKF analysis, such as either clipping (reducing to a reasonable value) or removing innovations that are greater than a given value, or using a robust variation of the EnKF (Roh *et al.*, 2013). It may also be possible to use non-gaussian distributions within the EnKF as has recently been discussed by Fowler and Van Leeuwen (2013). Of course, redefinition of the sub-compartment database shapefile to better align with reality would also be of benefit, though may be prohibited by cost at the national scale.

The assimilation of the top height from the LiDAR did little to reduce uncertainty in the other two state variables (number of stems and tubular volume). This is to be expected when there was little reduction in the uncertainty of top height through assimilation. The reduction in uncertainty would have been passed on through the covariance matrices which are used in the calculation of the Kalman gain value (K_e). Therefore, to reduce uncertainty in these variables, it would be necessary to have a reduction in the top height uncertainty, or perhaps more useful would be to provide observations of number of stems and tubular volume in the future. These could be provided from remote sensing, such as aerial and terrestrial LiDAR. Individual stems may be identified using either variable window filters or wavelet analysis (Falkowski *et al.*, 2006), and tubular volume might be estimated using terrestrial LiDAR measurements (Maas *et al.*, 2008). Even a single estimate of these made in concert with the top height estimates could better constrain the state space of each sub-compartment.

The ground-based measurements should have been useful as a benchmark of forecasts made following the final assimilation of the LiDAR data with the EnKF. Unfortunately, the lack of replication within each stand limits the usefulness. The most that can be inferred is that following assimilation, the models forecasts are mostly consistent with ground-based measurements. A more thorough program

of ground measurement could be used to better benchmark, or indeed provide additional inputs for the EnKF in future.

If nothing else, this paper illustrates the potential for the use of the EnKF in the future of forest inventory. The EnKF is relatively simple to implement, and requires modest computing power when the models are not too complex. While there are obviously issues to address, this method has not previously been applied in this field and so such issues are to be expected. This method could easily be applied to any single species stands with an appropriate growth model and observation data. In future it could even be applied to more complex stands given an appropriate mixed species model and accurate enough observations. As forest data becomes cheaper to obtain through new techniques of data capture, it is useful to have tools such as the EnKF to take advantage of them. However, care must also be taken to ensure that such data is fit for purpose.

Chapter 5

Synthesis and conclusions

5.1 Summary

The aim of this work was to investigate models for forecasting UK forest growth, and reducing uncertainty in predictions. A number of approaches to the modelling of growth of the two most important conifer species (Sitka spruce and Scots pine) in UK forests have been presented here. The Stand Level Dynamic Growth (SLeDG) model structure allows the forecasting of any stand from any point in state-space, regardless of previous management. This is an improvement over existing look-up table models similar to those of Edwards and Christie (1981) which do not allow for deviations from predetermined management regimes. Models such as Physiological Principles Predicting Growth (3PG)N represent the underlying physiological processes with more realism than SLeDG models, making them useful for providing growth forecasts given climatic change. Different tradeoffs were indentified. The extra complexity of process-based models can lead to greater uncertainties if insufficient data are available for parameterisation, whereas parameterisation of the SLeDG model is relatively robust even when only a small dataset is available. The SLeDG model is also relatively simple with only three or four (See Chapter 2.) transition functions to forecast the state of a stand. This has made it very suitable for demonstrating the use of Bayesian techniques for model selection, calibration, and inventory revision using remote sensing observations.

Bayesian techniques provide a useful structure for the modelling of forest growth, whilst allowing for an enhanced understanding of the uncertainties involved, compared with a frequentist approach. Bayesian model comparison provides a probabilistic way of selecting models: be it comparing different models (e.g. van Oijen *et al.* (2013)) or simply different structures of a single model, as demonstrated in Chapter 3. Bayesian calibrations explore parameter space in order to quantify the whole posterior distribution. The Differential Evolution

Markov Chain (DE-MC) method provides efficiencies in the way that parameter space is explored in order to reduce the computational cost of randomly exploring parameter space. In empirical models such as a SLeDG type model, often the parameters do not represent physical constraints that might be present in process-based models (e.g. photosynthetically active radiation (PAR)). Thus parameter space may be constrained in the specification of priors consistent with previous (frequentist) calibrations of models. With loose enough constraints, it has been possible to parameterise two separate species for the UK, and it is possible that the constraints will work for other conifer species in the UK. These calibrations result in predictions that are consistent with existing forecasts, but provide additional information regarding the uncertainties of parameters and thus uncertainties of model outputs when conducting forecasts.

The information on parameter uncertainty is particularly of use when performing data assimilations with an Ensemble Kalman Filter (EnKF). Data assimilation may allow for a reduction of uncertainty when repeated observations (measurements) are available to narrow the uncertainty in model only predictions. As ground measurements of forest inventory are time intensive (and thus have a high cost), modern light detection and ranging (LiDAR) techniques can provide large scale inventories for reasonable cost. Data assimilation of LiDAR top height with the EnKF was shown to have potential for improving inventory uncertainty. However, observational uncertainty restricted the uncertainty reduction. Adjustments to the EnKF analysis, as well as the processing and cleaning of observations, may reduce this observational uncertainty in the future and enhance this method for improved forest inventory at the national scale.

The variety of modelling methods presented in this thesis are discussed below: how they relate and reasons for their selection. The findings of this thesis also have a number of wider implications for future forest growth forecasting in the UK. Thus I will also discuss ideas that should be considered, both in modelling forest growth

and in models that themselves rely on forest growth models. Additionally, it is important to consider the data requirements for future forest modelling efforts and this is also discussed. Areas for further research are also discussed based on this research and predicted future needs.

5.2 Modelling techniques used

Throughout the thesis, the SLeDG model has been used as a method for forecasting forest growth. In Chapter 2, a non-Bayesian method is used to calibrate the SLeDG model, whereas Chapters 3 and 4 utilised Bayesian methods. The initial non-Bayesian method was selected for use in Chapter 2 in order to familiarise and understand how SLeDG models had recently been parameterised (for example García *et al.* (2011) and García and Ruiz (2003)). Once this was achieved it allowed an easier transition to using Bayesian methods to calibrate the SLeDG model, as the model's structure and function had been explored.

The Bayesian methods used in Chapters 3 and 4 were the author's first attempts at using Bayesian statistics to calibrate models. The decision was made to only use the three directly measured state variables in the SLeDG model to reduce model complexity and increase understanding of Bayesian methods, thus occupancy was not included. In future calibrations, occupancy could be included, and the Bayesian framework of Chapter 3 should be considered well suited to include latent variables with associated uncertainties. Indeed, a Bayesian model comparison could be used in the future to determine whether there is benefit to including occupancy in the SLeDG model.

It should be noted that the Ensemble Kalman Filter (EnKF) used in Chapter 4 is a special case of the Bayesian method used in Chapter 3 (Evensen, 2009), in that the posterior distribution is generated based on the prior distribution

being updated by the addition of evidence, given in this instance by LiDAR measurements. It was therefore useful to create the model ensemble in Chapter 4 using the distributions generated in Chapter 3, a technique that does not appear to have been used previously in the peer-reviewed literature.

5.3 Modelling implications

Are the models currently used in the UK for prediction of forest growth fit for purpose? While the M1 model and its predecessors (Edwards and Christie, 1981; Hamilton and Christie, 1971) may produce clear outputs when used for forecasting timber production, the outputs lack flexibility at a time where forest management is aiming to provide more services than just timber production (Welsh Assembly Government, 2009; Scottish Executive, 2006; Forestry Commission, 1998). Uncertainty estimates are increasingly important to forest managers (Kangas, 1999; Lohmander, 1988), and currently employed models have not been documented in the peer-reviewed literature for identification and quantification of uncertainty. This also has knock-on effects for models that are reliant on growth predictions, such as the C-FLOW model used in national land use, land use change and forestry (LULUCF) inventory reporting (Dyson *et al.*, 2009). In the past, computational costs may have limited forecasters to using Sitka spruce of an intermediated yield class to represent all conifer stands in the UK for carbon reporting (Cannell and Dewar, 1995; Milne *et al.*, 1998), however modern computing power should allow all stands to be forecast with species and productivity class-specific models that take into account differences in forest management. Indeed, while using a single intermediate value at a national scale may lead to an acceptable national estimate of carbon storage, it does not provide enough detail for forest managers to improve the carbon storage potential of complex and varied forest landscapes.

In the future, process-based models such as 3PG (Landsberg and Waring, 1997) may be more widely applied to forest growth forecasting, as they provide the kind of flexible predictions required to accomodate changes in management, and also climate (e.g. (Xenakis *et al.*, 2012)). However, at present the uncertainty in such models due to their large parameter sets limits their applicability in forest management.

SLeDG style models provide a middle ground with more flexibility than M1, but without the ability of accurately adjusting to environmental changes. They can be applied at a national scale, as demonstrated in Ireland (Broad and Lynch, 2006) and New Zealand (García, 1983), and may be parameterised with moderate datasets, as demonstrated in Chapter 2. They would be well suited to use in LULUCF reporting, and could easily drive the growth model component of wind risk (Gardiner and Quine, 2000) and timber quality models (Leban, 2003). Chapter 3 has created a Bayesian framework for species-specific calibrations suitable for other conifers in the UK (or elsewhere) and so efforts to calibrate the other major conifer species in the UK should be undertaken.

Beyond model calibration and model selection Bayesian methods may also provide further opportunities to combine multiple forest growth models for optimising forecasts. Several growth forecasts from different models could be combined using Bayesian model averaging, weighted according to the models' probabilities (Bullock and Boone, 2007). Additionally, new computational methods (e.g. MT-DREAM$_{zs}$ (Laloy and Vrugt, 2012)) and tools (e.g. rjags (Plummer, 2013)) for exploring parameter space are always being developed, and have potential to be applied in forest growth modelling. Bayesian methods have the potential to become commonplace in forest growth modelling given a level of explanation and documentation in applications appropriate to both modellers and potential users.

Indeed, more generally the documentation and publishing of growth models for

further benchmarking and criticism is important. With no plans to publish the M1 model (Jenkins, 2009) there is little scope for improvement of the model, for example attempt Bayesian calibration or model averaging. While innovation is required for publishing in peer-reviewed journals there are no shortage of platforms for publishing model details online and databases such as FORMODEL (Meredieu *et al.*, 2011) are also available. With more documented models, there is greater opportunity to apply them using techniques such as data assimilation demonstrated in Chapter 4.

5.4 Inventory implications

Further development of both models and data assimilation techniques require measurement and inventory data for parameterisation and assimilation respectively. The timescales involved in forestry make this a particular challenge, as permanent sample plot (PSP)s set out for producing inputs to provide model calibration inputs may not be fit for purpose by the time a usable dataset has been collected, and so as much data as possible should be collected when measuring PSPs to avoid inadequacy. Equally, as technology which reduces the cost of inventory becomes more widespread there are issues with dealing with very large datasets. Thus efforts to provide ways of processing and cleaning data from multiple sources in both a cost and time effective manner should be investigated. The availability of 'Big Data' sources is starting to be recognised in ecology (Hampton *et al.*, 2013) and methods applied in such fields may be applicable in forest inventory and modelling. Linked to this is the question of data availability. As with publishing model details, the open sharing of forest mensuration data among stakeholders is equally important for providing the most accurate and precise estimates of the state of forests. Policies by Research Councils instigating open

publication to justify the use of public funds may help to push such a trend further.

Modern LiDAR techniques can be used in forest inventory, and a number of suggestions are made in the discussion of Chapter 4 as to how advanced processing techniques may be applied to reduce measurement uncertainty. It is also possible to combine the use of LiDAR with satellite observations to provide both a further constrain and a wider observational area for data assimilation. Spatial statistics such as the k-Nearest Neighbour technique used by McInerney *et al.* (2010) could provide observations for the EnKF at a larger scale than a LiDAR flight. Larger scale data assimilation could be applied using a combination of LiDAR and satellite observations at a national scale to improve the national forest inventory. Another area for further investigation is to consider data assimilation with multiple measurements made at the same time. Chasmer *et al.* (2006) used coincident terrestrial and aerial LiDAR data capture and identified problems with each capture, however if both of these captures were combined with a model using an EnKF it may be possible to have a greater reduction in state variable uncertainty.

If there was to be an effort in the future to improve the UK forest inventory, a model-data fusion approach supported by data assimilation should be considered. It would allow for a larger scale area to be studied, with a great reduction in uncertainty.

5.5 Conclusions

All forest growth models have strengths and weaknesses. Mathematical models seek to represent a system by simplifying it to a series of equations. It is in the selection of how a system is represented that models differ. Models should be

developed (or selected) based on providing outputs for a given purpose. Modern UK forests are multi-functional, and require models that are flexible to changes in management (and potentially climate) in addition to having measures of accuracy and precision in forecasts. Bayesian statistics provide a useful probabilistic framework for parameterising and comparing models, and should be more widely applied in forest growth modelling. Modern forest inventory techniques such as LiDAR can be used in conjunction with growth models to provide a more accurate estimate of forest productivity. Having an improved understanding of the uncertainty in forest productivity can enhance models which are dependent on growth models, enhancing carbon storage estimates, wind risk predictions, and timber quality assessment. These enhancements all combine to improve the value of UK forests.

References

Aldhous, J.R. (1961). Provenance of Sitka spruce. *Forestry Commission Report on Forest Research for 1961*, 147–154.

Allen, J.I., Eknes, M. and Evensen, G. (2003). An Ensemble Kalman Filter with a complex marine ecosystem model: hindcasting phytoplankton in the Cretan Sea. *Annales Geophysicae*, **21**, 399–411.

Almeida, A.C., Siggins, A., Batista, T.R., Beadle, C., Fonseca, S. and Loos, R. (2010). Mapping the effect of spatial and temporal variation in climate and soils on Eucalyptus plantation production with 3-PG, a process-based growth model. *Forest Ecology and Management*, **259**, 1730–1740.

Anderson, J.E., Plourde, L.C., Martin, M.E., Braswell, B.H., Smith, M.L., Dubayah, R.O., Hofton, M.a. and Blair, J.B. (2008). Integrating waveform lidar with hyperspectral imagery for inventory of a northern temperate forest. *Remote Sensing of Environment*, **112**, 1856–1870.

Andrén, O. and Kätterer, T. (1997). ICBM: the introductory carbon balance model for exploration of soil carbon balances. *Ecological Applications*, **7**, 1226–1236.

Annan, J., Hargreaves, J., Edwards, N. and Marsh, R. (2005). Parameter estimation in an intermediate complexity earth system model using an ensemble Kalman filter. *Ocean Modelling*, **8**, 135–154.

Assmann, E. (1970). *The principles of forest yield study. Studies in the organic production, structure, increment and yield of forest stands*. Pergamon Press, Oxford, UK.

Balzter, H., Luckman, a., Skinner, L., Rowland, C. and Dawson, T. (2007). Observations of forest stand top height and mean height from interferometric SAR and LiDAR over a conifer plantation at Thetford Forest, UK. *International Journal of Remote Sensing*, **28**, 1173–1197.

Blanco, J., Seely, B., Welham, C. and Scoullar, K. (2008). Complexity in modelling forest ecosystems: How much is enough? *Forest Ecology and Management*, **256**, 1646–1658.

Broad, L.R. and Lynch, T. (2006). Growth models for Sitka spruce in Ireland. *Irish Forestry*, **63**, 53–79.

Bullock, B.P. and Boone, E.L. (2007). Deriving tree diameter distributions using Bayesian model averaging. *Forest Ecology and Management*, **242**, 127–132.

Cannell, M. and Dewar, R. (1995). The carbon sink provided by plantation forests and their products in Britain. *Forestry*, **68**, 35–48.

Chasmer, L., Hopkinson, C. and Treitz, P. (2006). Investigating laser pulse penetration through a conifer canopy by integrating airborne and terrestrial lidar. *Canadian Journal of Remote Sensing*, **32**, 116–125.

Chen, M., Liu, S. and Tieszen, L. (2008). An improved state-parameter analysis of ecosystem models using data assimilation. *Ecological Modelling*, **219**, 317–326.

Clark, J., Wolosin, M. and Dietze, M. (2007). Tree growth inference and prediction from diameter censuses and ring widths. *Ecological Applications*, **17**, 1942–1953.

Clutter, J.L. (1963). Compatible Growth and Yield Models for Loblolly Pine. *Forest Science*, **9**, 354–371.

Coops, N. and Waring, R. (2001). The use of multiscale remote sensing imagery to derive regional estimates of forest growth capacity using 3-PGS. *Remote Sensing of Environment*, **75**, 324–334.

Coops, N. and Waring, R. (2011). A process-based approach to estimate lodgepole pine (Pinus contorta Dougl.) distribution in the Pacific Northwest under climate change. *Climatic Change*, 1–16.

Coops, N., Waring, R.H. and Landsberg, J. (1998). Assessing forest productivity in Australia and New Zealand using a physiologically-based model driven with averaged monthly weather data and satellite-derived estimates of canopy photosynthetic capacity. *Forest Ecology and Management*, **104**, 113–127.

Davies, O. and Kerr, G. (2011). The Costs and Revenues of Transformation to Continuous Cover Forestry continuous cover forestry : options with Sitka spruce. Tech. Rep. March, Forest Research, Farnham, UK.

De Wit, A. and van Diepen, C. (2007). Crop model data assimilation with the Ensemble Kalman filter for improving regional crop yield forecasts. *Agricultural and Forest Meteorology*, **146**, 38–56.

Defra (2007). A Strategy for England's Trees, Woods and Forests. Tech. rep., The Department for Environment, Food and Rural Affairs, London.

Dixon, B.L. and Howitt, R. (1979). Continuous forest inventory using a linear filter. *Forest Science*, **25**, 675–689.

Duursma, R., Falster, D., Valladares, F., Sterck, F., Pearcy, R., Lusk, C., Sendall, K., Nordenstahl, M., Houter, N., Atwell, B., Kelly, N., Kelly, J., Liberloo, M., Tissue, D., Medlyn, B. and Ellsworth, D. (2012). Light interception efficiency explained by two simple variables: a test using a diversity of small-to medium-sized woody plants. *New Phytologist*, **193**, 397–408.

Dyson, K.E., Thomson, A.M., Mobbs, D.C., Milne, R., Skiba, U., Clark, A., Levy, P., Jones, S., Billett, M., Dinsmore, K., van Oijen, M., Ostle, N., Foereid, B., Smith, P., Matthews, R., Mackie, E., Bellamy, P., Rivas-Casado, M., Jordan, C., Higgins, A., Tomlinson, R.W., Grace, J., Parrish, P., Williams, M., Clement, R., Moncrieff, J. and Manning, A. (2009). Inventory and projections of UK emissions by sources and removals by sinks due to land use, land use change and forestry. Annual report July 2009. Tech. rep., Department for the Environment, Food and Rural Affairs. Climate, Energy and Ozone: Science and Analysis Division.

Edwards, P.N. and Christie, J. (1981). *Yield models for forest management*. HMSO, London.

Evans, D.L., Roberts, S.D. and Parker, R.C. (2006). LiDAR - A new tool for forest measurements? *Forestry Chronicle*, **82**, 211–218.

Evensen, G. (1994). Sequential data assimilation with a nonlinear quasi-geostrophic model using Monte Carlo methods to forecast error statistics. *Journal of Geophysical Research*, **99**, 10,143–10,162.

Evensen, G. (2003). The Ensemble Kalman Filter: theoretical formulation and practical implementation. *Ocean Dynamics*, **53**, 343–367.

Evensen, G. (2009). *Data assimilation: the ensemble Kalman filter*. Springer, Berlin, 2nd edn.

Evensen, G. and Leeuwen, P.V. (1996). Assimilation of Geosat altimeter data for the Agulhas current using the ensemble Kalman filter with a quasigeostrophic model. *Monthly Weather Review*, **124**, 85–96.

Falkowski, M., Smith, A. and Hudak, A. (2006). Automated estimation of individual conifer tree height and crown diameter via two-dimensional spatial wavelet analysis of lidar data. *Canadian Journal of Remote Sensing*, **32**, 153–161.

Fonweban, J., Gardiner, B.A., Macdonald, E. and Auty, D. (2011). Variable-top merchantable volume equations for Scots pine (Pinus sylvestris) and Sitka spruce (Picea sitchensis (Bong.) Carr.) in Northern Britain. *Forestry*, **84**, 237–253.

Forest Research (2001). ForestYield Software, Version 1.1. Available from Forestry Commission Research Agency.

Forestry Commission (1998). England Forestry Strategy: A New Focus for England's Woodlands. Tech. rep., Forestry Commission National Office For England, Cambridge,UK.

Forestry Commission (2003). National inventory of woodland and trees: Great Britain. Tech. rep., Forest Research, Northern Research Station, Edinburgh.

Forestry Commission (2011). Standing timber volume for coniferous trees in Britain: National Forest Inventory Report. Tech. rep., Forestry Commission, Edinburgh.

Forestry Commission (2013). Woodland Area , Planting and Restocking. Tech. Rep. June, Forestry Commission: Economics and Statistics, Edinburgh.

Fortin, M. and DeBlois, J. (2010). A statistical estimator to propagate height prediction errors into a general volume model. *Canadian Journal of Forest Research*, **40**, 1930–1939.

Fowler, A. and Van Leeuwen, P.J. (2013). Observation impact in data assimilation: The effect of non-gaussian observation error. *Tellus, Series A: Dynamic Meteorology and Oceanography*, **65**, 1–16.

Gao, C., Wang, H., Weng, E., Lakshmivarahan, S., Zhang, Y. and Luo, Y. (2011). Assimilation of multiple data sets with the ensemble Kalman filter to improve forecasts of forest carbon dynamics. *Ecological applications : a publication of the Ecological Society of America*, **21**, 1461–73.

García, O. (1979). Modelling stand development with stochastic differential equations. In D. Elliott, ed., *Mensuration for Management Planning of Exotic Forest plantations. New Zealand Forest Service, FRI Symposium*, 20, 315–333.

Garcia, O. (1983). A stochastic differential equation model for the height growth of forest stands. *Biometrics*, **39**, 1059–1072.

García, O. (1983). New class of growth models for even-aged stands: Pinus radiata in Golden Downs Forest. *New Zealand Journal of Forestry Science*, **14**, 65–88.

García, O. (2006). Site Index: concept and Methods. In C.J. Cieszewski and M. Strub, eds., *The 2nd International Conference on Forest Measurements and Quantitative Methods and Management*, June, 275–283, Hot Springs, Arkansas.

García, O. (2009). A simple and effective forest stand mortality model. *Mathematical and Computational Forestry & Natural-Resource Sciences (MCFNS)*, **1**, 1–9.

García, O. (2010). A parsimonious dynamic stand model for interior spruce in British Columbia. *Forest Science*, **57**, 265–280.

García, O. (2013). Building a dynamic growth model for trembling aspen in western Canada without age data. *Canadian Journal of Forest Research*, **43**, 256–265.

García, O. and Ruiz, F. (2003). A growth model for eucalypt in Galicia, Spain. *Forest Ecology and Management*, **173**, 49–62.

García, O., Burkhart, H.E. and Amateis, R.L. (2011). A biologically-consistent stand growth model for loblolly pine in the Piedmont physiographic region, USA. *Forest Ecology and Management*, **262**, 2035–2041.

Gardiner, B., Suárez, J., Achim, A., Hale, S. and Nicoll, B. (2004). Forest GALES A PC-based wind risk model User's Guide. Forest Research Published Software.

Gardiner, B.A. and Quine, C.P. (2000). Management of forests to reduce the risk of abiotic damage – a review with particular reference to the effects of strong winds. *Forest Ecology and Management*, **135**, 261–277.

Gelman, A. and Hill, J. (2007). *Data analysis using regression and multilevel/hierarchical models*. Cambridge University Press, Cambridge, UK.

Gelman, A. and Rubin, D. (1992). Inference from iterative simulation using multiple sequences. *Statistical science*, **7**, 457–472.

Gertner, G.Z. (1984). Localizing a Diameter Increment Model with a Sequential Bayesian Procedure. *Forest Science*, **30**, 851–864.

Green, E. and Strawderman, W. (1996). Predictive posterior distributions from a Bayesian version of a slash pine yield model. *Forest science*, **42**, 456–464.

Green, E.J., Strawderman, W.E. and Thomas, C.E. (1992). Empirical Bayes Development of Honduran Pine Yield Models. *Forest Science*, **38**, 21–33.

Green, E.J., MacFarlane, D.W. and Valentine, H.T. (2000). Bayesian synthesis for quantifying uncertainty in predictions from process models. *Tree Physiology*, **20**, 415–419.

Guerif, M. and Duke, C. (2000). Adjustment procedures of a crop model to the site specific characteristics of soil and crop using remote sensing data assimilation. *Agriculture, Ecosystems & Environment*, **81**, 57–69.

Hamilton, G.J. (1975). *Forest Mensuration Handbook*. HMSO, London.

Hamilton, G.J. and Christie, J. (1971). *Forest Management Tables (Metric)*. HMSO, London.

Hampton, S.E., Strasser, C.A., Tewksbury, J.J., Gram, W.K., Budden, A.E., Batcheller, A.L., Duke, C.S. and Porter, J.H. (2013). Big data and the future of ecology. *Frontiers in Ecology and the Environment*, **11**, 156–162.

Härkönen, S., Tokola, T., Packalén, P., Korhonen, L. and Mäkelä, a. (2013). Predicting forest growth based on airborne light detection and ranging data, climate data, and a simplified process-based model. *Canadian Journal of Forest Research*, **43**, 364–375.

Hasenauer, H. (1994). *A single-tree growth simulator for uneven spruce-pine and beech-spruce mixed stands [in German]*.. Austrian Society for Forest Ecosystem Research and Experimental Tree Research, Vienna, Austria.

Haugen, V.E.J. and Evensen, G. (2002). Assimilation of SLA and SST data into an OGCM for the Indian Ocean. *Ocean Dynamics*, **52**, 133–151.

Hibberd, B.G. (1991). *Forestry practice. Forestry Commission Handbook No 6*.. HMSO, London.

Hopkinson, C. and Chasmer, L. (2004). Assessing forest metrics with a ground-based scanning lidar. *Journal of Forest*, **583**, 573–583.

Houllier, F., Leban, J. and Colin, F. (1995). Linking growth modelling to timber quality assessment for Norway spruce. *Forest Ecology and Management*, **74**, 91–102.

Houtekamer, P.L. and Mitchell, H.L. (2001). A Sequential Ensemble Kalman Filter for Atmospheric Data Assimilation. *Monthly Weather Review*, **129**, 123–137.

Houtekamer, P.L. and Mitchell, H.L. (2005). Ensemble Kalman filtering. *Quarterly Journal of the Royal Meteorological Society*, **131**, 3269–3289.

Hu, Z. and García, O. (2010). A height-growth and site-index model for interior spruce in the Sub-Boreal Spruce biogeoclimatic zone of British Columbia. *Canadian Journal of Forest Research*, **40**, 1175–1183.

Hudak, A.T., Lefsky, M.A., Cohen, W.B. and Berterretche, M. (2002). Integration of lidar and Landsat ETM+ data for estimating and mapping forest canopy height. *Remote Sensing of Environment*, **82**, 397–416.

Hummel, F.C. and Christie, J. (1953). *Revised yield tables for conifers in Great Britain, Forestry Commission, Forest Record, No. 24*. HMSO, London.

Hyde, P., Nelson, R., Kimes, D. and Levine, E. (2007). Exploring LiDAR–RaDAR synergy—predicting aboveground biomass in a southwestern ponderosa pine forest using LiDAR, SAR and InSAR. *Remote Sensing of Environment*, **106**, 28–38.

IPCC (2003). *Intergovernmental Panel on Climate Change Good Practice Guidance for Land Use, Land-Use Change and Forestry*. IPCC National Greenhouse Gas Inventories Programme Technical Support Unit, Hayama, Japan.

Jandl, R., Lindner, M., Vesterdal, L., Bauwens, B., Baritz, R., Hagedorn, F., Johnson, D., Minkkinen, K. and Byrne, K. (2007). How strongly can forest management influence soil carbon sequestration? *Geoderma*, **137**, 253–268.

Jenkins, T. (2009). Growth and yield models for improved Sitka spruce. Talk to the Timber Quality Steering Group, available at: www.forestry.gov.uk.

Kalman, R. (1960). A new approach to linear filtering and prediction problems. *Journal of basic Engineering*, **82**, 35–45.

Kangas, A. (1999). Methods for assessing uncertainty of growth and yield predictions. *Canadian Journal of Forest Research*, **29**, 1357–1364.

Kangas, A.S. (1997). On the prediction bias and variance in long-term growth projections. *Forest Ecology and Management*, **96**, 207–216.

Kass, R. and Raftery, A. (1995). Bayes factors. *Journal of the American Statistical Association*, **90**, 773–795.

Kerr, G. (1999). The use of silvicultural systems to enhance the biological diversity of plantation forests in Britain. *Forestry*, **72**, 191–205.

Koch, B. (2010). Status and future of laser scanning, synthetic aperture radar and hyperspectral remote sensing data for forest biomass assessment. *ISPRS Journal of Photogrammetry and Remote Sensing*, **65**, 581–590.

Koohkan, M.R. and Bocquet, M. (2012). Accounting for representativeness errors in the inversion of atmospheric constituent emissions: application to the retrieval of regional carbon monoxide fluxes. *Tellus B*, **64**, 1–17.

Korzukhin, M., Ter-Mikaelian, M. and Wagner, R. (1996). Process versus empirical models: which approach for forest ecosystem management? *Canadian Journal of Forest Research*, **26**, 879–887.

Kutner, M.H., Nachtsheim, C. and Neter, J. (2004). *Applied linear regression models*. McGraw-Hill, New York.

Laloy, E. and Vrugt, J.A. (2012). High-dimensional posterior exploration of hydrologic models using multiple-try DREAM (ZS) and high-performance computing. *Water Resources Research*, **48**, W01526.

Landsberg, J. (2003). Physiology in forest models: history and the future. *Forest Biometry, Modelling and Information Sciences*, **1**, 49–63.

Landsberg, J. and Waring, R. (1997). A generalised model of forest productivity using simplified concepts of radiation-use efficiency, carbon balance and partitioning. *Forest Ecology and Management*, **95**, 209–228.

Landsberg, J., Waring, R. and Coops, N. (2003). Performance of the forest productivity model 3-PG applied to a wide range of forest types. *Forest Ecology and Management*, **172**, 199–214.

Leban, J. (2003). Models for the timber quality assessment of the actual forest resource. Methodology for Sitka spruce. Tech. rep., Forest Reseach UK.

Lefsky, M., Cohen, W., Hudak, A., Acker, S. and Ohmann, J. (1999). Integration of lidar, Landsat ETM+ and forest inventory data for regional forest mapping. *International Archives of Photogrammetry and Remote Sensing*, **32**, 119–126.

Lehtonen, A., Mäkipää, R. and Heikkinen, J. (2004). Biomass expansion factors (BEFs) for Scots pine, Norway spruce and birch according to stand age for boreal forests. *Forest Ecology and Management*, **188**, 211–224.

Levy, P.E., Hale, S.E. and Nicoll, B.C. (2004). Biomass expansion factors and root : shoot ratios for coniferous tree species in Great Britain. *Forestry*, **77**, 421–430.

Li, R., Stewart, B. and Weiskittel, A. (2011). A Bayesian approach for modelling non-linear longitudinal/hierarchical data with random effects in forestry. *Forestry*, **85**, 17–25.

Lohmander, P. (1988). Continuous extraction under risk. *Systems Analysis Modelling Simulation*, **5**, 339–354.

Lonsdale, J., Xenakis, G., Mencuccini, M. and Perks, M. (2015). A comparison of models for quantifying growth and standing carbon in uk scots pine forests. *iForest-Biogeosciences and Forestry*, 638–647.

Low, A.J. (1987). Sitka spruce silviculture in Scottish forests. *Proceedings of the Royal Society of Edinburgh Section B: Biology*, **93**, 93–106.

Luenberger, D.G. (1979). *Introduction to dynamic systems*, vol. 19. John Wiley.

Maas, H.G., Bienert, A., Scheller, S. and Keane, E. (2008). Automatic forest inventory parameter determination from terrestrial laser scanner data. *International Journal of Remote Sensing*, **29**, 1579–1593.

Mäkelä, A., Landsberg, J., Ek, A.R., Burk, T.E., Ter-Mikaelian, M., Agren, G.I., Oliver, C.D. and Puttonen, P. (2000). Process-based models for forest

ecosystem management: current state of the art and challenges for practical implementation. *Tree Physiology*, **20**, 289–298.

Mason, E.G., Methol, R. and Cochrane, H. (2011). Hybrid mensurational and physiological modelling of growth and yield of Pinus radiata D.Don. using potentially useable radiation sums. *Forestry*, **84**, 99–108.

Mayer, D. and Butler, D. (1993). Statistical validation. *Ecological Modelling*, **68**, 21–32.

McInerney, D.O., Suarez-Minguez, J., Valbuena, R. and Nieuwenhuis, M. (2010). Forest canopy height retrieval using LiDAR data, medium-resolution satellite imagery and kNN estimation in Aberfoyle, Scotland. *Forestry*, **83**, 195–206.

McIntosh, R. (1995). The history and multi-purpose management of Kielder Forest. *Forest Ecology and Management*, **79**, 1–11.

McRoberts, R. and Lessard, V. (2000). The effects of uncertainty in diameter growth model predictions on annual inventory estimates. In *Second Annual Forest Inventory and Analysis (FIA) Symposium*, 70–75, Salt Lake City, UT.

Meredieu, C., Orazio, C., Baptista-Coelho, M. and Tomé, M. (2011). Internet database on forest models. Tech. rep., European Forest Institute, Joensuu, Finland.

Metcalf, C.J.E., McMahon, S.M. and Clark, J.S. (2009). Overcoming data sparseness and parametric constraints in modeling of tree mortality: a new nonparametric Bayesian model. *Canadian Journal of Forest Research*, **39**, 1677–1687.

Metropolis, N., Rosenbluth, A.W., Rosenbluth, M.N., Teller, A.H. and Teller, E. (1953). Equation of State Calculations by Fast Computing Machines. *The Journal of Chemical Physics*, **21**, 1087–1092.

Milne, R., Brown, T. and Murray, T. (1998). The effect of geographical variation of planting rate on the uptake of carbon by new forests of Great Britain. *Forestry*, **71**, 297–310.

Minunno, F., Xenakis, G., Perks, M.P. and Mencuccini, M. (2010). Calibration and validation of a simplified process-based model for the prediction of the carbon balance of Scottish Sitka spruce (Picea sitchensis) plantations. *Canadian Journal of Forest Research*, **40**, 2411–2426.

Minunno, F., van Oijen, M., Cameron, D.R., Cerasoli, S., Pereira, J.S. and Tomé, M. (2012). Analysing structural error and parameter uncertainty of two Eucalyptus models differing in representation of autotrophic respiration. In A. Abbasi and N. Giesen, eds., *EGU General Assembly Conference Abstracts*, vol. 14 of *EGU General Assembly Conference Abstracts*, 1250.

Minunno, F., van Oijen, M., Cameron, D. and Pereira, J. (2013). Selecting parameters for Bayesian calibration of a process-based model: a methodology based on canonical correlation analysis. *SIAM/ASA Journal on Uncertainty Quantification*, **1**, 370–385.

Mitchell, K.J. (1975). Dynamics and Simulated Yield of Douglas-fir. *Forest Science Monograph*, **17**, 1–39.

Mitchell, K.J. (1988). SYLVER: Modelling the impact of silviculture on yield, lumber value, and economic return. *The Forestry Chronicle*, **64**, 127–131.

Mohren, G.M.J., Bartelink, H.H. and Jansen, J.J. (1994). *Contrasts between biologically-based process models and management-oriented growth and yield models*. Elsevier, Amsterdam.

Monserud, R.a. (2003). Evaluating forest models in a sustainable forest management context. *Forest Biometry, Modelling and Information*, **1**, 35–47.

Monteith, J.L. (1972). Solar Radiation and Productivity in Tropical Ecosystems. *The Journal of Applied Ecology*, **9**, 747.

Moradkhani, H., Sorooshian, S., Gupta, H.V. and Houser, P.R. (2005). Dual state-parameter estimation of hydrological models using ensemble Kalman filter. *Advances in Water Resources*, **28**, 135–147.

Morison, J., Matthews, R., Miller, G., Perks, M., Randle, T., Vanguelova, E., White, M. and Yamulki, S. (2011). Understanding the Carbon and Greenhouse Gas Balance of UK Forests - A Review. Tech. Rep. March, Forest Research, Farnham, UK.

Næsset, E. and Økland, T. (2002). Estimating tree height and tree crown properties using airborne scanning laser in a boreal nature reserve. *Remote Sensing of Environment*, **79**, 105–115.

Nijnik, M., Mather, A., Reynolds, K.M., Thomson, A.J., Köhl, M., Shannon, M.A., Ray, D., Rennolls, K. and Others (2007). Analysing institutions and public perspectives to identify the future of British forests. *Sustainable Forestry: From Monitoring and Modelling to Knowledge Management and Policy Science, CABI publishers*, 171–188.

Patenaude, G., Milne, R., Van Oijen, M., Rowland, C.S. and Hill, R.A. (2008). Integrating remote sensing datasets into ecological modelling: a Bayesian approach. *International Journal of Remote Sensing*, **29**, 1295–1315.

Pérez-Cruzado, C. and Muñoz Sáez, F. (2011). Combining empirical models and the process-based model 3-PG to predict Eucalyptus nitens plantations growth in Spain. *Forest Ecology and Management*, **262**, 1067–1077.

Pinjuv, G., Mason, E.G. and Watt, M. (2006). Quantitative validation and comparison of a range of forest growth model types. *Forest Ecology and Management*, **236**, 37–46.

Plummer, M. (2013). rjags: Bayesian graphical models using MCMC (Software). R package version 3-10, http://cran.r-project.org/package=rjags.

Pommerening, A. and Murphy, S. (2004). A review of the history, definitions and methods of continuous cover forestry with special attention to afforestation and restocking. *Forestry*, **77**, 27–44.

Popescu, S. (2007). Estimating biomass of individual pine trees using airborne lidar. *Biomass and Bioenergy*, **31**, 646–655.

Popescu, S., Wynne, R. and Scrivani, J. (2004). Fusion of small-footprint lidar and multispectral data to estimate plot-level volume and biomass in deciduous and pine forests in Virginia, USA. *Forest Science*, **50**, 551–565.

Prisley, S. and Mortimer, M. (2004). A synthesis of literature on evaluation of models for policy applications, with implications for forest carbon accounting. *Forest Ecology and Management*, **198**, 89–103.

Pyatt, G., Ray, D. and Fletcher, J. (2001). An ecological site classification for forestry in Great Britain. Tech. rep., Forestry Commission, Edinburgh.

QGIS Development Group (2014). QGIS Geographic Information System. Open Source Geospatial Foundation Project.

Quaife, T., Lewis, P., Dekauwe, M., Williams, M., Law, B., Disney, M. and Bowyer, P. (2008). Assimilating canopy reflectance data into an ecosystem model with an Ensemble Kalman Filter. *Remote Sensing of Environment*, **112**, 1347–1364.

R Development Core Team (2012). *R: A Language and Environment for Statistical Computing*. R Foundation for Statistical Computing, Vienna, Austria.

Radtke, P. and Robinson, a. (2006). A Bayesian strategy for combining predictions from empirical and process-based models. *Ecological Modelling*, **190**, 287–298.

Radtke, P.J., Burk, T.E. and Bolstad, P.V. (2002). Forest Ecosystem Model with correlated inputs. *Forest Science*, **48**, 701–711.

Rennolls, K. (1995). Forest height growth modelling. *Forest Ecology and Management*, **71**, 217–225.

Roh, S., Genton, M.G., Jun, M., Szunyogh, I. and Hoteit, I. (2013). Observation Quality Control with a Robust Ensemble Kalman Filter. *Monthly Weather Review*, **141**, 4414–4428.

Rykiel, E. (1996). Testing ecological models: the meaning of validation. *Ecological Modelling*, **90**, 229–244.

Sands, P. and Landsberg, J. (2001). Parameterisation of 3-PG for plantation grown Eucalyptus globulus. *Forest Ecology and Management*, **163**, 273–292.

Schreuder, H.T., Ernst, R.L. and Ramirez-Maldonado, H. (2004). *Statistical techniques for sampling and monitoring natural resources*. US Department of Agriculture, Forest Service, Rocky Mountain Research Station, Fort Collins, CO, USA.

Scottish Executive (2006). The Scottish Forestry Strategy. Tech. rep., Forestry Commission Scotland, Edinburgh.

Scottish Executive (2012). Woodland Creation - Productive Conifer (high cost) woodlands (RP22301B). Website. Accessed: 14/1/14, www.scotland.gov.uk/Topics/farmingrural/SRDP/RuralPriorities/Options/WoodlandCreation/ConiferHighCost.

Sharpe, P.J.H. and Rykiel, E.J. (1991). *Modelling integrated response of plants to multiple stresses*. Academic Press, San Diego, California.

Smith, J. and Heath, L. (2001). Identifying influences on model uncertainty: an application using a forest carbon budget model. *Environmental Management*, **27**, 253–267.

Soares, P., Tome, M., Skovsgaard, J. and Vanclay, J. (1995). Evaluating a growth model for forest management using continuous forest inventory data. *Forest Ecology and Management*, **71**, 251–265.

St-Onge, B., Hu, Y. and Vega, C. (2008). Mapping the height and above-ground biomass of a mixed forest using lidar and stereo Ikonos images. *International Journal of Remote Sensing*, **29**, 1277–1294.

Stage, A. (1973). Prognosis model for stand development. Research Paper INT-137. Tech. rep., USDA Forest Service, Ogden, Utah.

Stan Development Team (2014). Stan Modeling Language User's Guide and Reference Manual (Software). Accessed: 14/1/14, http://mc-stan.org.

Suarez, J.C., Ontiveros, C., Smith, S. and Snape, S. (2005). Use of airborne LiDAR and aerial photography in the estimation of individual tree heights in forestry. *Computers and Geosciences*, **31**, 253–262.

Swatantran, A., Dubayah, R., Roberts, D., Hofton, M. and Blair, J.B. (2011). Mapping biomass and stress in the Sierra Nevada using lidar and hyperspectral data fusion. *Remote Sensing of Environment*, **115**, 2917–2930.

Swenson, J., Waring, R., Fan, W. and Coops, N. (2005). Predicting site index with a physiologically based growth model across Oregon, USA. *Canadian Journal of Forest Research*, **35**, 1697–1707.

ter Braak, C.J.F. (2006). A Markov Chain Monte Carlo version of the genetic algorithm Differential Evolution: easy Bayesian computing for real parameter spaces. *Statistics and Computing*, **16**, 239–249.

ter Braak, C.J.F. and Vrugt, J.A. (2008). Differential Evolution Markov Chain with snooker updater and fewer chains. *Statistics and Computing*, **18**, 435–446.

Tuomi, M., Vanhala, P., Karhu, K., Fritze, H. and Liski, J. (2008). Heterotrophic soil respiration—Comparison of different models describing its temperature dependence. *Ecological Modelling*, **211**, 182–190.

UNFCCC (1997). Kyoto Protocol to the United Nations Framework Convention for Climate Change. http://www.unfccc.de/, Kyoto, Japan.

Valentine, H. and Green, E. (2012). Models relating stem growth to crown length dynamics: application to loblolly pine and Norway spruce. *Trees*, **26**, 469–478.

Valentine, H.T. and Mäkelä, A. (2005). Bridging process-based and empirical approaches to modeling tree growth. *Tree Physiology*, **25**, 769–79.

van Leeuwen, M. and Nieuwenhuis, M. (2010). Retrieval of forest structural parameters using LiDAR remote sensing. *European Journal of Forest Research*, **129**, 749–770.

van Oijen, M., Rougier, J. and Smith, R. (2005). Bayesian calibration of process-based forest models: bridging the gap between models and data. *Tree Physiology*, **25**, 915–27.

van Oijen, M., Reyer, C., Bohn, F.J., Cameron, D.R., Deckmyn, G., Flechsig, M., Härkönen, S., Hartig, F., Huth, A., Kiviste, A., Lasch, P., Mäkelä, A., Mette, T., Minunno, F. and Rammer, W. (2013). Bayesian calibration, comparison and averaging of six forest models, using data from Scots pine stands across Europe. *Forest Ecology and Management*, **289**, 255–268.

Vanclay, J. and Skovsgaard, J. (1997). Evaluating forest growth models. *Ecological Modelling*, **98**, 1–12.

Vanclay, J.K. (1994). *Modelling forest growth and yield*. CAB International, Oxon, UK.

Vuokila, Y. (1965). Functions for variable density yield tables of pine based on temporary sample plots. *Communicationes Instituti Forestalis Fenniae*, **60**, 1–86.

Walters, D.D.K., Burkhart, H.E., Reynolds, M.R. and Gregoire, T.T.G. (1991). A Kalman Filter Approach to Localizing Height-Age Equations. *Forest Science*, **37**, 1526–1537.

Waterworth, R., Richards, G., Brack, C. and Evans, D. (2007). A generalised hybrid process-empirical model for predicting plantation forest growth. *Forest Ecology and Management*, **238**, 231–243.

Weiskittel, A., Maguire, D. and Monserud, R. (2007). *Development of a Hybrid Model for Intensively Managed Douglas-fir in the Pacific Northwest*, 49–67. August, USDA, Portland, OR.

Weiskittel, A.R., Maguire, D.A., Monserud, R.A. and Johnson, G.P. (2009). A hybrid model for intensively managed Douglas-fir plantations in the Pacific Northwest, USA. *European Journal of Forest Research*, **129**, 325–338.

Welsh Assembly Government (2009). Woodlands for Wales. Tech. rep., Forestry Commission Wales, http://gov.wales/topics/environmentcountryside/forestry/woodlandsforwales/woodland-for-wales-action-plan-2012/?lang=en.

Wernsdörfer, H., Colin, A., Bontemps, J.D., Chevalier, H., Pignard, G., Caurla, S., Leban, J.M., Hervé, J.C. and Fournier, M. (2012). Large-scale dynamics of a heterogeneous forest resource are driven jointly by geographically varying growth conditions, tree species composition and stand structure. *Annals of Forest Science*, **69**, 829–844.

Williams, M., Schwarz, P.a., Law, B.E., Irvine, J. and Kurpius, M.R. (2005). An improved analysis of forest carbon dynamics using data assimilation. *Global Change Biology*, **11**, 89–105.

Woodland Expansion Advisory Group (2012). Report of the Woodland Expansion Advisory Group. Tech. Rep. June, Cabinet Secretary for Rural Affairs and Environment, Richard Lochhead, MSP, Edinburgh.

Woollons, R., Snowdon, P. and Mitchell, N. (1997). Augmenting empirical stand projection equations with edaphic and climatic variables. *Forest Ecology and Management*, **98**, 267–275.

Xenakis, G. (2007). *Assessment of carbon sequestration and timber production of Scots pine across Scotland using the process-based model 3-PGN*. Ph.D. thesis, University of Edinburgh, Edinburgh.

Xenakis, G., Ray, D. and Mencuccini, M. (2008). Sensitivity and uncertainty analysis from a coupled 3-PG and soil organic matter decomposition model. *Ecological Modelling*, **219**, 1–16.

Xenakis, G., Ray, D. and Mencuccini, M. (2012). Effects of climate and site characteristics on Scots pine growth. *European Journal of Forest Research*, **131**, 427–439.

Yoda, K. (1963). Self-thinning in over-crowded pure stands under cultivated and natural conditions.(In-traspecific competition among higher plants. XI.). *Journal of Biology Osaka City University*, **14**, 107–129.

Zeide, B. (1978). Standardization of growth curves. *Journal of Forestry*, **76**, 289–292.

Appendix A

SLeDG parameterisation details

A.1 Height growth and site index

Height was measured as stand top height, commonly defined in UK forestry as the average height of the 100 largest trees by diameter at breast-height (dbh) per hectare. Top height was used as it is relatively invariant to different stand densities compared to mean height. Height growth was thus parameterised as an independent sub-model which also classified the site general productivity: a site index model.

The site index model relating top height to stand age was estimated using the *EasySDE* package (`http://forestgrowth.unbc.ca/sde`). This models height growth with a differential form of the von Bertalanffy model, whereby the change in height at any point in time was a function of the current height:

$$\frac{dH^{b_3}}{dt} = b_2(b_1^{b_3} - H^{b_3}) \tag{A.1}$$

The parameters $b_1 - b_3$ may either be local (and thus site quality dependent) or global parameters. Two ways of including site quality were tested:

1. b_1 as local parameter q
2. b_2 as local parameter q

Each model was fitted using all 51 permanent sample plot (PSP) sites. The two models were compared by the log-likelihood of each formulation, in addition to Akaike information criterion (AIC) which attributes a cost to the addition of extra parameters.

Integration of equation (A.1) allowed height to be predicted at a point forward in time:

$$H_2 = b_1 \left(1 - \left[1 - \left(\frac{H_1}{b_1} \right)^{b_3} \right] e^{-b_2(t_2 - t_1)} \right)^{1/b_3} \tag{A.2}$$

Here H_1 was the initial height, H_2 predicted height and $t_2 - t_1$ the time change between heights. Site index (H_s) may be determined from this given a fixed origin $[t_1, H_1] = [0, 0]$, and a reference age for site index t_s:

$$H_s = b_1(1 - e^{-b_2 t_s})^{1/b_3} \tag{A.3}$$

The log-likelihoods provided by *EasySDE* for each of the two alternative ways of including site quality in the site index model are given in Table A.1 along with calculated AIC values. The best parameterisation for the site index (SI) model was selected by both log-likelihood and AIC as model 1.

Table A.1: Log-likelihood and Akaike information criterion (AIC) values of the two alternative parameterisations for including site quality (a local parameter) in the height growth model

Model number	1	2
Log-likelihood	726.1	701.7
AIC	-1444.2	-1395.4

A.2 Mortality

Mortality was modelled as a function of the stand height and current number of stems. Basal area is excluded as an explanatory variable, as previous accumulation of woody tissue should not cause mortality in itself. As height is determined by site quality in the model, mortality is thus linked with site quality. The model is given here as:

$$\frac{dN}{dH} = -b_4 H^{b_5} N^{b_6} \tag{A.4}$$

The equation may be expressed in terms of dN/dt by multiplying by dH/dt: equation (A.1). The 3 parameters (b_4, b_5, b_6) were estimated using least-squares method using consecutive pairs of PSP measures from unthinned plots representing natural mortality. Thinned plots were excluded due to lack of information concerning the timing of thinnings. A log transformation of the integral of equation (A.4) allowed the parameters to be estimated more efficiently:

$$\log(N_2) = \log\left(N_1^{1-b_6} + \left[b_4 \frac{b_6 - 1}{b_5 + 1}(H_2{}^{b_5+1} - H_1{}^{b_5+1})\right]\right) / 1 - b_6 \tag{A.5}$$

A.3 Basal area and Occupancy

Basal area is modelled indirectly, by predicting the increase in the product of B and H: W. W is linearly related to both biomass and volume, and additionally W behaves more simply than B alone.

Change in W is given by the balance of the gross increment (W^+) increase and stem wood loss (W^-) decrease for a given change in H:

$$\frac{dW}{dH} = W^+ - W^-$$

The gross increment is modelled by simple function of H and N. The function is:

$$W^+ = b_7 H^{b_8} N^{b_9} \tag{A.6}$$

Loss of stem wood (W^-) is a function of the relative size of of trees lost due to mortality defined in the previous section:

$$W^- = -k\frac{W}{N}\frac{dN}{dH} \tag{A.7}$$

Where k represents the relative size of dead trees. Here it is assumed a constant and equal to b_9.

A complication to the previous approach (Equation A.6.) of estimation of gross increment is that it applies only to stands with maximum canopy closure. Recently established or thinned stands have not yet occupied all available space both above ground with foliage, and below ground in root systems. The maximum resource utilisation potential is thus not being reached. This is represented in the model by occupancy (Ω): a proportion of maximum productivity achieved at stand closure. This is analogous to an interception efficiency: an index of the rate of gross photosynthesis versus a maximum potential rate, where a stand has enough leaves to intercept all photosynthetically active radiation (PAR).

Occupancy is an unobserved variable, but the relative closure (R) represents the physical extent of foliage and roots compared to a closed stand. It is similar to a Leaf Area Index (LAI), but avoids issues with LAI measurement common in forests. R and Ω are non-linearly related: close to stand closure, additional leaves at the base of the canopy will not greatly increase productivity, but in open stands it is expected that resource capture and productivity is more closely linked to the amounts of root and foliage. The relationship suggested is:

$$\Omega = 1 - (1 - R)^{b_{10}} \tag{A.8}$$

The exponent in this function (b_{10}) is dependent on shade tolerance. The initial value of R at stand establishment is determined by a parameter b_{12} representing a planting density at which the stand would be considered fully closed. The initial value of R is the percentage that the initial planting density (N_b) makes up of b_{12}, unless N_b is greater than b_{12} in which case $R = 1$. Occupancy at planting (Ω_b) is thus derived from (A.8) as:

$$\Omega_b = 1 - (1 - \min\{N_b/b_{12}, 1\})^{b_{10}} \tag{A.9}$$

The value of R changes following a stand thinning. It is assumed proportional to basal area loss such that: $R_{\text{after}} = (B_{\text{after}}/B_{\text{before}})R_{\text{before}}$.

The rate of change of occupancy with top height is a function of height raised to the same exponent employed in equation (A.6) for W^+:

$$\frac{d\Omega}{dH} = b_{11}H^{b_8}(1 - \Omega) \tag{A.10}$$

When occupancy reaches a value of 1 (representing optimum resource use) it no longer increases, and productivity is at its maximum value. The equation for W^+ (A.6) is multiplied by Ω to account for these changes in occupancy:

$$W^+ = b_7\Omega H^{b_8}W^{b_9} \tag{A.11}$$

Parameters b_7 - b_{12} from Equations (A.9), (A.10), and (A.11) were estimated simultaneously using the `optim` function in the R statistical system, version 2.15 (R Development Core Team, 2012) to minimise root mean standard error (RMSE)

in estimates of B. Simultaneous estimation helps reduce model error. Preliminary investigations fixed values for b_9, b_{10}, and b_{12} equal to those estimated for loblolly pine (García *et al.*, 2011), and then freed to see if any model improvement resulted. Non-overlapping intervals were utilised in the parameterisation to reduce temporal autocorrelation.

A.4 Volume and Biomass

The merchantable volume (V) is linearly related to W and is thus estimated as:

$$V = \beta_v W + c_v \tag{A.12}$$

β_v and c_v are the slope and intercept of the relationship respectively. An intercept is included as a stand's top height may be shorter than 1.3m, with B and W equal to zero, yet there may still be a merchantable volume.

Whole tree biomass is is estimated using the biomass expansion factors (BEF) and root:shoot ratios of Levy *et al.* (2004). Merchantable volume is multiplied by the biomass expansion factors (BEF) and wood density to give the above ground biomass. Whole tree biomass is then given by calculating root:shoot ratio (0.301 for Scots pine) to determine root mass, and adding this to the above ground biomass. The biomass expansion factors (BEF) is determined by tree height for Scots pine according to the equation:

$$\text{BEF} = 1.392 - 0.4812\log(H) \tag{A.13}$$